

**Aggregation behavior of cholic acid derivatives  
in organic solvents and in water**

**Promotor**

Prof. dr. E.J.R. Sudhölter, hoogleraar in de organische chemie,  
Wageningen Universiteit

**Co-promotor**

Dr. A.T.M. Marcelis, universitair docent, Laboratorium voor Organische Chemie,  
Wageningen Universiteit

**Promotiecommissie**

Prof. dr. M.A. Cohen Stuart, Wageningen Universiteit

Prof. dr. J.B.F.N. Engberts, Rijksuniversiteit Groningen

Prof. dr. Ae. de Groot, Wageningen Universiteit

Dr. P. Terech, Commissariat à l'Energie Atomique, Grenoble, France

**Hendra M. Willemen**

**Aggregation behavior of cholic acid derivatives  
in organic solvents and in water**

Proefschrift

ter verkrijging van de graad van doctor

op gezag van de rector magnificus

van Wageningen Universiteit,

Prof. dr. ir. L. Speelman,

in het openbaar te verdedigen

op dinsdag 8 oktober 2002

des namiddags te half twee in de Aula.

Willemen, H.M.

Aggregation behavior of cholic acid derivatives in organic solvents and in water

Thesis Wageningen University - with summaries in English and Dutch

ISBN 90-5808-714-X

Today is the tomorrow I worried about yesterday

.....and all is well.



## Table of contents

<b>Chapter 1</b> Introduction	<b>1</b>
<b>Chapter 2</b> <i>N</i> -Cholyl amino acid alkyl esters: a novel class of organogelators	<b>15</b>
<b>Chapter 3</b> Alkyl derivatives of cholic acid as organogelators: one-component and two-component gels	<b>31</b>
<b>Chapter 4</b> A small angle neutron scattering study on cholic acid based organogel systems	<b>47</b>
<b>Chapter 5</b> Aggregation of different amino acid conjugates of cholic acid in aqueous solution	<b>67</b>
<b>Chapter 6</b> Micellization, thermodynamics, and antimicrobial activity of cholic acid based facial amphiphiles carrying three permanent ionic head groups	<b>77</b>
<b>Chapter 7</b> General discussion	<b>91</b>
<b>Summary</b>	<b>101</b>
<b>Samenvatting</b>	<b>104</b>
<b>Dankwoord</b>	<b>107</b>
<b>Curriculum vitae</b>	<b>110</b>
<b>List of publications</b>	<b>111</b>





# 1

## Introduction

*This chapter gives a brief introduction to the subject of this thesis. First, an introduction to aggregation chemistry is given with the emphasis on micelles and organogels. Then, a short overview is given about bile acids in general and about the use of cholic acid derivatives as functional molecules in particular. Finally, the content of this thesis is outlined.*

## 1.1 AGGREGATION IN SOLUTION

The process of spontaneous aggregation of single molecules in solution into larger structures with a certain order is an important phenomenon in every-day-life as well as in science. The best-known example of aggregation in every-day-life is the formation of micelles by detergent molecules. The most important type of aggregation, which is essential to life, is the formation of the lipid bilayer membrane by phospholipids. It has inspired chemists and physicists to study and mimic this and other types of aggregates.<sup>1</sup>

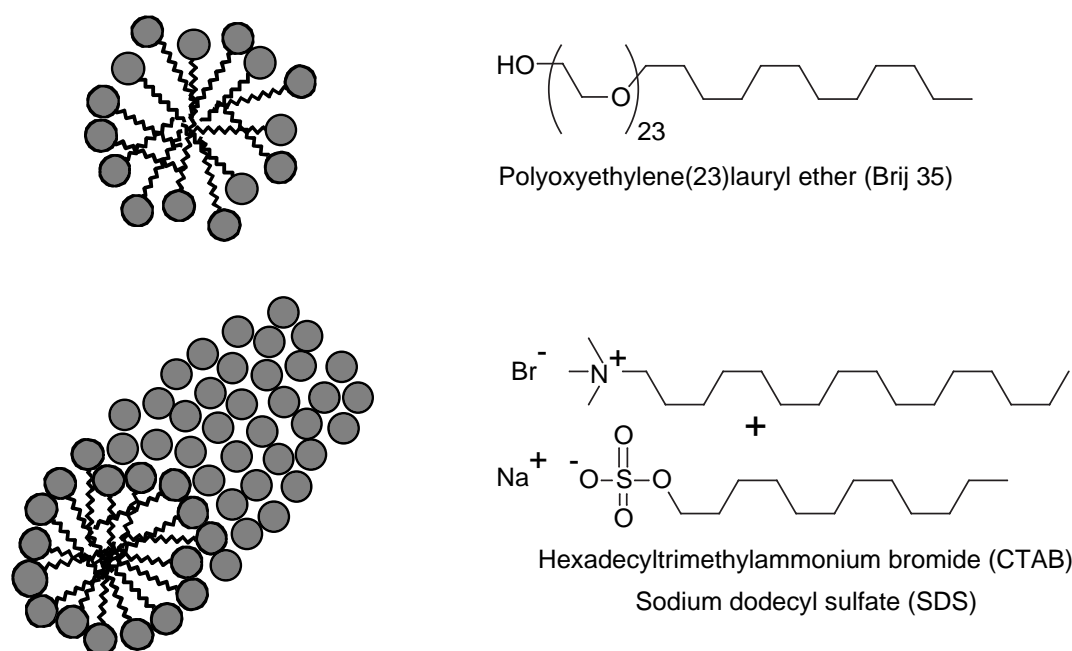
Aggregation of molecules often occurs at the borderline of solubility. An important molecular property in this respect is polarity, for which solubility follows the rule 'like dissolves like'. Polar (hydrophilic) compounds are well soluble in polar solvents, e.g. salt in water, and the same goes for apolar (hydrophobic) compounds and solvents, e.g. vitamin E in oil. Furthermore, polar compounds are insoluble in apolar solvents and vice versa. Things become interesting when a compound has amphiphilic properties, i.e. when it contains a polar as well as an apolar part. These compounds are most comfortable when each part is located in an appropriate environment, which is only possible at the interface between two media. Therefore, amphiphilic compounds are also called surface active agents, or short: surfactants.<sup>2</sup> When they are placed in a solvent, the urge to minimize the unfavorable polar-apolar interaction causes them to aggregate. This usually happens spontaneously above a certain concentration (the critical aggregation concentration or cac). Also a minimum temperature (the Krafft point<sup>3</sup>) is necessary to assure that the solubility of the surfactant equals the cac. The shape and size of the aggregates can vary considerably, depending on the shape of the surfactant and the character of the solvent. A few examples are described below.

### 1.1.1 AGGREGATION IN WATER

Different types of aggregates can be formed in water. The best-known type of aggregate that is formed in water is the micelle. Micelles are spontaneously formed, dynamic systems with a lifetime in the order of milliseconds. The monomers continuously exchange with the surrounding medium with a residence time in the micelle in the order of microseconds.<sup>1</sup> Most micelle-forming surfactants have a

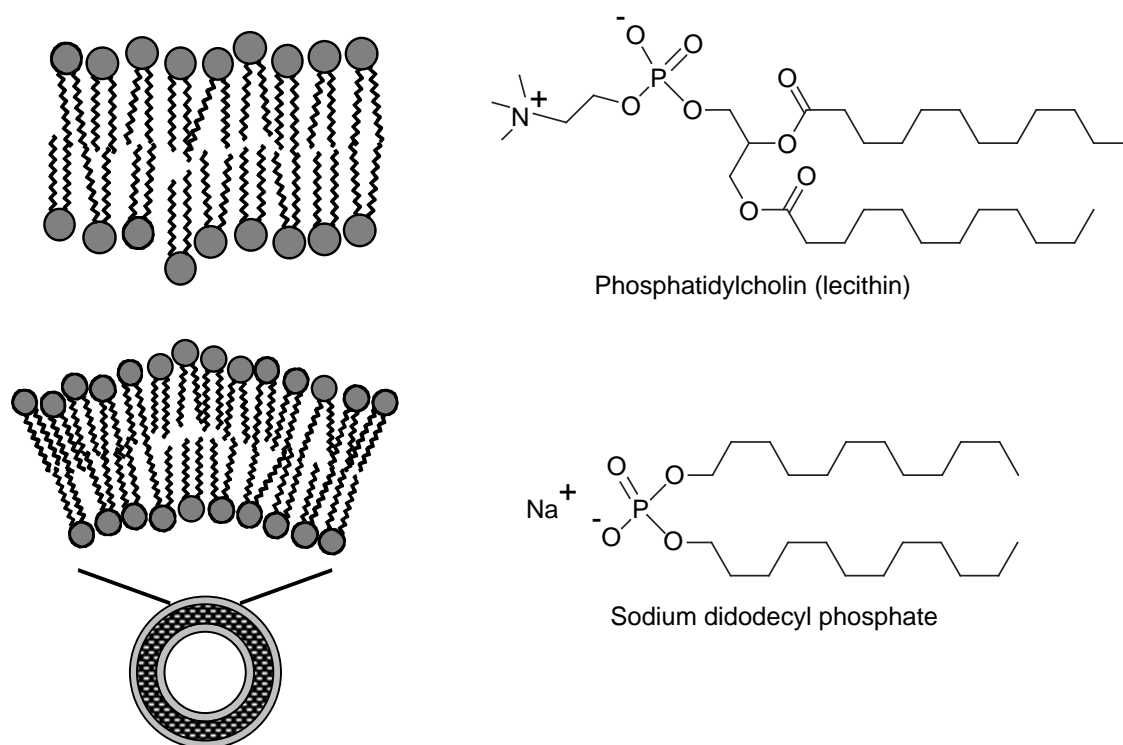
hydrophilic head group, often ionic, and a hydrophobic part, usually an alkyl chain. The polar head groups are located on the outside of the micelle, where they are in full contact with the surrounding water. The alkyl tails are concentrated inside the micelle, where they are shielded from the polar environment.

The driving force for spontaneous micellization lies in the hydrophobic effect, in which hydrophobic hydration and hydrophobic interactions play a role.<sup>4</sup> When the surfactants are present as monomers in solution, the hydrophobic tails are hydrated. This involves increased hydrogen bond interactions and a loss of freedom for the hydration water molecules as compared to bulk water. Upon micellization, there is van der Waals interaction between the hydrophobic tails, which gives a considerable decrease in the hydrophobic hydration. The consequent breaking of the extra hydrogen bonds results in an unfavorable enthalpy effect, which is compensated by a large entropy gain, due to increased freedom of the water molecules. This favorable entropy effect also compensates for two smaller effects: the entropy loss for the tails themselves and the enthalpy increase due to head group repulsion, especially in the case of ionic surfactants. However, the binding of counter ions also relieves this repulsion by decreasing the overall surface charge.



**Scheme 1.1** Schematic representation of a spherical micelle (top) and a worm-like micelle (bottom) and typical surfactants that form these aggregates

Depending on the geometry of the surfactant, different types of micelles can be formed. Two types of micelles and typical surfactants, which can form these aggregates, are shown in Scheme 1.1. The simplest type of micelle is the spherical micelle. This is a sphere-shaped aggregate with an aggregation number of 50-100 (i.e. the number of molecules that take part in the micelle). The surfactants usually possess one head group and one apolar tail. Since the cross-sectional area of the hydrated head group exceeds the diameter of the tail, they are considered cone-shaped, which explains the formation of a sphere-shaped aggregate. Its average diameter is 5-10 nm. Another type of micelle is the worm-like, or cylindrical, micelle. This type of micelle can be formed by the addition of strongly binding counter ions, which decreases the effective head group area. They can also be formed by ion pair surfactants: a mixture of anionic and cationic surfactants, each with one alkyl tail. Because of the attraction between these oppositely charged head groups, the effective head group area decreases, which enables closer packing of the monomers.<sup>2</sup> Worm-like micelles often cause an increase in the viscosity of the solution.



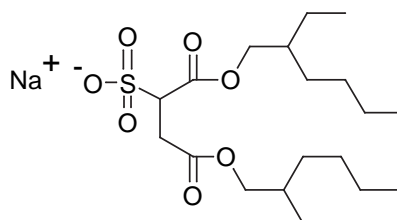
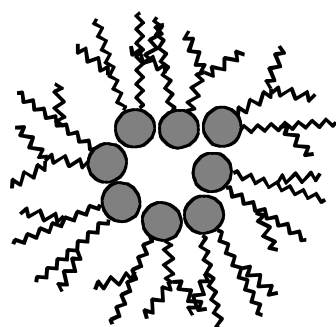
**Scheme 1.2** Schematic representation of a bilayer (top) and a vesicle (bottom) and typical surfactants that form these aggregates

Another type of aggregate that is formed in water is the bilayer and, related to that, the vesicle. These are schematically drawn in Scheme 1.2, together with some typical surfactants that form these aggregates. In the bilayer two molecules face each other with the apolar parts, and numerous of these pairs are stacked next to each other. Since the head groups are located on the outside, both sides of the layer are polar and the interior is apolar. These structures are usually formed by surfactants with one head group and two hydrophobic tails. The head group area is almost equal to the cross section of the two tails and the cylinder-shaped molecules can pack in a flat bilayer. A vesicle can be considered as a bilayer with a small curvature, which is closed at the ends. They seldom form spontaneously because of the often limited solubility of the monomers. Instead they can be prepared by ultrasonication, by microfiltration or via a thin film.<sup>2</sup> Vesicles can be uni- or multilamellar and their diameters range from 20 nm to several micrometers.

There are many more possible aggregates in aqueous solution, such as hydrogels and lyotropic liquid crystalline phases.<sup>5</sup> Formation of these aggregates depends on the structure of the surfactant (bolaform, gemini surfactants) and the surfactant concentration. This lies however outside the scope of this thesis and will therefore not be discussed.

### 1.1.2 AGGREGATION IN ORGANIC SOLVENTS

As is the case in water, also different types of aggregates can be formed in organic solvents. A type of aggregate that is the opposite of the micelle is the inverted micelle, shown in Scheme 1.3.

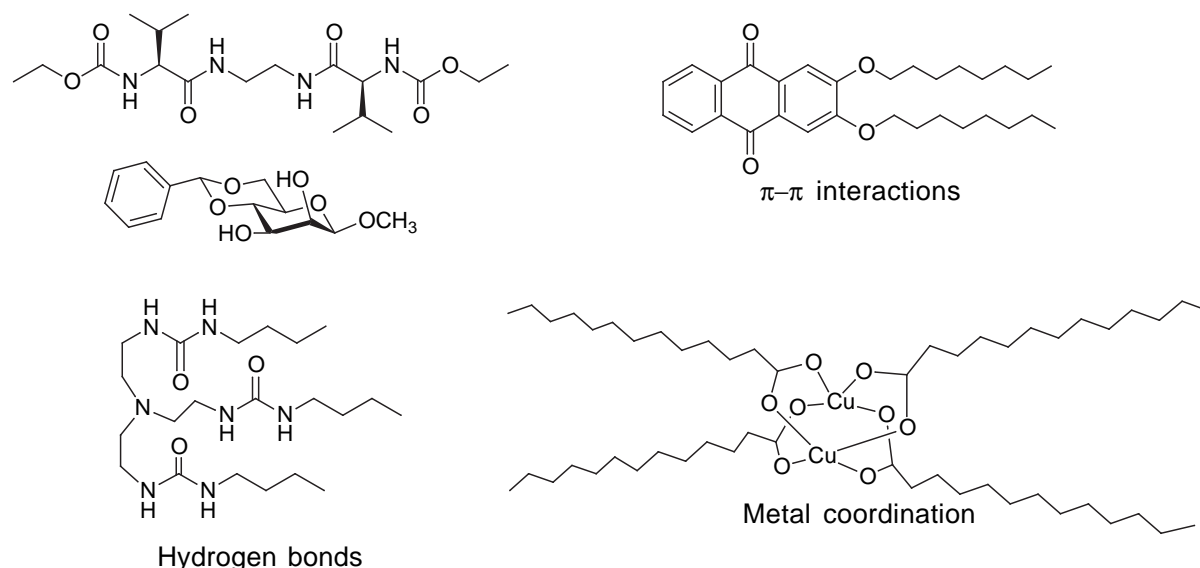


Sodium bis(2-ethylhexyl) sulfosuccinate (AOT)

**Scheme 1.3** Schematic representation of a reversed micelle and a typical surfactant that forms this aggregate

Here the head groups are located in the core of the aggregate and the apolar tails are on the outside, facing the apolar medium. Generally, there is a small water pool in the center, for hydration of the head groups. Surfactants that form these inverted structures usually have a bulky hydrophobic part, e.g. a branched alkyl tail, so they are considered to be 'reversed cone'-shaped molecules.

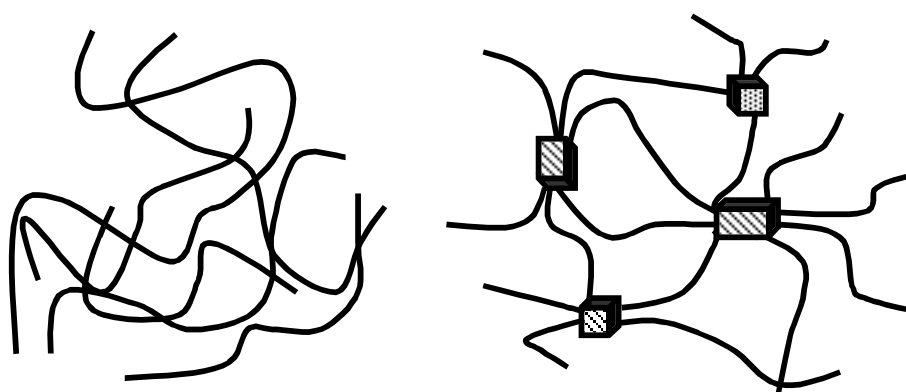
An important type of aggregate formed in organic solvents is the organogel. Organogels based on polymers are known for a longer period, but in this thesis only the relatively new organogels based on low molecular mass organogelators (LMOGs or just: organogelators) are considered.<sup>6,7</sup> Research on them started about two decades ago and new knowledge is gained every day. There is still no consensus on the description of what an organogel is. Generally, an organogel is an organic solvent with a considerable increase in viscosity by means of formation of a 3D-network of entangled fibers, which are formed by aggregation of organogelator molecules. The driving force for this aggregation of organogelators into fibers can be through different interactions. This leads to a great diversity in organogelators, of which some typical examples are depicted in Scheme 1.4.



**Scheme 1.4** Typical organogelators for different bonding types<sup>8,10,13,16,18</sup>

Gelators that assemble by means of hydrogen bonds usually possess hydroxyl groups, amide groups, or urea groups,<sup>8,9</sup> and they are often based on amino acids<sup>10-12</sup>

or sugars.<sup>13,14</sup> n-Alkanes with 24 to 36 carbon atoms are simple gelators,<sup>15</sup> which assemble by means of van der Waals interactions in various organic solvents. Gelation can also be driven by the coordination of metal-containing gelators.<sup>16,17</sup> Gelators with large conjugated systems, such as anthraquinones<sup>18</sup> or porphyrins,<sup>19</sup> aggregate through  $\pi$ - $\pi$  stacking. There are also gelators that combine two of the above mentioned interactions.<sup>20,21</sup> The large number of different organogelators is expanded with new discoveries regularly, often by chance, but recently there is a tendency to actively design new organogelators.<sup>22-24</sup> There are however no standard requirements, which molecules should possess in order to act as organogelators. A moderate solubility could be regarded as a requirement, because gelation is a process that occurs at the borderline of solubility. A poorly soluble compound, that also has difficulty with crystallization, will have a tendency to form a gel. This is the reason why most organogels are formed upon heating and subsequently cooling of a solution of organogelator in an appropriate solvent. Only a small amount of organogelator is necessary to form a network and to gel a large amount of solvent: concentrations of about 1 wt % of organogelator are usually sufficient. Besides the variation in which organogelators aggregate inside the fibers, there is also variation in the interaction between the fibers in the 3D network.<sup>25,26</sup> Scheme 1.5 shows examples of loose, transient interactions and crystalline microdomains at the positions where the fibers meet. The structure of the network has influence on the macroscopic properties of organogels, such as viscosity.

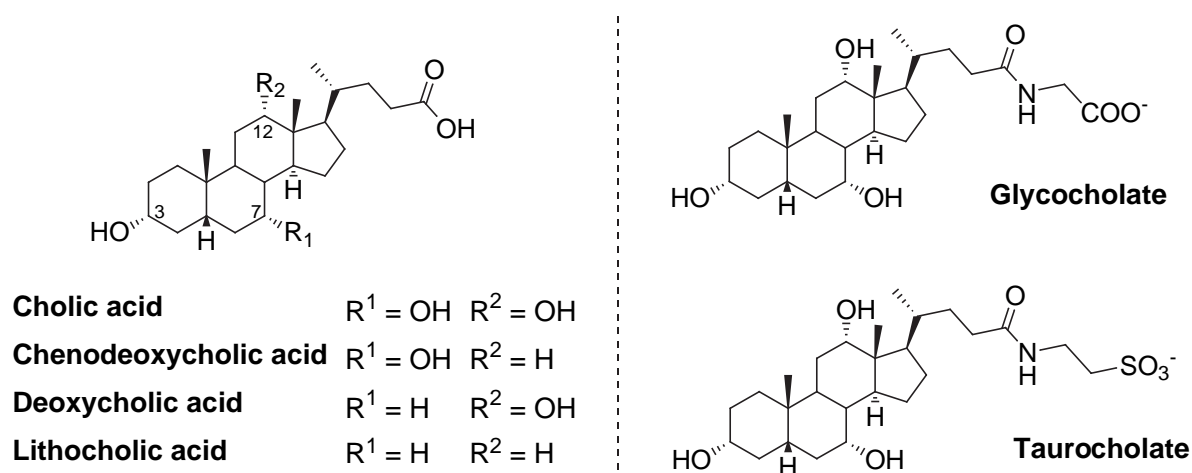


**Scheme 1.5** Schematic representation of possible organogel networks: transient interactions (left) and microcrystalline knots (right) at positions where the fibers meet

## 1.2 CHOLIC ACID

### 1.2.1 BILE ACIDS

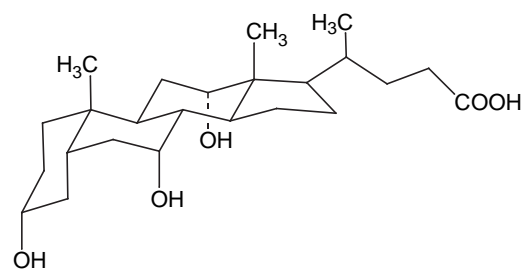
Bile acids are important biosurfactants with a role in mammalian digestion. The most important bile acids are presented in Scheme 1.6. Cholic acid and chenodeoxycholic acid are so-called primary bile acids. They are synthesized in the liver from cholesterol in several steps, such as introduction of one or two hydroxyl groups to the steroid unit, epimerization of the  $3\alpha$ -hydroxyl group, and subsequent oxidation of the side chain.<sup>27</sup> Deoxycholic acid and lithocholic acid are secondary bile acids, which are derived from  $7\alpha$ -dehydroxylation of the primary bile acids by colon bacteria. Bile salts are formed from the bile acids by means of conjugation with amino acids. The two amino acids that are coupled to bile acids in humans are glycine and taurine. These conjugates (also depicted in Scheme 1.6) are the actual biologically active compounds, which are stored in the gall bladder, and finally released as components of bile into the duodenum. The function of the conjugation is to lower the  $pK_a$  value and therefore increase the water solubility at the physiological pH in the duodenum (pH 6-8). Furthermore, this ionic state prevents premature absorption of these compounds through the intestine wall, and thus ensures a sufficient concentration in the intestines.<sup>28</sup>



**Scheme 1.6** Structures of bile acids (left) and bile salts (right)



The structure of bile acids does not resemble that of the classical head-tail surfactant, described in the previous paragraph. They have an ionic carboxylate group as head group. But the 'hydrophobic' part of the molecule contains a bulky steroid unit and it possesses some polar hydroxyl groups, which are all located on one side of the steroid unit. For cholic acid this is shown in Scheme 1.7. Therefore, it is also called a facial amphiphile: polar on one side, apolar on the other.



**Scheme 1.7**

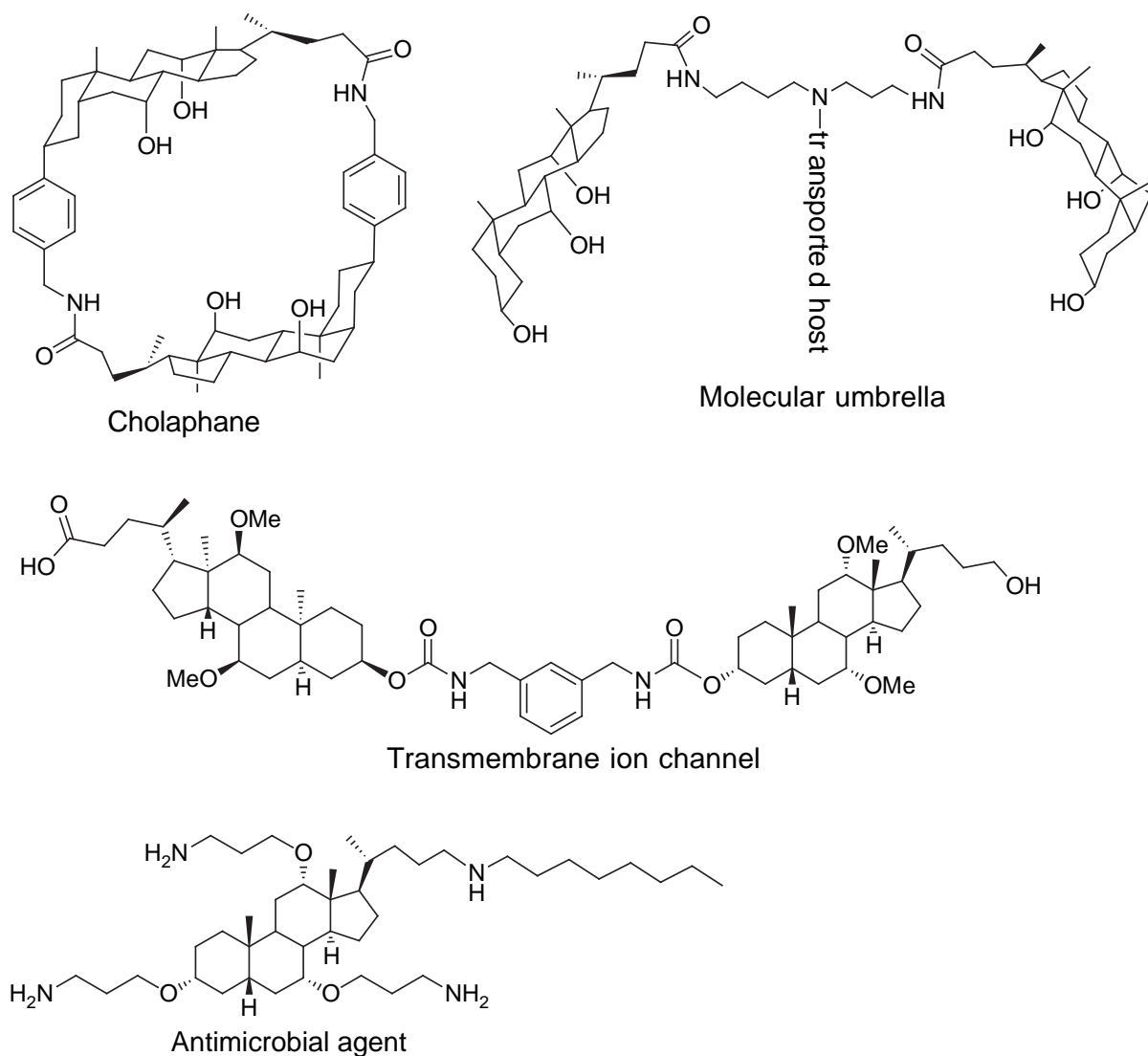
Consequently, their aggregates in water are different from classical surfactants. Small primary micelles are formed with 4 to 10 molecules in which the apolar sides of the steroid units are lying toward each other in the middle and the polar hydroxyl groups are on the outside. At high concentrations these primary micelles form larger clusters by means of hydrogen bonds between the hydroxyl groups and secondary micelles are formed.<sup>29-32</sup>

### 1.2.2 CHOLIC ACID DERIVATIVES AS FUNCTIONAL MOLECULES

Cholic acid is one of the main bile acids in mammals. It is commercially available at low cost. Furthermore, it has an unusual molecular structure with some special characteristics, such as the facial amphiphilicity. The carboxylic acid and the three hydroxyl groups can act as synthesis handles. For these reasons cholic acid is a suitable building block for new functional molecules. Various examples are described below, of which a few are shown in Scheme 1.8.

Because of the difference in steric hindrance each hydroxyl group can be derivatized individually.<sup>33</sup> Therefore cholic acid can be used as a scaffold for combinatorial chemistry<sup>34</sup> and asymmetric synthesis.<sup>35</sup> Not only the co-directed hydroxyl groups are useful for these purposes, but also the side-chain with a

carboxylic group is important since it provides an attachment point to the solid phase. The rigid steroid unit of cholic acid has a curvature, which facilitates the construction of cyclic compounds, so-called cholaphanes. These compounds are widely used as receptors for small molecules.<sup>36,37</sup> Also many other types of receptors were built from cholic acid in which usually two or more molecules were linked together to form a tweezer-type of receptor.<sup>38</sup>



**Scheme 1.8** Examples of functional cholic acid derivatives<sup>36,39,41,44</sup>

The facial amphiphilicity of the steroid unit is used in so-called molecular umbrellas.<sup>39</sup> These transport molecules can carry a polar host molecule across a bilayer membrane by shielding it from the environment with two or more cholic acid units.<sup>40</sup> Also bilayer incorporated trans-membrane channels for ion transport were

reported that are based on cholic acid. The wall of such a channel is formed by several cholic acid units, which are held together by spontaneous assembly<sup>41</sup> or by a covalently bound linker.<sup>42</sup> The hydrophilicity of the hydroxyl groups of cholic acid can be emphasized, which leads to new, micelle-forming facial amphiphiles.<sup>43</sup> A number of them display antimicrobial activity.<sup>44</sup> These compounds have nitrogen-containing groups attached to the hydroxyl groups, which permeabilize the outer bacterial membrane. A short alkyl chain at the place of the carboxylic group promotes transport through the membrane. Because of their interaction with bilayers cholic acid derived facial amphiphiles can also be used as membrane fusogens.<sup>45</sup> Other medical applications of cholic acid derivatives are as drug-delivery agents,<sup>46</sup> as transfection agents,<sup>47</sup> and as X-ray contrast agents.<sup>48</sup> In all these cases cholic acid facilitates transport of more polar molecules across the membrane bilayer by shielding them from the apolar interior. Cholic acid derivatives have been used for chiral separations, e.g. as stationary phase for HPLC<sup>49</sup> and in inclusion chemistry.<sup>50</sup> In the crystal packing of such an inclusion complex one enantiomer of, for example, a small ketone favorably fits between the antiparallel layers of head-to-tail arranged cholic acid molecules, whereas the other enantiomer remains in solution. Thermosensitive polymers containing cholic acid in the side chain have been reported<sup>51</sup> and also some cholic acid-based organogelators.<sup>52,53</sup>

### 1.3 OUTLINE OF THIS THESIS

The research that is reported in this thesis involves the synthesis of cholic acid derivatives and a study of their aggregation behavior in solution. The emphasis lies on the relation between the molecular structure and the aggregation properties of a variety of compounds. The research can be divided into two parts, based on the medium in which aggregation takes place. The first part of the thesis (chapters 2-4) deals with organogel formation in organic solvents and the last part (chapters 5-6) deals with micelle formation in aqueous solution.

In chapter 2 a series of cholic acid derivatives with  $\alpha$ -amino acid alkyl esters is presented, which act as organogelators for aromatic solvents. Variation in structure provides information about the molecular requirements for gelation. In chapter 3

alkyl derivatives of cholic acid with different connecting groups are presented as possible organogelators. The influence of the connecting group on the gelation ability is investigated. Besides these one-component organogels, a new type of two-component gel is described. For some gels described in chapters 2 and 3, a study on the network structure using small angle neutron scattering measurements is reported in chapter 4. This study provides detailed information about the type of network and its dimensions in relation to the gelator's molecular structure.

In chapter 5 a series of  $\alpha$ -amino acid derivatives of cholic acid is presented, which are derived from the compounds described in chapter 2. These compounds form micellar aggregates in water. The effect of the molecular structure on micellization behavior is investigated. In chapter 6 cholic acid derivatives with three ionic groups are presented, which are micelle forming facial amphiphiles in water. Their aggregation behavior is studied as a function of two aspects of their molecular structure. Furthermore, the thermodynamics of micellization and their antimicrobial activity are investigated.

In chapter 7 some general points are discussed and relations between the former chapters are established to provide answers for some remaining questions.

## REFERENCES AND NOTES

- 1 J.H. Fuhrop, J. Köning, *Membranes and Molecular Assemblies: the Synkinetic Approach*, The Royal Society of Chemistry - Cambridge, **1994**.
- 2 J.H. Clint, *Surfactant Aggregation*, Blackie - Glasgow/London, **1992**.
- 3 Y. Moroi, *Micelles, Theoretical and Applied Aspects*, Plenum Press - New York, **1992**.
- 4 J. Israelachvili, *Intermolecular and Surface Forces*, 2nd ed., Academic Press - London, **1991**, pp. 129-132.
- 5 D. Myers, *Surfactant Science and Technology*, 2nd ed., VCH Publishers - New York, **1992**.
- 6 P. Terech, R.G. Weiss, *Chem. Rev.* **1997**, 97, 3133-3159.
- 7 D.J. Abdallah, R.G. Weiss, *Adv. Mater.* **2000**, 12, 1237-1247.
- 8 M. de Loos, A.G.J. Ligtenbarg, J. van Esch, H. Kooijman, A.L. Spek, R. Hage, R.M. Kellogg, B.L. Feringa, *Eur. J. Org. Chem.* **2000**, 3675-3678.
- 9 U. Beginn, B. Tartsch, *Chem. Commun.* **2001**, 1924-1925.
- 10 K. Hanabusa, R. Tanaka, M. Suzuki, M. Kimura, H. Shirai, *Adv. Mater.* **1997**, 9, 1095-1097.
- 11 K. Hanabusa, M. Matsumoto, M. Kimura, A. Kakehi, H. Shirai, *J. Colloid Interface Sci.* **2000**, 224, 231-244.
- 12 N. Yamada, T. Imai, E. Koyama, *Langmuir* **2001**, 17, 961-963.
- 13 O. Gronwald, S. Shinkai, *Chem. Eur. J.* **2001**, 7, 4329-4334.
- 14 R.J.H. Hafkamp, M.C. Feiters, R.J.M. Nolte, *J. Org. Chem.* **1999**, 64, 412-426.
- 15 D.J. Abdallah, R.G. Weiss, *Langmuir* **2000**, 16, 352-355.
- 16 P. Terech, V. Schaffhauser, P. Maldavi, J.M. Guenet, *Europhys. Lett.* **1992**, 17, 515-521.
- 17 R.J.H. Hafkamp, B.P.A. Kokke, I.M. Danke, H.P.M. Geurts, A.E. Rowan, M.C. Feiters, R.J.M. Nolte, *Chem. Commun.* **1997**, 545-546.

- 18 G.M. Clavier, J.F. Brugger, H. Bouas-Laurent, J.L. Pozzo, *J. Chem. Soc., Perkin Trans. 2* **1998**, 2527-2534.
- 19 S. Tamaru, M. Nakamura, M. Takeuchi, S. Shinkai, *Org. Lett.* **2001**, 3, 3631-3634.
- 20 C. Geiger, M. Stanescu, L. Chen, D.G. Whitten, *Langmuir* **1999**, 15, 2241-2245.
- 21 N. Amanokura, Y. Kanekiyo, S. Shinkai, D.N. Reinhoudt, *J. Chem. Soc., Perkin Trans.* **1999**, 1995-2000.
- 22 J.H. van Esch, B.L. Feringa, *Angew. Chem., Int. Ed.* **2000**, 39, 2263-2266.
- 23 G. Mieden-Gundert, L. Klein, M. Fischer, F. Vögtle, K. Heuzé, J.L. Pozzo, M. Vallier, F. Fages, *Angew. Chem., Int. Ed.* **2001**, 40, 3164-3166.
- 24 S. Tamaru, M. Nakamura, M. Takeuchi, S. Shinkai, *Org. Lett.* **2001**, 3, 3631-3634.
- 25 P. Terech, *Progr. Colloid Polym. Sci.* **1996**, 102, 64-70.
- 26 P. Terech, *Ber. Bunsenges. Phys. Chem.* **1998**, 102, 1630-1643.
- 27 H. Danielsson in *The Bile Acids Vol. 2 Physiology and Metabolism*, Eds. P.P. Nair, D. Kritchevsky, Plenum Press - New York, **1973**, pp. 1-32.
- 28 J.B. Carey Jr. in *The Bile Acids, Vol. 2 Physiology and Metabolism*, Eds. P.P. Nair, D. Kritchevsky, Plenum Press - New York, **1973**, pp. 55-82.
- 29 D.M. Small in *The Bile Acids, Vol. 1 Chemistry*, Eds. P.P. Nair, D. Kritchevsky, Plenum Press - New York, **1971**, pp. 302-326.
- 30 G. Li, L.B. McGown, *J. Phys. Chem.* **1994**, 98, 13711-13719.
- 31 B.R. Simonovic, M. Momirovic, *Mikrochim. Acta* **1997**, 127, 101-104.
- 32 O. Rinco, M.H. Kleinman, C. Bohne, *Langmuir* **2001**, 17, 5781-5890.
- 33 H. Gao, J.R. Dias, *Org. Prep. Proced. Int.* **1999**, 31, 145-166.
- 34 J.F. Barry, A.P. Davis, M.N. Perez-Payan, M.R.J. Elsegood, R.F.W. Jackson, C. Gennari, U. Piarulli, M. Gude, *Tetrahedron Lett.* **1999**, 40, 2849-2852.
- 35 U. Maitra, *Current Science* **1996**, 71, 617-624.
- 36 A.P. Davis, *Chem. Soc. Rev.* **1993**, 243-253.
- 37 Y. Li, J.R. Dias, *Chem. Rev.* **1997**, 97, 283-304.
- 38 J. Tamminen, E. Kolehmainen, *Molecules* **2001**, 6, 21-64.
- 39 V. Janout, M. Lanier, S.L. Regen, *J. Am. Chem. Soc.* **1997**, 119, 640-647.
- 40 V. Janout, L. Zhang, I.V. Staina, C. Di Giorgio, S.L. Regen, *J. Am. Chem. Soc.* **2001**, 123, 5401-5406.
- 41 C. Goto, M. Yamamura, A. Satake, Y. Kobuke, *J. Am. Chem. Soc.* **2001**, 123, 12152-12159.
- 42 P. Bandyopadhyay, V. Janout, L. Zhang, S.L. Regen, *J. Am. Chem. Soc.* **2001**, 123, 7691-7696.
- 43 U. Taotafa, D.B. McMullin, S.C. Lee, L.D. Hansen, P.B. Savage, *Org. Lett.* **2000**, 2, 4117-4120.
- 44 E.J. Schmidt, J.S. Boswell, J.P. Walsh, M.M. Schellenberg, T.W. Winter, C. Li, G.W. Allman, P.B. Savage, *J. Antimicrob. Chemother.* **2001**, 47, 671-674.
- 45 Y.R. Vandenburg, B.D. Schmidt, M.N. Perez-Payan, A.P. Davis, *J. Am. Chem. Soc.* **2000**, 122, 3252-3253.
- 46 A. Kannan, E. De Clercq, C. Pannecouque, M. Witvrouw, T.L. Hartman, J.A. Turpin, R.W. Buckheit Jr., M. Cushman, *Tetrahedron* **2001**, 57, 9385-9391.
- 47 S. Walker, M.J. Sofia, R. Kakarla, N.A. Kogan, L. Wierichs, C.B. Longley, K. Bruker, H.R. Axelrod, S. Midha, S. Babu, D. Kahne, *Proc. Natl. Acad. Sci. USA* **1996**, 93, 1585-1590.
- 48 P. G. Singh, J. Klaveness, F. Rise, A.J. Aasen, *ARKIVOC* **2001**, 2, NIL\_32-NIL\_41.
- 49 L. Vaton-Chanvrier, H. Oulyadi, Y. Combret, G. Coquerel, J.C. Combret, *Chirality* **2001**, 13, 668-674.
- 50 V. Bertolasi, O. Bortolini, M. Fogagnolo, G. Fantin, P. Pedrini, *Tetrahedron Asymm.* **2001**, 12, 1479-1483.
- 51 A. Benrebouh, D. Avoce, X.X. Zhu, *Polymer* **2001**, 4031-4038.
- 52 Y. Hishikawa, K. Sada, R. Watanabe, M. Miyata, K. Hanabusa, *Chem. Lett.* **1998**, 795-796.
- 53 K. Nakano, Y. Hishikawa, K. Sada, M. Miyata, K. Hanabusa, *Chem. Lett.* **2000**, 1170-1171.



# 2

## **N-Cholyl amino acid alkyl esters: a novel class of organogelators**

*Several N-cholyl amino acid alkyl esters were found to act as novel, potent organogelators for aromatic solvents and cyclohexene. These novel organogelators afford stable, transparent, and thermoreversible gels. Modification of the molecular structure and IR-measurements show that gelation takes place by means of a hydrogen bonded network and involves at least the amide bond and several hydroxyl groups of the cholic acid component. The chiral center of the amino acid component seems to play an important role in gelation. Although a wide variety of derivatives display gelation behavior, a small change in molecular structure can have a dramatic effect on the gelling capability. Electron microscopy reveals a fibrous structure in the gels. Differential scanning calorimetry shows several transitions in the melting behavior of the gels.*

This chapter was published in *Eur. J. Org. Chem.* **2001**, 2329-2335.

## 2.1 INTRODUCTION

Research in the field of organogels has received more and more attention over the last several years, and the number of low molecular mass organogelators is rapidly growing.<sup>1-8</sup> The gelling capability of these compounds is not yet understood in detail, but one important requirement is the ability of the gelator molecules to form aggregates spontaneously, which encapsulate the solvent in a three-dimensional network. For many organogelators, the gel network consists of fibers, which in turn assemble into larger aggregates.<sup>9</sup> Aggregation of low molecular mass organogelators is usually driven by specific noncovalent intermolecular forces, such as hydrogen bond formation, metal coordination bond formation, hydrophobic interactions, dipole-dipole interactions, or van der Waals interactions. Cholesterol-based organogelators usually aggregate by means of hydrophobic or van der Waals interactions.<sup>5,10</sup> Many other low molecular mass organogelators contain strongly hydrogen bonding groups. Literature reports several organogelators containing amide and urea groups<sup>11-14</sup> and gelators based on amino acids.<sup>15-19</sup>

Generally, the gelled state can be seen as a metastable state between solution and crystallization. If a compound is moderately soluble, it will have the tendency to crystallize or precipitate upon cooling. However, if crystal packing is hampered, the occurrence of a metastable state, such as the gelled state, will be more likely. Cholic acid, one of the main bile acids, has been frequently used in crystal inclusion chemistry. With cholic acid or its derivatives as a host, inclusion crystals have been formed with small ketones, alcohols, and esters. The cholic acid molecules are arranged in stacked bilayers, providing hydrophobic, channel-like voids in which the guest molecules can be accommodated.<sup>20,21</sup> It was found by chance that one of these compounds, *N*-isopropylcholamide, produced not only inclusion crystals and guest-free crystals but also organogels, depending on the mixture of solvents used.<sup>22</sup> This example illustrates the influence of the solvent on the type of aggregate that is observed. Literature reports another example of bile acid derived organogelators: a two-component gel system mediated by electron donor-acceptor interaction and based on the bile acid backbone, with two derivatized hydroxyl groups.<sup>23</sup>

We found that several compounds in which cholic acid is coupled to an  $\alpha$ -amino acid ester act as gelators for aromatic solvents, producing transparent and

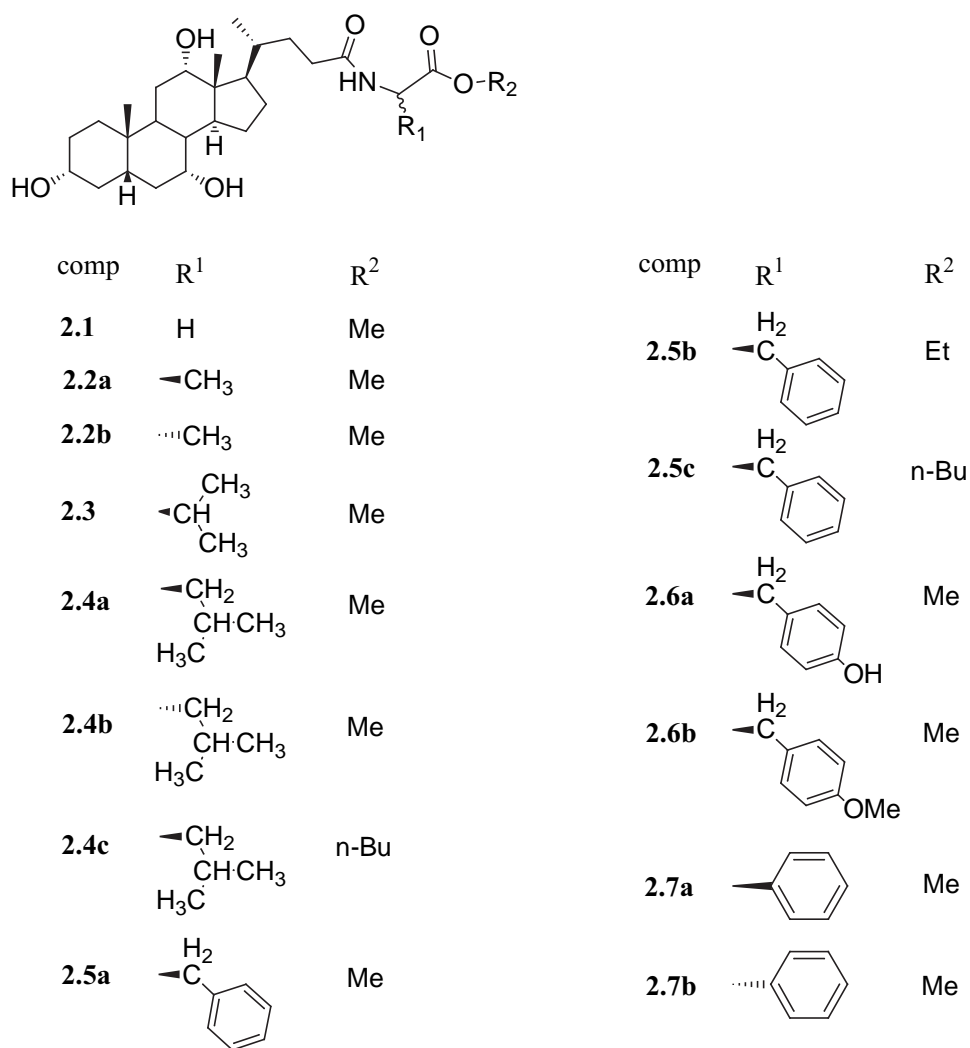


stable gels. Thus, a novel class of organogelators, composed of two natural building blocks, has been found. Structural modifications were performed in order to assess the structural elements necessary for gel formation, and infrared spectroscopy was used to study the hydrogen bond interactions in the gel. Scanning electron microscopy gave information on the fibrous structure, while the melting points and thermal behavior of all gels were measured using differential scanning calorimetry (DSC). As occasionally reported in literature,<sup>24-26</sup> DSC is an easy and precise method for investigation of the thermal behavior of organogels.

## 2.2 RESULTS AND DISCUSSION

A series of novel compounds was prepared by coupling cholic acid to  $\alpha$ -amino acid esters, with diethylphosphoryl cyanide (DEPC) as a coupling reagent,<sup>27</sup> resulting in formation of an amide bond. The compounds synthesized are shown in Scheme 2.1. Thin layer chromatography, <sup>1</sup>H NMR, and elemental analyses confirmed the structures and purities of the compounds. Most compounds were obtained as glasses ( $T_g \sim 100$  °C). Upon prolonged heating or solvation, some of the compounds slowly crystallized.

All compounds were tested for their gelling abilities in several solvents. In a typical gelation experiment, a capped test tube was filled with solvent and about 1.5 wt% of compound, and was then heated until the solid had dissolved. After cooling, gelation was checked by monitoring the disappearance of flow. In several cases, lower concentrations of gelator were sufficient. It was found that the absence of water is crucial for gelation. Adding a small drop of water or methanol to a gel caused immediate restoration of the solvent's flow and sometimes precipitation of the gelator. To obtain reproducible and stable gels, a small quantity of 4 Å molsieves was added to the gelation mixture. This observation indicates that hydrogen bonds play an important role in assembling the gel network. Given the structure of the gelators, which possess an amide bond, an ester bond, and three hydroxyl groups, this seems a reasonable assumption.



Scheme 2.1.

In benzene and toluene, a clear, transparent, and thermoreversible gel was found for most compounds. Some compounds provide transparent gels at concentrations as high as 20 wt%. The organogels have a remarkably high degree of stability towards mechanical agitation. Furthermore, they can be stored for several months at room temperature without disruption or precipitation. Several other aromatic solvents were found to be less suitable for gelation. 4-Butylbenzene, chlorobenzene, and anisole gave isotropic solutions for most compounds; only a few compounds were able to gel these solvents. The only nonaromatic solvents that were found to be capable of gel formation with these compounds were cyclohexene and cyclooctene; these gave similar results and so only those for cyclohexene are reported here. Results of the gelation experiments are summarized in Table 2.1. The melting behavior of 25 mM gels (about 1.5 wt%) in benzene, as determined using DSC, is

given in Table 2.2. Higher concentrations of gelator resulted in higher melting points, which is analogous to increasing solubility of a compound at higher temperatures.

**Table 2.1.** Gelation results of different N-cholyl amino acid alkyl esters<sup>[a]</sup>

compound	benzene	toluene	4-butyl- benzene	chloro- benzene	anisole	cyclo- hexene
<b>2.1</b>	s	n	n	p	s (p)	n
<b>2.2a</b>	g <sub>t</sub>	g <sub>t</sub>	p	s	s	p
<b>2.2b</b>	n	n	n	n	n	n
<b>2.3</b>	g <sub>t</sub>	g <sub>t</sub>	g <sub>c</sub> (p)	s (p)	s	g <sub>c</sub> (p)
<b>2.4a</b>	g <sub>t</sub>	g <sub>t</sub>	g <sub>t</sub>	g <sub>t</sub>	s	g <sub>t</sub>
<b>2.4b</b>	g <sub>t</sub>	g <sub>t</sub>	g <sub>t</sub>	g <sub>t</sub>	g <sub>t</sub>	g <sub>t</sub>
<b>2.4c</b>	g <sub>t</sub>	g <sub>t</sub>	g <sub>t</sub>	s	s	g <sub>t</sub>
<b>2.5a</b>	g <sub>t</sub>	g <sub>t</sub>	g <sub>t</sub>	s	s	g <sub>t</sub> (g <sub>c</sub> )
<b>2.5b</b>	g <sub>t</sub> (g <sub>c</sub> )	g <sub>t</sub> (g <sub>c</sub> )	g <sub>t</sub> (g <sub>c</sub> )	s (p)	s	g <sub>t</sub> (g <sub>c</sub> )
<b>2.5c</b>	g <sub>t</sub>	g <sub>t</sub>	g <sub>t</sub>	s	s	g <sub>t</sub>
<b>2.6a</b>	n	n	n	n	n	n
<b>2.6b</b>	g <sub>t</sub>	g <sub>t</sub>	g <sub>c</sub> (p)	s	s	p
<b>2.7a</b>	n	n	n	n	n	n
<b>2.7b</b>	n	n	n	n	n	n
<b>2.8</b>	s	s	s	s	s	p
<b>2.9</b>	s (p)	s (p)	s (p)	s	s	p
<b>2.10</b>	p	s (p)	n	s	s	n

<sup>[a]</sup> g<sub>t</sub> = transparent gel; g<sub>c</sub> = cloudy gel; s = soluble; n = not soluble; p = precipitation; observation was made immediately after cooling, changes after 24 h in parentheses

Compound **2.1** showed no gelling behavior, but was moderately soluble in benzene. This result is intriguing, because compounds **2.2a**, **2.3** and **2.4a** with small, apolar tails in the amino acid, gave stable gels in benzene, with similar melting points. Comparison of compound **2.1** with compound **2.2a** shows that the former lacks only a methyl group. One explanation for this phenomenon is that the presence of an alkyl group at this position results in lower solubility and therefore gelation. Another explanation could be that an asymmetric group next to the amide bond is essential for gelation of these types of compounds.

**Table 2.2.** Melting behavior of 25 mM gels in benzene<sup>[a]</sup>

compound	pre-melting transitions (°C)		mpt (°C)
<b>2.2a</b>		49 (b)	53
<b>2.3</b>		40 (b)	42
<b>2.4a</b>		40 (b)	43
<b>2.4b</b>		54 (b)	56
<b>2.4c</b>		32 (b)	33
<b>2.5a</b>	30 (b)	42 (b)	46
<b>2.5b</b>		26 (b)	27
<b>2.5c</b>	25 (bs)	32 (b)	33
<b>2.6b</b>	35 (b)	43 (b)	48

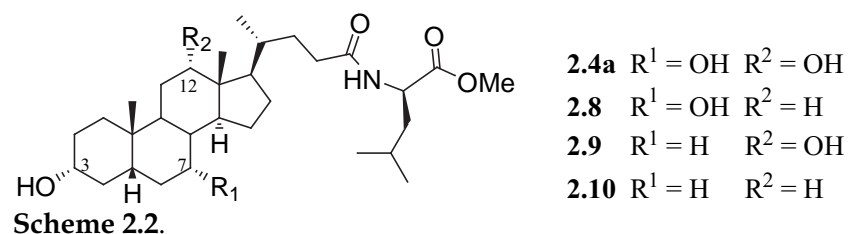
<sup>[a]</sup> b = broad peak, bs = broad shoulder; determined using DSC, heating rate 0.5 °C/min

To study the influence of the chiral center at the amino acid  $\alpha$ -carbon atom, compounds **2.2b** and **2.4b** (D-isomers) were synthesized and their gelling ability was compared to that of compounds **2.2a** and **2.4a** (L-isomers). It was found that compound **2.2b** was insoluble in benzene and in the other solvents and gave no gelation. This is probably connected with the fact that this compound was directly obtained in a crystalline state, whereas other compounds were obtained as glasses. Compound **2.4b** was soluble in warm benzene and gave gelation upon cooling. Interestingly, the melting point of the gel with compound **2.4b** was 13 °C higher than that with compound **2.4a**. However, when heated in benzene for a longer period, precipitation of compound **2.4b** in the crystalline state occurred, after which it was insoluble. Furthermore, compound **2.4b** produced a gel in anisole, whereas compound **2.4a** did not. These findings indicate a crucial role for the chiral center at the amino acid  $\alpha$ -carbon. Similar results were recently reported for another class of chiral organogelators.<sup>28</sup>

Introduction of a phenyl group into the amino acid component of the molecule seems to have little effect on the gelling ability. Compound **2.5a** in benzene afforded a stable, transparent gel similar to those produced by compounds **2.2a**, **2.3** and **2.4**. The tyrosine derivative **2.6a** showed no gelling behavior: this compound was

insoluble in benzene. However, compound **2.6b**, which was prepared from compound **2.6a** by methylation of the hydroxyl group, proved to be a potent gelator for benzene. Apparently compound **2.6a** is too polar to dissolve in benzene, even at high temperature. Compounds **2.7a** and **2.7b** were not soluble in the tested solvents and did not form any gels. This lack of gelation is comparable to the case of compound **2.2b**, since compound **2.7a** was also obtained in a crystalline state and compound **2.7b** easily crystallized in solution.

For the behavior of compounds **2.4c**, **2.5b**, and **2.5c**, with alkyl ester groups longer than methyl moieties, no clear trend was observed. The ethyl ester derivative, compound **2.5b**, was a poor gelator for many solvents. In most cases a gel was initially formed, but was not stable. Within one day the gelator had precipitated, indicating that for this compound the energetically more favorable crystalline state is easily reached. On the other hand, the butyl ester derivatives **2.4c** and **2.5c** gave stable gels in the same solvents as had the corresponding methyl ester derivatives, although the melting points of gels of the butyl esters were about 10 °C lower than those of the methyl esters.



In view of the supposed importance of hydrogen bond formation in the production of the gel network, the question arises whether all hydroxyl groups of the cholic acid component are required for gelation to take place. In order to investigate this, compounds **2.8**, **2.9**, and **2.10** were prepared (see Scheme 2.2). These compounds are also based on natural bile acids: chenodeoxycholic acid, deoxycholic acid, and lithocholic acid, respectively. All of them lack one or two hydroxyl groups at the 7 and 12 positions, compared to cholic acid. Compounds **2.8-2.10** did not form gels in any of the tested solvents; these results are also summarized in Table 2.1. Apparently, the hydroxyl groups at the 7 and 12 positions are both needed to build

the hydrogen bonded gel network. This is an important difference from cholesterol-based organogelators, since the cholesterol skeleton lacks both hydroxyl groups.

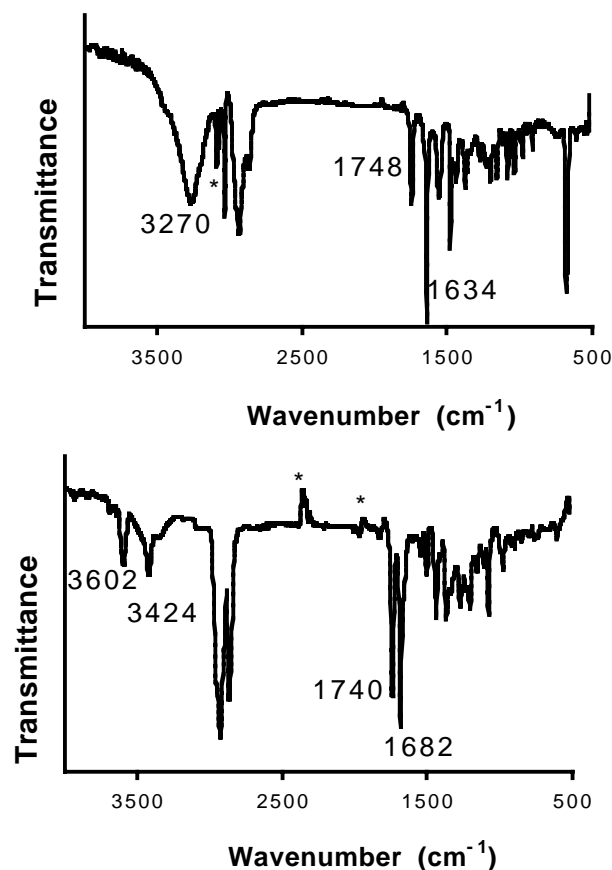


**Figure 2.1.** FT-IR spectra of compounds **2.4b** (top) and **2.8** (bottom) in benzene; \* = residual solvent peak

The presence of hydrogen bonds in the gels was further investigated with FT-IR measurements. IR-spectra of gels in benzene were recorded for compounds **2.3**, **2.4b** and **2.6b**. Compounds **2.1** and **2.8** were measured as solutions in benzene. Typical spectra are shown in Figure 2.1 and the relevant data are listed in Table 2.3. All compounds showed two strong and sharp carbonyl signals. The signal from the ester carbonyl group was found at about 1745 cm<sup>-1</sup> in all cases. The signal from the amide carbonyl group gave different values: about 1634 cm<sup>-1</sup> for gelating compounds and about 1682 cm<sup>-1</sup> for nongelating compounds. These values agree with literature values for amides in the solid and dissolved state, respectively. Intermolecular hydrogen bonding of amides causes a marked decrease in the amide carbonyl stretching frequency.<sup>29</sup> Another difference between the spectra of the gelating and nongelating compounds was seen in the O-H and N-H stretch signals. For the gels,

one broad signal around  $3270\text{ cm}^{-1}$  was found, which points to a hydrogen bonded N-H. This peak had a shoulder between  $3450$  and  $3500\text{ cm}^{-1}$ , which is in the range for hydrogen bonded hydroxyl groups. The nongelating compounds gave two sharp peaks at about  $3602$  and  $3424\text{ cm}^{-1}$ , indicative of dissolved O-H and N-H groups, not involved in hydrogen bonding.

**Table 2.3.** FT-IR data for several gelating and nongelating compounds in benzene<sup>[a]</sup>

compound	state	$\nu$ OH/NH ( $\text{cm}^{-1}$ )	$\nu$ C=O ester ( $\text{cm}^{-1}$ )	$\nu$ C=O amide ( $\text{cm}^{-1}$ )
<b>2.3</b>	gel	3265 (b)	1746	1636
<b>2.4b</b>	gel	3270 (b)	1748	1634
<b>2.6b</b>	gel	3270 (b)	1746	1636
<b>2.1</b>	solution	3580 (s)/3400 (s)	1750	1686
<b>2.8</b>	solution	3602 (s)/3424 (s)	1740	1682

[a] b = broad peak, s = sharp peak

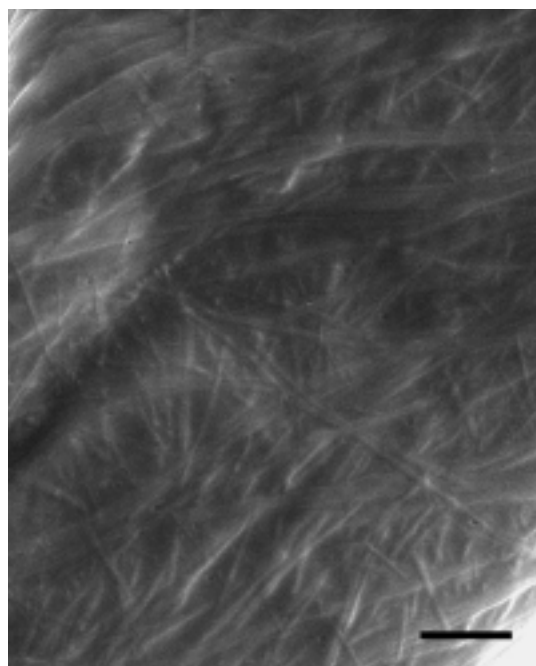


**Figure 2.2.** SEM-image of a 25 mM gel of compound **2.4b** in benzene; bar indicates  $1\text{ }\mu\text{m}$

Scanning electron microscopy (SEM) of a 25 mM gel of compound **2.4b** in benzene showed fibers with a diameter of about 50 nm and a length of several  $\mu\text{m}$ , as can be seen in Figure 2.2. No helical shape is visible within the fibers. Occasionally, several single fibers seem to aggregate in a bundle, with a parallel arrangement.

DSC measurements on the thermoreversible benzene gels showed several transitions in the heating curves. For gels produced with compounds **2.2a**, **2.3**, and **2.4**, two endothermic transition peaks were found: a broad one at lower temperature and a sharp one at higher temperature. For gels with the aromatic amino acid compounds **2.5a**, **2.5c**, and **2.6b**, three endothermic transition peaks were found: a second broad peak appeared at low temperature. Typical thermograms of both kinds of compounds are shown in Figure 2.3. The melting points of the gels (defined as the temperature above which macroscopic flow appears) were also determined by visually monitoring the flow of the gels in a thermally controlled bath. If these values are compared to the DSC thermograms, it can be concluded that the sharp transition peak in the thermogram corresponds with the actual melting of the gel. At the temperatures of the broad transitions, there was no visual change in the gels at macroscopic level. An explanation for the appearance of these pre-melting transitions is partial melting of the gelator network. It can be imagined that an assembly of fibers is broken down upon heating, prior to complete disintegration of the single fibers.

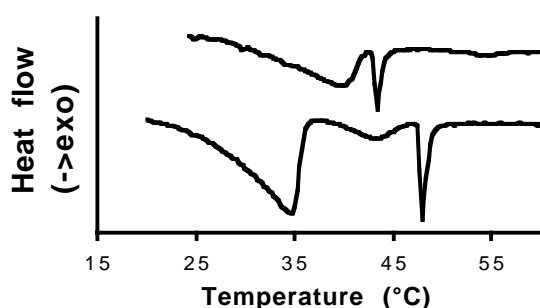


**Figure 2.3.** Heating curves of 25 mM gels of compounds **2.4a** (top) and **2.6b** (bottom) in benzene; heating rate 0.5 °C/min

## 2.3 CONCLUSIONS

A variety of *N*-cholyl  $\alpha$ -amino acid alkyl esters were found to behave as novel organogelators, forming stable, transparent, and thermoreversible gels in aromatic solvents. Gelation was only observed for compounds that did not crystallize easily and takes place through a network of fibers of about 50 nm thickness. Molecular requirements for gelation are the amide bond and several hydroxyl groups of the



cholic acid component, since these groups are responsible for the hydrogen bonded aggregation within the fibers. There are indications that chirality also plays a role in the aggregation of these novel organogelators. It was found that a small difference in structure can have a large influence on the gelling capability; it is assumed that in these cases a change in structure leads to a change in packing of the molecules. The gels go through one or two pre-melting transitions before actual melting takes place, indicating a partial melting of the network upon heating.

## 2.4 EXPERIMENTAL SECTION

**General Remarks:**  $^1\text{H}$ -NMR spectra (200 MHz) were recorded on a Bruker AC200 spectrometer at ambient temperature. - Melting points were measured using an Olympus BH-2 microscope with a Mettler FP82HT hot stage and a FP80HT temperature controller. - Elemental analyses were performed with an Elemental Analyzer EMASyst1106. - FT-IR spectra were recorded on a BIO-RAD FTS-7 spectrophotometer with a resolution of  $4\text{ cm}^{-1}$ . Compounds were measured as a solid in KBr or as a solution or a gel in benzene. - For SEM, drops of gel were air-dried on Carbon adhesive taps (Electron Microscopy Sciences, Washington), that were mounted on specimen stubs. Specimen were placed in a dedicated preparation chamber (CT 1500 HF, Oxford Instruments), sputtercoated with Pt, 10 nm. Samples were analyzed on the SEM (JSM 6300 F, Jeol Japan) at ambient temperature and images were digitally recorded. - DSC thermograms were recorded on a Setaram micro-DSC III. Approximately 500 mg of a 25 mM solution of gelator in benzene above the gel melting temperature was brought into a metal, screw-capped cup and was allowed to cool to room temperature thus forming a gel. A reference cup contained the same amount of benzene. Two heating and cooling cycles were recorded with a rate of  $1\text{ }^\circ\text{C}/\text{min}$  and  $0.5\text{ }^\circ\text{C}/\text{min}$ , respectively, and the second heating curves were compared. This procedure assured that gels were formed under reproducible conditions.

**Synthesis:** Used solvents were of p.a. quality. The different bile acids were purchased, as were glycine methyl ester hydrochloride, L-leucine methyl ester hydrochloride, L-phenylalanine ethyl ester hydrochloride, L-tyrosine methyl ester hydrochloride, and diethylphosphoryl cyanide (DEPC). L-valine methyl ester hydrochloride, D-leucine methyl ester hydrochloride, and L-phenylalanine methyl ester hydrochloride were prepared by adding the amino acids to a cold solution of thionyl chloride in methanol.<sup>30</sup> Acid-catalysed

esterification of L-leucine to 1-butanol was described before.<sup>31</sup> The purity of the products was verified with NMR, TLC and elemental analysis.

**General procedure for the synthesis of *N*-cholyl amino acid alkyl esters:** 2.05 g of cholic acid (5.0 mmol) and 5.0 mmol of the appropriate  $\alpha$ -amino acid alkyl ester were dissolved in 35 ml dry *N,N*-dimethylformamide. After cooling to 0°C 0.825 ml (5.5 mmol) DEPC was added. An excess of triethylamine (3.5 ml) was gradually added during a period of 10 minutes. The mixture was stirred at 0°C for 45 minutes and subsequently at room temperature for 24 hours. Afterwards the triethylammonium salt was filtered off and DMF and triethylamine were evaporated in vacuum. The residue was purified by flash column chromatography on silica using dichloromethane:methanol (95:5) as an eluent. Evaporation of the product-containing fractions in vacuum gave a white solid, generally in about 70% yield.

***N*-Cholyl glycine methyl ester (2.1):** <sup>1</sup>H-NMR: (CDCl<sub>3</sub>)  $\delta$  = 6.27 (bt, 1H, NH); 4.03 (d, 2H, CH<sub>2</sub>); 3.97 (bs, 1H, 12 $\alpha$ -CH); 3.83 (bs, 1H, 7 $\alpha$ -CH); 3.75 (s, 3H, OCH<sub>3</sub>); 3.48 (m, 1H, 3 $\alpha$ -CH); 2.32-1.02 (m, 24H, aliphatic H); 0.99 (d, 3H, 21-CH<sub>3</sub>); 0.88 (s, 3H, 19-CH<sub>3</sub>); 0.67 (s, 3H, 18-CH<sub>3</sub>). IR: (KBr)  $\nu$  = 3421, 2929, 2861, 1744, 1654, 1540. Anal. calcd for C<sub>27</sub>H<sub>45</sub>NO<sub>6</sub>·0.9H<sub>2</sub>O: C 65.4, H 9.51, N 2.83; found C 65.37, H 9.76, N 2.85.

***N*-Cholyl L-alanine methyl ester (2.2a):** <sup>1</sup>H-NMR: (CDCl<sub>3</sub>)  $\delta$  = 6.41 (bd, 1H, NH); 4.57 (m, 1H, C<sup>\*</sup>H); 3.97 (bs, 1H, 12 $\alpha$ -CH); 3.84 (bs, 1H, 7 $\alpha$ -CH); 3.73 (s, 3H, OCH<sub>3</sub>); 3.46 (m, 1H, 3 $\alpha$ -CH); 2.28-1.05 (m, 27H, aliphatic H); 0.98 (d, 3H, 21-CH<sub>3</sub>); 0.87 (s, 3H, 19-CH<sub>3</sub>); 0.67 (s, 3H, 18-CH<sub>3</sub>). IR: (KBr)  $\nu$  = 3388, 2935, 2867, 1743, 1650, 1540. Anal. calcd for C<sub>28</sub>H<sub>47</sub>NO<sub>6</sub>·0.7H<sub>2</sub>O: C 66.42, H 9.64, N 2.77; found C 66.35, H 9.97, N 2.76.

***N*-Cholyl D-alanine methyl ester (2.2b):** <sup>1</sup>H-NMR: (CDCl<sub>3</sub>)  $\delta$  = 6.60 (bs, 1H, NH); 4.58 (m, 1H, C<sup>\*</sup>H); 3.98 (bs, 1H, 12 $\alpha$ -CH); 3.84 (bs, 1H, 7 $\alpha$ -CH); 3.73 (s, 3H, OCH<sub>3</sub>); 3.45 (m, 1H, 3 $\alpha$ -CH); 2.26-1.09 (m, 27H, aliphatic H); 0.98 (d, 3H, 21-CH<sub>3</sub>); 0.87 (s, 3H, 19-CH<sub>3</sub>); 0.67 (s, 3H, 18-CH<sub>3</sub>). IR: (KBr)  $\nu$  = 3448, 3364, 2937, 2868, 1758, 1641, 1544. HMRS calcd for C<sub>28</sub>H<sub>47</sub>NO<sub>6</sub> (M<sup>+</sup>): 493.3403; found 493.3403.

***N*-Cholyl L-valine methyl ester (2.3):** <sup>1</sup>H-NMR: (CDCl<sub>3</sub>)  $\delta$  = 6.06 (bd, 1H, NH); 4.55 (dd, 1H, C<sup>\*</sup>H); 3.98 (bs, 1H, 12 $\alpha$ -CH); 3.84 (bs, 1H, 7 $\alpha$ -CH); 3.73 (s, 3H, OCH<sub>3</sub>); 3.48 (m, 1H, 3 $\alpha$ -CH); 2.30-1.03 (m, 25H, aliphatic H); 0.99 (d, 3H, 21-CH<sub>3</sub>); 0.93 (d, 6H, 2 Val-CH<sub>3</sub>); 0.88 (s, 3H, 19-CH<sub>3</sub>); 0.68 (s, 3H, 18-CH<sub>3</sub>). IR: (KBr)  $\nu$  = 3428, 2934, 2861, 1739, 1656, 1536. Anal. calcd for C<sub>30</sub>H<sub>51</sub>NO<sub>6</sub>·0.7H<sub>2</sub>O: C 67.43, H 9.89, N 2.62; found C 67.35, H 10.10, N 2.72.

***N*-Cholyl L-leucine methyl ester (2.4a):** <sup>1</sup>H-NMR: (CDCl<sub>3</sub>)  $\delta$  = 6.06 (bd, 1H, NH); 4.55 (dd, 1H, C<sup>\*</sup>H); 3.98 (bs, 1H, 12 $\alpha$ -CH); 3.84 (bs, 1H, 7 $\alpha$ -CH); 3.73 (s, 3H, OCH<sub>3</sub>); 3.48 (m, 1H, 3 $\alpha$ -CH); 2.30-1.04 (m, 27H, aliphatic H); 0.99 (d, 3H, 21-CH<sub>3</sub>); 0.93 (d, 6H, 2 Leu-CH<sub>3</sub>); 0.88 (s, 3H,

19-CH<sub>3</sub>); 0.68 (s, 3H, 18-CH<sub>3</sub>). IR: (KBr)  $\nu$  = 3418, 2948, 2869, 1740, 1655, 1545. Anal. calcd for C<sub>31</sub>H<sub>53</sub>NO<sub>6</sub>·H<sub>2</sub>O: C 67.23, H 10.01, N 2.53; found C 67.33, H 10.35, N 2.86.

**N-Cholyl D-leucine methyl ester (2.4b):** <sup>1</sup>H-NMR: (CDCl<sub>3</sub>)  $\delta$  = 6.42 (bs, 1H, NH); 4.63 (m, 1H, C<sup>\*</sup>H); 3.98 (bs, 1H, 12 $\alpha$ -CH); 3.85 (bs, 1H, 7 $\alpha$ -CH); 3.71 (s, 3H, OCH<sub>3</sub>); 3.48 (m, 1H, 3 $\alpha$ -CH); 2.27-1.02 (m, 27H, aliphatic H); 0.98 (d, 3H, 21-CH<sub>3</sub>); 0.92 (d, 6H, 2 Leu-CH<sub>3</sub>); 0.88 (s, 3H, 19-CH<sub>3</sub>); 0.67 (s, 3H, 18-CH<sub>3</sub>). IR: (KBr)  $\nu$  = 3397, 2948, 2869, 1744, 1655, 1540. Anal. calcd for C<sub>31</sub>H<sub>53</sub>NO<sub>6</sub>·0.7H<sub>2</sub>O: C 67.90, H 10.00, N 2.55; found C 67.90, H 10.29, N 2.67.

**N-Cholyl L-leucine *n*-butyl ester (2.4c):** <sup>1</sup>H-NMR: (CDCl<sub>3</sub>)  $\delta$  = 6.18 (d, 1H, NH); 4.62 (m, 1H, C<sup>\*</sup>H); 4.10 (t, 2H, OCH<sub>2</sub>); 3.97 (bs, 1H, 12 $\alpha$ -CH); 3.84 (bs, 1H, 7 $\alpha$ -CH); 3.45 (m, 1H, 3 $\alpha$ -CH); 2.30-1.03 (m, 31H, aliphatic H); 0.99-0.87 (m, 15H, 5 CH<sub>3</sub>); 0.66 (s, 3H, 18-CH<sub>3</sub>). IR: (KBr)  $\nu$  = 3388, 2958, 2870, 1739, 1656, 1544. Anal. calcd for C<sub>34</sub>H<sub>59</sub>NO<sub>6</sub>·0.5H<sub>2</sub>O: C 69.58, H 10.31, N 2.39; found C 69.64, H 10.63, N 2.53.

**N-Cholyl L-phenylalanine methyl ester (2.5a):** <sup>1</sup>H-NMR: (CDCl<sub>3</sub>)  $\delta$  = 7.25 (m, 3H, aromatic H); 7.08 (m, 2H, aromatic H); 6.07 (bd, 1H, NH); 4.87 (m, 1H, C<sup>\*</sup>H); 3.95 (bs, 1H, 12 $\alpha$ -CH); 3.83 (bs, 1H, 7 $\alpha$ -CH); 3.71 (s, 3H, OCH<sub>3</sub>); 3.43 (m, 1H, 3 $\alpha$ -CH); 3.10 (m, 2H, CH<sub>2</sub>-Ph); 2.36-1.05 (m, 24H, aliphatic H); 0.95 (d, 3H, 21-CH<sub>3</sub>); 0.87 (s, 3H, 19-CH<sub>3</sub>); 0.65 (s, 3H, 18-CH<sub>3</sub>). IR: (KBr)  $\nu$  = 3407, 3033, 2933, 2867, 1741, 1650, 1536. Anal. calcd for C<sub>34</sub>H<sub>51</sub>NO<sub>6</sub>·1.1H<sub>2</sub>O: C 69.26, H 9.10, N 2.38; found C 69.18, H 9.08, N 2.50.

**N-Cholyl L-phenylalanine ethyl ester (2.5b):** <sup>1</sup>H-NMR: (CDCl<sub>3</sub>)  $\delta$  = 7.25 (m, 3H, aromatic H); 7.09 (m, 2H, aromatic H); 6.07 (bd, 1H, NH); 4.85 (m, 1H, C<sup>\*</sup>H); 4.15 (q, 2H, OCH<sub>2</sub>); 3.94 (bs, 1H, 12 $\alpha$ -CH); 3.82 (bs, 1H, 7 $\alpha$ -CH); 3.43 (m, 1H, 3 $\alpha$ -CH); 3.09 (m, 2H, CH<sub>2</sub>-Ph); 2.33-1.02 (m, 27H, aliphatic H); 0.95 (d, 3H, 21-CH<sub>3</sub>); 0.87 (s, 3H, 19-CH<sub>3</sub>); 0.65 (s, 3H, 18-CH<sub>3</sub>). IR: (KBr)  $\nu$  = 3407, 3027, 2932, 2861, 1737, 1655, 1530. Anal. calcd for C<sub>35</sub>H<sub>53</sub>NO<sub>6</sub>·0.6H<sub>2</sub>O: C 70.70, H 9.19, N 2.36; found C 70.74, H 9.35, N 2.57.

L-Phenylalanine *n*-butyl ester hydrochloride: 3.30 g (20 mmol) of L-phenylalanine was dissolved in 15 ml 1-butanol and heated to 80°C. 1.5 ml of 37% hydrochloric acid was added and the mixture was stirred overnight. After evaporation of the solvent in vacuum, the residue was dissolved in a small amount of methanol and precipitated with ether to give 2.96 g (11.5 mmol, 57%) of a white powder. <sup>1</sup>H-NMR: (CDCl<sub>3</sub>)  $\delta$  = 8.75 (bs, 2H, NH<sub>2</sub>); 7.29 (m, 5H, aromatic H); 4.36 (m, 1H, C<sup>\*</sup>H); 4.08 (t, 2H, OCH<sub>2</sub>); 3.41 (m, 2H, CH<sub>2</sub>-C<sup>\*</sup>); 1.49 (q, 2H, CH<sub>2</sub>); 1.22 (q, 2H, CH<sub>2</sub>); 0.85 (t, 3H, CH<sub>3</sub>). HRMS calcd for C<sub>13</sub>H<sub>20</sub>NO<sub>2</sub>Cl: (M<sup>+</sup> - 36) 221.1416; found 221.1419.

**N-Cholyl L-phenylalanine *n*-butyl ester (2.5c):** <sup>1</sup>H-NMR: (CDCl<sub>3</sub>)  $\delta$  = 7.26 (m, 3H, aromatic H); 7.09 (m, 2H, aromatic H); 6.03 (d, 1H, NH); 4.86 (m, 1H, C<sup>\*</sup>H); 4.19 (t, 2H, OCH<sub>2</sub>); 3.96 (bs, 1H, 12 $\alpha$ -CH); 3.83 (bs, 1H, 7 $\alpha$ -CH); 3.43 (m, 1H, 3 $\alpha$ -CH); 3.09 (m, 2H, CH<sub>2</sub>-Ph); 2.31-1.02 (m,

28H, aliphatic H); 0.96-0.87 (m, 9H, 3 CH<sub>3</sub>); 0.66 (s, 3H, 18-CH<sub>3</sub>). IR: (KBr)  $\nu$  = 3403, 3027, 2933, 2869, 1737, 1650, 1536. Anal. calcd for C<sub>37</sub>H<sub>57</sub>NO<sub>6</sub>·0.5H<sub>2</sub>O: C 71.58, H 9.42, N 2.26; found C 71.61, H 9.61, N 2.48.

**N-Cholyl L-tyrosine methyl ester (2.6a):** <sup>1</sup>H-NMR: (CDCl<sub>3</sub>/CD<sub>3</sub>OD)  $\delta$  = 6.88 (m, 2H, aromatic H); 6.69 (m, 2H, aromatic H); 6.34 (bd, 1H, NH); 4.74 (m, 1H, C\*H); 3.89 (bs, 1H, 12 $\alpha$ -CH); 3.79 (bs, 1H, 7 $\alpha$ -CH); 3.69 (s, 3H, OCH<sub>3</sub>); 3.35 (m, 1H, 3 $\alpha$ -CH); 3.06 (m, 2H, CH<sub>2</sub>-Ph); 2.60-1.01 (m, 24H, aliphatic H); 0.88 (d, 3H, 21-CH<sub>3</sub>); 0.84 (s, 3H, 19-CH<sub>3</sub>); 0.61 (s, 3H, 18-CH<sub>3</sub>). <sup>13</sup>C-NMR: (CDCl<sub>3</sub>/CD<sub>3</sub>OD)  $\delta$  = 174.1 (s); 172.6 (s); 155.8 (s); 130.3(d); 126.7(s); 115.6(d); 73.3(d); 71.9(d); 68.5(d); 52.9(d); 52.4(q); 46.5(d); 46.2(s); 45.8(t); 41.6(d); 41.4(d); 39.3(d); 36.9(t); 36.7(s); 35.4(d); 34.7(t); 32.9(t); 31.8(t); 30.2(t); 28.0(t); 27.5(t); 26.3(d); 23.2(t); 22.4(q); 17.2(q); 12.4(q). IR: (KBr)  $\nu$  = 3397, 3030, 2931, 2861, 1741, 1646, 1517.

**N-Cholyl 4-methoxyphenylalanine methyl ester (2.6b):** 0.30 g (0.48 mmol) of compound 2.6a was dissolved in 15 ml butanone and 0.5 g of methyl iodide and 0.5 g of potassium carbonate were added. After refluxing the mixture overnight butanone was evaporated in vacuum. Dichloromethane was added and the salts were filtered off. After evaporation of the solvent in vacuum, the crude product was purified with flash column chromatography on silica gel using dichloromethane:methanol (95:5) as an eluent, affording 0.28 g (0.40 mmol, 92%) of a white solid. <sup>1</sup>H-NMR: (CDCl<sub>3</sub>)  $\delta$  = 7.00 (m, 2H, aromatic H); 6.81 (m, 2H, aromatic H); 5.96 (bd, 1H, NH); 4.83 (q, 1H, C\*H); 3.96 (bs, 1H, 12 $\alpha$ -CH); 3.84 (m, 1H, 7 $\alpha$ -CH); 3.77 (s, 3H, OCH<sub>3</sub>); 3.71 (s, 3H, OCH<sub>3</sub>); 3.44 (m, 1H, 3 $\alpha$ -CH); 3.04 (m, 2H, CH<sub>2</sub>-Ph); 2.24-1.25 (m, 24H, aliphatic H); 0.95 (d, 3H, 21-CH<sub>3</sub>); 0.88 (s, 3H, 19-CH<sub>3</sub>); 0.66 (s, 3H, 18-CH<sub>3</sub>). IR: (KBr)  $\nu$  = 3423, 3040, 2930, 2857, 1740, 1661, 1513. Anal. calcd for C<sub>35</sub>H<sub>53</sub>NO<sub>7</sub>·0.5H<sub>2</sub>O: C 69.05, H 8.94, N 2.30; found C 69.09, H 9.19, N 2.37.

**N-Cholyl L-phenylglycine methyl ester (2.7a):** <sup>1</sup>H-NMR: (CDCl<sub>3</sub>)  $\delta$  = 7.35 (m, 5H, aromatic H); 6.80 (m, 1H, NH); 5.58 (s, 1H, C\*H); 3.95 (bs, 1H, 12 $\alpha$ -CH); 3.84 (bs, 1H, 7 $\alpha$ -CH); 3.73 (s, 3H, OCH<sub>3</sub>); 3.42 (m, 1H, 3 $\alpha$ -CH); 2.39-1.05 (m, 24H, aliphatic H); 0.98 (d, 3H, 21-CH<sub>3</sub>); 0.88 (s, 3H, 19-CH<sub>3</sub>); 0.66 (s, 3H, 18-CH<sub>3</sub>). IR: (KBr)  $\nu$  = 3449, 3293, 3033, 2930, 2866, 1758, 1659, 1531. Anal. calcd for C<sub>33</sub>H<sub>49</sub>NO<sub>6</sub>·0.5H<sub>2</sub>O: C 70.18, H 8.92, N 2.48; found C 70.20, H 8.86, N 2.27.

**N-Cholyl D-phenylglycine methyl ester (2.7b):** <sup>1</sup>H-NMR: (CDCl<sub>3</sub>)  $\delta$  = 7.35 (m, 5H, aromatic H); 6.78 (d, 1H, NH); 5.59 (d, 1H, C\*H); 3.95 (bs, 1H, 12 $\alpha$ -CH); 3.83 (bs, 1H, 7 $\alpha$ -CH); 3.72 (s, 3H, OCH<sub>3</sub>); 3.43 (m, 1H, 3 $\alpha$ -CH); 2.38-1.03 (m, 24H, aliphatic H); 0.97 (d, 3H, 21-CH<sub>3</sub>); 0.88 (s, 3H, 19-CH<sub>3</sub>); 0.64 (s, 3H, 18-CH<sub>3</sub>). IR: (KBr)  $\nu$  = 3417, 3033, 2933, 2861, 1745, 1657, 1529. Anal. calcd for C<sub>33</sub>H<sub>49</sub>NO<sub>6</sub>·H<sub>2</sub>O: C 69.08, H 8.96, N 2.44; found C 69.23, H 9.11, N 2.42.

**N-Chenodeoxycholyl L-leucine methyl ester (2.8):** <sup>1</sup>H-NMR: (CDCl<sub>3</sub>)  $\delta$  = 5.92 (bd, 1H, NH); 4.66 (m, 1H, C\*H); 3.86 (bs, 1H, 7 $\alpha$ -CH); 3.73 (s, 3H, OCH<sub>3</sub>); 3.49 (m, 1H, 3 $\alpha$ -CH); 2.35-1.12

(m, 29H, aliphatic H); 0.94 (m, 9H, 21-CH<sub>3</sub> + 2 Leu-CH<sub>3</sub>); 0.90 (s, 3H, 19-CH<sub>3</sub>); 0.66 (s, 3H, 18-CH<sub>3</sub>). IR: (KBr)  $\nu$  = 3385, 2931, 2868, 1745, 1655, 1544. Anal. calcd for C<sub>31</sub>H<sub>53</sub>NO<sub>5</sub>·0.2H<sub>2</sub>O: C 71.14, H 10.29, N 2.68; found C 71.12, H 10.54, N 2.77.

**N-Deoxycholyl L-leucine methyl ester (2.9):** <sup>1</sup>H-NMR: (CDCl<sub>3</sub>)  $\delta$  = 6.02 (bd, 1H, NH); 4.66 (m, 1H, C<sup>\*</sup>H); 3.99 (bs, 1H, 12 $\alpha$ -CH); 3.73 (s, 3H, OCH<sub>3</sub>); 3.64 (m, 1H, 3 $\alpha$ -CH); 2.32-1.10 (m, 29H, aliphatic H); 0.96 (d, 3H, 21-CH<sub>3</sub>); 0.92 (d, 6H, 2 Leu-CH<sub>3</sub>); 0.87 (s, 3H, 19-CH<sub>3</sub>); 0.68 (s, 3H, 18-CH<sub>3</sub>). IR: (KBr)  $\nu$  = 3394, 2938, 2866, 1744, 1650, 1540. Anal. calcd for C<sub>31</sub>H<sub>53</sub>NO<sub>5</sub>·0.3H<sub>2</sub>O: C 70.90, H 10.29, N 2.67; found C 70.88, H 10.59, N 2.81.

**N-Lithocholyl L-leucine methyl ester (2.10):** <sup>1</sup>H-NMR: (CDCl<sub>3</sub>)  $\delta$  = 5.76 (d, 1H, NH); 4.65 (m, 1H, C<sup>\*</sup>H); 3.72 (s, 3H, OCH<sub>3</sub>); 3.61 (m, 1H, 3 $\alpha$ -CH); 2.32-1.05 (m, 31 H, aliphatic H); 0.94 (d, 3H, 21-CH<sub>3</sub>); 0.91 (d, 6H, 2 Leu-CH<sub>3</sub>); 0.89 (s, 3H, 19-CH<sub>3</sub>); 0.62 (s, 3H, 18-CH<sub>3</sub>). IR: (KBr)  $\nu$  = 3426, 3328, 2942, 2868, 1754, 1656, 1535. Anal. calcd for C<sub>31</sub>H<sub>53</sub>NO<sub>4</sub>: C 73.91, H 10.61, N 2.78; found C 74.28, H 11.02, N 2.87.

## REFERENCES AND NOTES

- 1 P. Terech, R.G. Weiss, *Chem. Rev.* **1997**, 97, 3133-3159.
- 2 K. Yoza, Y. Ono, K. Yoshihara, T. Akao, H. Shinmori, M. Takeuchi, S. Shinkai, D.N. Reinhoudt, *J. Chem. Soc., Chem. Commun.* **1998**, 907-908.
- 3 R. Oda, I. Huc, S.J. Candau, *Angew. Chem., Int. Ed.* **1998**, 37, 2689-2691.
- 4 G.M. Clavier, J.F. Brugger, H. Bouas-Laurent, J.L. Pozzo, *J. Chem. Soc., Perkin Trans. 2* **1998**, 2527-2534.
- 5 C. Geiger, M. Stanescu, L. Chen, D.G. Whitten, *Langmuir* **1999**, 15, 2241-2245.
- 6 N. Amanokura, Y. Kanekiyo, S. Shinkai, D.N. Reinhoudt, *J. Chem. Soc., Perkin Trans.* **1999**, 1995-2000.
- 7 D.J. Abdallah, R.G. Weiss, *Langmuir* **2000**, 16, 352-355.
- 8 D.J. Abdallah, R.G. Weiss, *Adv. Mater.* **2000**, 12, 1237-1247.
- 9 P. Terech, *Ber. Bunsenges. Phys. Chem.* **1998**, 102, 1630-1643.
- 10 L. Lu, T.M. Cocker, R.E. Bachman, R.G. Weiss, *Langmuir* **2000**, 16, 20-34.
- 11 M. de Loos, J. van Esch, I. Stokroos, R.M. Kellogg, B.L. Feringa, *J. Am. Chem. Soc.* **1997**, 119, 12675-12676.
- 12 K. Hanabusa, C. Koto, M. Kimura, H. Shirai, A. Kakehi, *Chem. Lett.* **1997**, 429-430.
- 13 K. Inoue, Y. Ono, Y. Kanekiyo, T. Ishi-i, K. Yoshihara, S. Shinkai, *J. Org. Chem.* **1999**, 64, 2933-2937.
- 14 U. Beginn, S. Keinath, M. Möller, *Macromol. Chem. Phys.* **1998**, 199, 2379-2384.
- 15 K. Hanabusa, H. Kobayashi, M. Suzuki, M. Kimura, H. Shirai, *Colloid Polym. Sci.* **1998**, 276, 252-259.
- 16 V.P. Vassilev, E.E. Simanek, M.R. Wood, C.H. Wong, *J. Chem. Soc., Chem. Commun.* **1998**, 1865-1866.
- 17 K. Hanabusa, R. Tanaka, M. Suzuki, M. Kimura, H. Shirai, *Adv. Mater.* **1997**, 9, 1095-1097.
- 18 S. Bhattacharya, S.N. Ghanashyam Acharya, *Chem. Mater.* **1999**, 11, 3121-3132.
- 19 K. Hanabusa, M. Matsumoto, M. Kimura, A. Kakehi, H. Shirai, *J. Colloid Interface Sci.* **2000**, 224, 231-244.
- 20 K. Miki, A. Masui, N. Kasai, M. Miyata, M. Shibakami, K. Takemoto, *J. Am. Chem. Soc.* **1988**, 110, 6594-6596.
- 21 K. Sada, T. Kondo, M. Ushioda, Y. Matsuura, K. Nakano, M. Miyata, K. Miki, *Bull. Chem. Soc. Jpn.* **1998**, 71, 1931-1937.
- 22 Y. Hishikawa, K. Sada, R. Watanabe, M. Miyata, K. Hanabusa, *Chem. Lett.* **1998**, 795-796.
- 23 U. Maitra, P.V. Kumar, N. Chandra, L.J. D'Souza, M.D. Prasanna, A.R. Raju, *J. Chem. Soc., Chem. Commun.* **1999**, 595-596.
- 24 K. Hanabusa, K. Shimura, K. Hirose, M. Kimura, H. Shirai, *Chem. Lett.* **1996**, 885-886.

- 25 J. van Esch, S. DeFeyter, R.M. Kellogg, F. DeSchryver, B.L. Feringa, *Chem. Eur. J.* **1997**, 3, 1238-1243.
- 26 P. Terech, J.J. Allegraud, C.M. Garner, *Langmuir* **1998**, 14, 3991-3998.
- 27 T. Shioiri, Y. Yokoyama, Y. Kasai, S. Yamada, *Tetrahedron* **1976**, 32, 2211-2217.
- 28 K. Hanabusa, Y. Maesaka, M. Kimura, H. Shirai, *Tetrahedron Lett.* **2000**, 40, 2385-2388.
- 29 D. Dolphin, A. Wick, *Tabulation of infrared spectral data*, Wiley - New York, **1977**.
- 30 W.J. Humphlett, C.V. Wilson, *J. Org. Chem.* **1961**, 26, 2507-2510.
- 31 W.T.J. Morgan, *J. Chem. Soc.* **1926**, 79-84.

# 3

## **Alkyl derivatives of cholic acid as organogelators: one-component and two-component gels**

*Cholic acid was coupled to an alkyl tail via three different connecting groups, amide, urea, and ester group, and the gelation capabilities of these compounds in different solvents were compared. Both amide and urea derivatives form one-component gels. They give transparent and stable gels in aromatic solvents through a hydrogen bonded network of monomolecular fibers. Structural variations give information about the molecular requirements for gelation. A new kind of two-component gel was found for the ester derivatives with two carbohydrates, isomannide and isosorbide. Formation of worm-like, inverted micelles causes gelation of apolar solvents. The optimal stoichiometry of the co-gelators lies close to 1:1.*

This chapter was accepted for publication in *Langmuir* **2002**.

### 3.1 INTRODUCTION

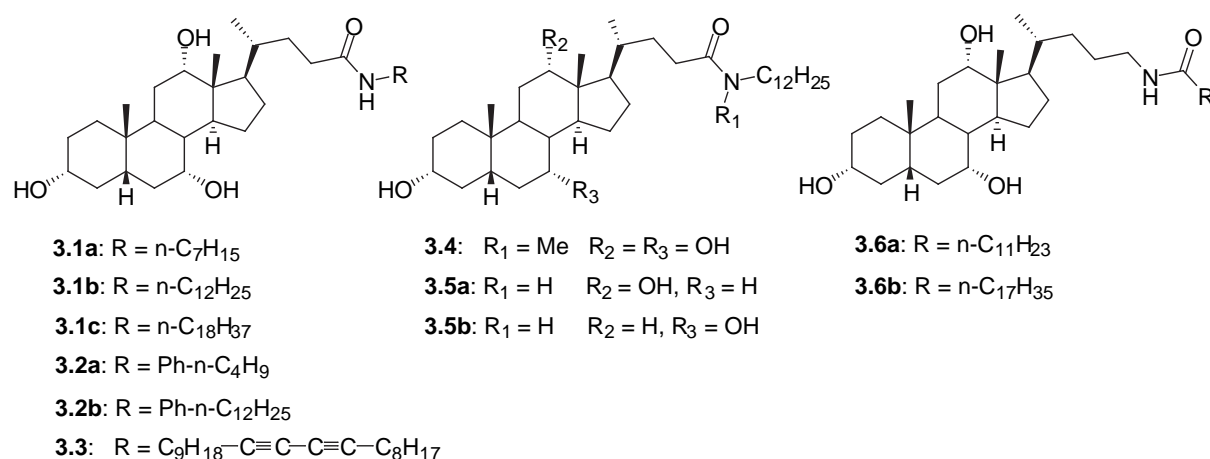
Research on organogels is relatively new and the number of organogelators has rapidly increased over the last 10-15 years.<sup>1,2</sup> In the past, discovery of new gelators often happened "by accident" and numerous studies have been dedicated to understanding the relation between a gelator's structure and its gelation behavior. Recently, there is a tendency to actively design new and simple organogelators.<sup>3-6</sup> A large number of organogelators forms aggregates by means of hydrogen bonds. For this class of gelators, the presence of potent hydrogen bonding groups, like amide or urea groups, is obligatory for gelation.<sup>7-11</sup> However, small changes in the rest of the molecular structure can have a drastic effect on the gelling capacity, as was reported earlier in a series of  $\alpha$ -amino acid derivatives of cholic acid, a bile acid.<sup>12</sup> Only a few bile acid based gelators are known,<sup>12-15</sup> whereas a large group of gelators based on the more apolar cholesterol has been reported.<sup>2,16,17</sup>

In this chapter, we compare a number of alkyl derivatives of cholic acid, connected by different groups: amide, urea and ester groups. By keeping the two structural units of the molecule the same, i.e. the cholic acid unit and the alkyl tail, the influence of the connecting group becomes more pronounced. Structural variations provide information on the molecular requirements for gelation. Besides the one-component gels, also a new type of co-gelation was found. So far, literature has reported few examples of combination gels.<sup>1,14,15,18-20</sup> Similar to one-component gels, the aggregation between co-gelators can be based on different interactions, such as hydrogen bonds,  $\pi$ - $\pi$  interactions, or van der Waals interactions. Two of the known combination gels involve bile acid derivatives,<sup>14,15</sup> but in both cases, the hydroxyl groups were derivatised, whereas we leave those intact. Investigations on this new type of combination gel with cholic acid derivatives are presented. Gels were studied with differential scanning calorimetry (DSC), infrared spectroscopy (IR), and transmission electron microscopy (TEM).

### 3.2 RESULTS AND DISCUSSION

A series of different alkyl derivatives of cholic acid with an amide group was synthesized (depicted in Scheme 3.1) and their gelation behavior was tested. Results are summarized in Table 3.1.





Scheme 3.1.

 Table 3.1. Gelation test of alkylcholamides<sup>[a]</sup>

Solvent	3.1a	3.1b	3.1c	3.2a	3.2b	3.3	3.5a	3.6a	3.6b
Benzene	<b>g</b> [54]	<b>g</b> [59]	<b>g</b> [53]	v	<b>g</b> [61]	<b>g</b> [40]	s	<b>g</b> [39]	<b>g</b> [38]
Toluene	<b>g</b>	<b>g</b>	<b>g</b>	n	n	<b>g</b>	s	<b>g</b>	<b>g</b>
Ethylbenzene	<b>g</b>	<b>g</b>	<b>g</b>	n	s(p)	<b>g</b>	s	s	<b>g</b>
Styrene	<b>g</b>	<b>g</b>	<b>g</b>	s(v)	s(g)	<b>g</b>	s	s(v)	s(g)
Chlorobenzene	<b>g</b>	<b>g</b>	<b>g</b>	n	n	<b>g</b>	s	s	<b>g</b>
Anisole	n	<b>g</b>	<b>g</b>	n	n	s	s	s	s(g)
Benzaldehyde	s	s	s	s	s		s	s	s
Acetophenone	s	s	s	s	s		s	s	s
Cyclohexene	<b>g</b>	<b>g</b> [80]	<b>g</b>	p(g <sub>c</sub> )	p(g <sub>c</sub> )	<b>g<sub>c</sub></b>	<b>g</b> [45]	<b>g<sub>c</sub></b>	<b>g</b>
n-Hexane	n	n	n	n	n		n	n	n

<sup>[a]</sup> conc 1.5 wt%; observation was made immediately after cooling; changes after 24 h in parentheses; **g** = gel, **g<sub>c</sub>** = cloudy gel, v = viscous solution, p = precipitate, s = soluble, n = not soluble; m.p. 25 mM gel in square brackets, determined using DSC, heating rate 0.5 °C/min

Alkylcholamides **3.1a-3.1c** formed gels in several aromatic solvents and in cyclohexene. The produced gels are completely transparent, thermoreversible, and stable for months. All three compounds produced gels of similar stability in concentrations of 1.5 wt%. So the influence of the alkyl tail length on gelation seems limited, although a certain minimum length is probably necessary.<sup>21,22</sup> Some melting points for the gels, determined with DSC, are given in Table 3.1. Increasing the concentration gave higher melting points, similar to the temperature dependence of normal solvation behavior. It is worth mentioning that the melting points for gels in

cyclohexene are higher than for gels in benzene. In fact, the cyclohexene gels are so stable that melting does not occur below the boiling point of the pure solvent.

In a TEM image of a gel of compound **3.1c** in benzene, shown in Figure 3.1, a fibrous structure is visible. The fibers have a very small diameter of about 5-6 nm. Since the length of compound **3.1c** in its fully stretched conformation is about 4 nm, the fibers are almost monomolecular in width. Most likely, the steroid units are located in the center of the fiber, connected by hydrogen bonds, and the alkyl tails are on the outside of the fiber, toward the solvent.

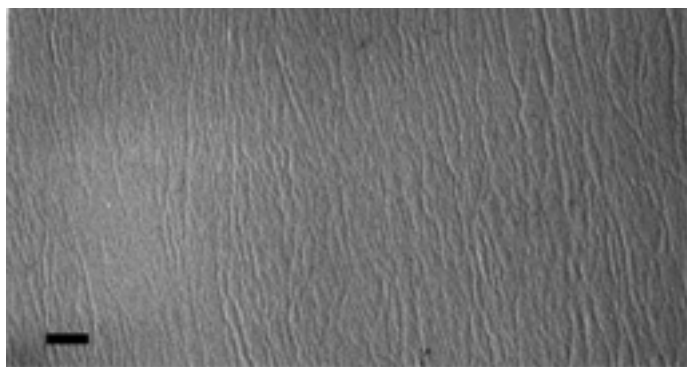


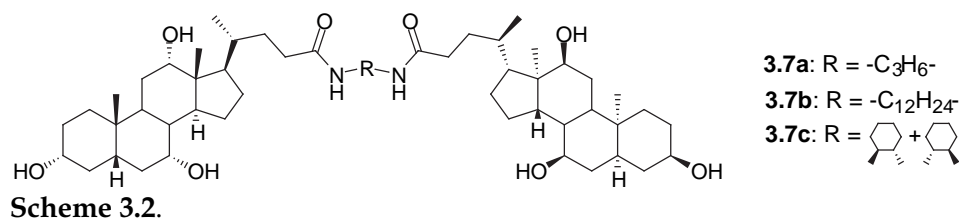
**Figure 3.1.** TEM-picture of 25 mM **3.1c** in benzene; bar indicates 500 nm

Introduction of an aromatic group in the alkyl tail deteriorates the gelation ability: compounds **3.2a** and **3.2b** produced rather unstable gels in a limited number of solvents. Compound **3.3**, with a 21-carbon alkyl tail, is a better gelator, despite the presence of a diacetylene functionality halfway along the alkyl tail. This compound **3.3** was able to form gels in the same aromatic solvents as compounds **3.1a-c**. It would be interesting if compound **3.3** could be polymerized in the gelled state, because in this way the gel network is stabilized,<sup>23-24</sup> but several attempts were unsuccessful. For polymerization, diacetylene functionalities have to be ordered in a parallel fashion. This is evidently not the case in benzene gels of compound **3.3**, confirming the idea of fibers in which the alkyl tails are on the outside, facing the solvent in all directions.

The driving force for aggregation of these gelators is hydrogen bonding between the amide group and the hydroxyl groups. This is evident from gelation experiments with compounds lacking one of these groups. Compound **3.4**, missing

the amide proton, and compounds **3.5a** and **3.5b**, with two hydroxyl groups, did not produce gels in any aromatic solvent. As the solubility in these solvents increases, the need for gelation decreases. Gelation of compound **3.5a** was found in cyclohexene and also in cyclooctadiene. However, compound **3.5b** did not form gels in these solvents. So the presence of two hydroxyl groups can be sufficient, but the precise packing of the H-bonded network appears to be a delicate process. The occurrence of hydrogen bonds was confirmed by IR spectroscopy. The stretching frequency of the amide carbonyl group for solutions of compounds **3.5a-b** in benzene was located at about  $1672\text{ cm}^{-1}$ , whereas for gels of compounds **3.1a-c** this value was lowered to about  $1638\text{ cm}^{-1}$  due to intermolecular hydrogen bonding.

Considering the importance of the amide bond, we were wondering if its direction could influence gelation. Compounds **3.6a** and **3.6b**, with a reversed amide bond, were prepared, starting from 24-aminocholane. They showed similar gelation behavior as the normal alkylcholamides: stable and transparent gels were obtained in aromatic solvents and cyclohexene. However, melting points of benzene gels of compounds **3.6a-b** were about  $15\text{ }^{\circ}\text{C}$  lower than those for compounds **3.1a-c**.



Three dimers were prepared (Scheme 3.2) in which two cholic acid units were connected via amide groups to a linear or cyclic alkyl spacer. Gelation was tested, but results are poor, as can be seen in Table 3.2. Compound **3.7a** gave gels in acetophenone and chloroform, but these gels were not as transparent or stable as the gels from compounds **3.1**, **3.3**, or **3.6**. The only transparent gel was obtained by compound **3.7c** in acetophenone, which had a melting point similar to that of compounds **3.1a-c** in benzene. It seems logical that the presence of two cholic acid units alters the solubility of the compounds to make them less soluble in more polar solvents. Since gelation is a process that occurs at the borderline of solubility (a poorly soluble compound, which has difficulty with crystallization, will have a

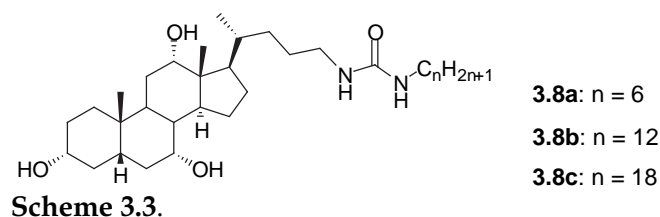
tendency to form a gel), the solvent in which gelation occurs, is also likely to have a more polar character.

**Table 3.2.** Gelation test of alkylcholamide dimers and alkylcholurea<sup>[a]</sup>

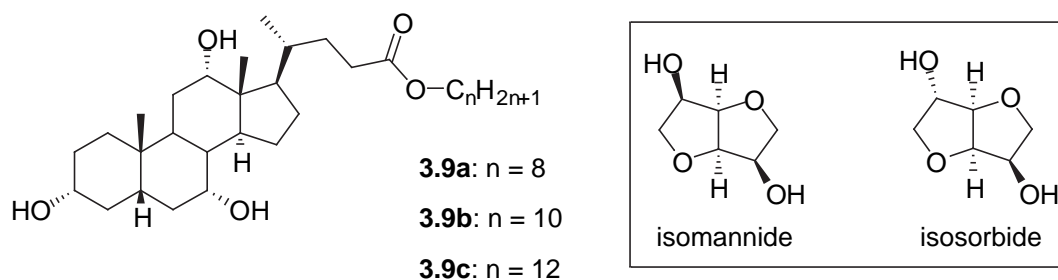
Solvent	3.7a	3.7b	3.7c	3.8a	3.8b	3.8c
Benzene	n	n	n	n	n	s(g)[54]
Toluene	n	n	n	n	n	<b>g</b>
Ethylbenzene	n	n	n	s(p)	s(p)	s(g)
Chlorobenzene	n	n	n	s	s	s
Anisole	n	n	n	n	s(v)	s(g)
Benzaldehyde	s	s	s	s	s	s
Acetophenone	<b>g<sub>c</sub></b>	n	s(g) [55]	s	s	s
Cyclohexene	n	n	n	n	n	n
Hexane	n	n	n	n	n	n
Octanol	s	s	s	s	s	s(v)
Chloroform	n( <b>g<sub>c</sub></b> )	v	s	s	s	s

<sup>[a]</sup> conc 1.5 wt%; observation was made immediately after cooling; changes after 24 h in parentheses; g = gel, g<sub>c</sub> = cloudy gel, p = precipitate, v = viscous solution, s = soluble, n = not soluble; m.p. 25 mM gel in square brackets, determined using DSC, heating rate 0.5 °C/min.

Because the urea group is often found in hydrogen bonded organogelators, we also used this group to couple cholic acid to an alkyl tail. Compounds **3.8a-c** (Scheme 3.3) were synthesized and their gelation behavior was tested. Results are given in Table 3.2. The gelling capability of these compounds was rather disappointing, as only compound **3.8c** was able to gel the aromatic solvents benzene, toluene, ethylbenzene, and anisole. The melting point of a gel of compound **3.8c** in benzene is comparable to that of compounds **3.1a-c**. Apparently, for the urea type of alkyl derivatives of cholic acid, a longer alkyl tail is necessary to form gels, in comparison with the amide derivatives.



A series of alkyl cholates **3.9a-c** (Scheme 3.4) with tails of 8, 10, and 12 carbon atoms was synthesized. As expected, the hydrogen bonding ability of esters is weaker than that of amides and no one-component gels were formed in aromatic solvents. However, in other apolar solvents aggregation of these compounds was noticed, in the form of solubilization of other compounds and even co-gelation. Compounds **3.9a-c** are highly soluble in solvents such as n-hexane, n-octane, or chloroform. In these solvents they can increase the solubility of more polar compounds, e.g. sugars and water. In a 0.1 M solution of compound **3.9a-c** in octane as much as 0.5 M water could be dissolved. At these high concentrations of compound **3.9b-c**, a thickening of the solution could be observed. This behavior indicates the formation of a microemulsion based gel (MBG)<sup>25</sup> based on inverted micelles. Also two specific carbohydrates, isomannide (IM) and isosorbide (IS) (inset Scheme 3.4), could be dissolved in a warm solution of compounds **3.9a-c** in hexane or octane, whereas they are insoluble in the pure solvents. To our surprise, we found that after cooling the combination of these compounds forms a thermoreversible and opaque gel, also at lower concentrations. This new type of combination gel was studied in more detail.



**Scheme 3.4**

Different combinations of alkyl cholates and carbohydrates were tried. There seems to be no difference in behavior between IM and IS: both carbohydrates give gels with alkyl esters **3.9a-c** in hexane and octane with similar thermal behavior. Also, the influence of the alkyl tail length of the cholate was not significant. No difference was found in the gel formation or stability with octyl, decyl, or dodecyl cholate.

A TEM image of a gel of compound **3.9b** and IM in octane shows a fibrous structure in which the fibers have a diameter of 10-12 nm and are occasionally bundled. An example is shown in Figure 3.2. The most likely aggregation structure consists of worm-like inverted micelles as a special kind of MBG. The carbohydrate will be located in the center of the fiber together with the steroid units of the alkyl cholates facing their polar side toward the carbohydrates and their apolar side and alkyl tail directed outward to the surrounding solvent.

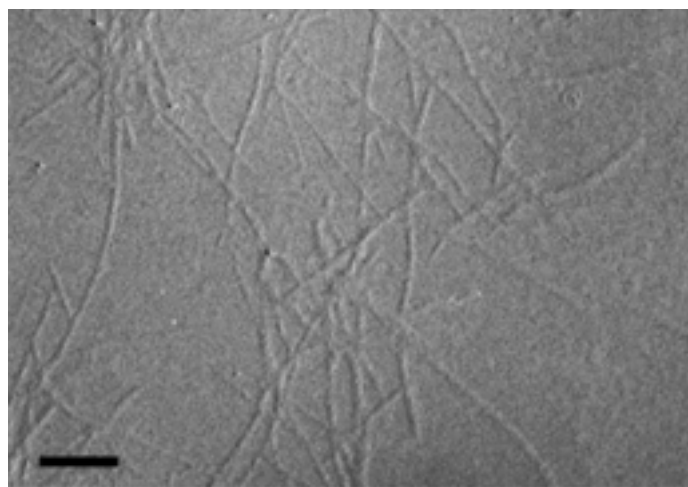


**Figure 3.2.** TEM-picture of 10 mM IM / 20 mM **3.9b** in octane; bar indicates 500 nm

Thermal behavior and stability of the gels were studied using DSC. Thermograms of these gels show three endothermic transition peaks upon heating: two broad transitions and one sharp peak. An example is shown in Figure 3.3.

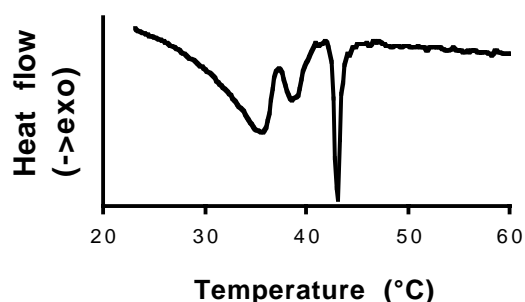


**Figure 3.3.** DSC thermogram of 10 mM IM / 15 mM **3.9b** in octane, heating rate 0.3 °C/min

The melting points of the gels (defined as the temperature above which macroscopic flow appears) were also determined by visually monitoring the flow of the gels in a thermally controlled bath. When these values are compared to the DSC

thermograms, it can be concluded that the sharp transition peak in the thermogram corresponds with the actual melting of the gel. At the temperatures of the broad transitions, there is no visual change in the gels at macroscopic level. For the physical interpretation of these pre-melting transitions, we assume that partial melting of the network takes place. The interaction between the fibers may be lost before the fibers themselves disintegrate. However, proof of this assumption requires detailed structural investigations.

**Table 3.3.** Melting behavior of gels of IM and **3.9b** in octane<sup>[a]</sup>

entry	Conc IM [mM]	Conc <b>3.9b</b> [mM]	Pre-melting transitions [°C]		M.p. [°C]
1	5	20	30	35	38
2	10	15	35	39	43
3	10	20	37	40	43
4	10	25	34	37	41
5	10	30	35	38	43
6	10	40	31	36	39
7	10	50	27	33	35
8	15	20	36	41	46

<sup>[a]</sup> determined using DSC; heating rate 0.3 °C/min

An important condition for these combination gels is that the concentration of alkyl cholate has to be higher than the concentration of carbohydrate in order to have complete dissolution of the latter. The ratio of concentrations was varied for compound **3.9b** and IM in octane and melting points for these gels are summarized in Table 3.3. Enthalpy values were also recorded, but there was only little variation between the values for different ratios and no clear trend was observed. Comparison of entries 1, 3, and 8 shows that with an increasing concentration of IM, the melting point of the gel also increases. However, with an increasing concentration of compound **3.9b**, as in entries 2-7, the melting point is rather constant. The only condition is that the concentration IM is no more than 4 times lower than the concentration of compound **3.9b**. When this happens, as can be seen in entries 6 and

7, the melting point decreases. So it is mainly IM, which contributes to the stability of the gels. The carbohydrate is the essential bridge with the right molecular structure to keep the alkyl cholates together through hydrogen bonds. This is also in line with the lower concentration of alkyl cholate required for this co-gelation in comparison with the concentration required for thickening in the presence of only water. If the amount of IM is too low, in comparison with the alkyl cholate, the aggregates are weak and the melting points decreases. So the optimal ratio carbohydrate:alkyl cholate should be as close to 1:1 as solubility allows, but not lower than 1:4.

### 3.3 CONCLUSIONS

Alkyl derivatives of cholic acid act as different kind of gelators in several organic solvents. Amide and urea derivatives act as one-component gelators in aromatic solvents and cycloalkenes, producing completely transparent gels. Thin, hydrogen bond-driven fibers are formed. The direction of the amide bond has little influence on gelation, while introduction of an aryl group decreases the gelling capability. For urea derivatives the alkyl tail has to be longer than for amides to cause gelation. Dimers containing two cholic acid units form organogels in more polar solvents. Ester derivatives form a new type of combination gel in octane with two specific carbohydrates, isomannide and isosorbide. The amount of carbohydrate determines the stability of the gel, which probably consists of worm-like, inverted micelles. The optimal ratio of both components lies close to 1:1.

### 3.4 EXPERIMENTAL SECTION

**General Remarks:**  $^1\text{H}$ - and  $^{13}\text{C}$ -NMR spectra were recorded at 200 and 50 MHz, respectively on a Bruker AC200 spectrometer at ambient temperature. - FT-IR spectra were recorded on a BIO-RAD FTS-7 spectrophotometer with a resolution of  $4\text{ cm}^{-1}$ . Compounds were measured as a solid in KBr or as a solution or a gel. - Elemental analyses were performed with an Elemental Analyzer EMASyst 1106. - HRMS and FAB data were obtained with a Finnigan MAT 95 mass spectrometer. - In a typical gelation experiment, a capped test tube was filled with solvent and about 1.5 wt% of a compound (unless stated otherwise) and heated until the solid was dissolved. After cooling, gelation was checked by monitoring the



disappearance of flow. The absence of water is crucial for gelation and to obtain reproducible and stable gels, a grain of molsieve 4 Å was added to each gelation mixture. - For TEM, drops of gel were spread and air-dried on Formvar/carbon-coated copper grids (400 mesh). Specimens were shadowed with Pt at an angle of 15° and at a distance of about 15 cm at  $2.6 \times 10^{-2}$  Pa. Samples were analyzed on a Jeol 1200 EX TEM at 80 kV. Photos were recorded on Agfa Scientia EM films and developed with diluted D19 developer. - DSC thermograms were recorded on a Setaram micro-DSC III. Approximately 500 mg of a solution of gelator above the gel melting temperature was brought into a metal, screw-capped cup and was allowed to cool to room temperature, thus forming a gel. A reference cup contained the same amount of pure solvent. Two heating and cooling cycles were recorded (rate for first 1 °C/min and for the second 0.3 or 0.5 °C/min) and the second heating curves were compared. This procedure assured that gels were formed under reproducible conditions. Transition temperatures refer to the peak minima.

**Synthesis:** Used solvents were of p.a. quality. The different bile acids were purchased, as were the alkyl alcohols, alkylamines, alkylcarboxylic acids, alkylisocyanates, diaminoalkanes, and diethylphosphoryl cyanide (DEPC). The 1-aminohenicosa-10,12-diyne was kindly provided by Dr. H.M. Barentsen. The methyldodecylamine was prepared according to literature.<sup>26</sup> The 24-aminocholane-3,7,12-triol hydrochloride was prepared according to a literature procedure<sup>27</sup> starting from 3,7,12-triformyloxycholic acid.<sup>28</sup> The purity of the products was verified with NMR, thin layer chromatography and elemental analyses.

General procedure for the synthesis of alkyl(di)cholamides is similar to the procedure described previously.<sup>12</sup> Compounds **3.6a** and **3.6b** were prepared by coupling 24-aminocholane-3,7,12-triol hydrochloride to the appropriate carboxylic acid using the same procedure.

**N-Heptylcholamide (3.1a):** <sup>1</sup>H NMR (CDCl<sub>3</sub>): δ = 5.99 (s, 1H, NH), 3.94 (br. s, 1H, 12α-CH), 3.83 (br. s, 1H, 7α-CH), 3.42 (m, 1H, 3α-CH), 3.20 (q, 2H, NCH<sub>2</sub>), 2.45-1.10 (m, 34H, aliphatic H), 0.97 (d, 3H, 21-CH<sub>3</sub>), 0.85 (m, 6H, 2 CH<sub>3</sub>), 0.65 (s, 3H, 18-CH<sub>3</sub>). - IR (KBr): ν = 3384, 2928, 2859, 1648, 1558. - C<sub>31</sub>H<sub>55</sub>NO<sub>4</sub>: calcd. C 73.62, H 10.96, N 2.77; found C 73.39, H 11.35, N 2.64.

**N-Dodecylcholamide (3.1b):** <sup>1</sup>H NMR (CDCl<sub>3</sub>): δ = 5.68 (s, 1H, NH), 3.97 (br. s, 1H, 12α-CH), 3.85 (br. s, 1H, 7α-CH), 3.45 (m, 1H, 3α-CH), 3.22 (q, 2H, NCH<sub>2</sub>), 2.32-1.08 (m, 44H, aliphatic H), 0.98 (d, 3H, 21-CH<sub>3</sub>), 0.86 (m, 6H, 2 CH<sub>3</sub>), 0.68 (s, 3H, 18-CH<sub>3</sub>). - <sup>13</sup>C NMR (CDCl<sub>3</sub>): δ = 174.0 (24-C), 73.1 (12-CH), 71.9 (3-CH), 68.5 (7-CH), 46.5 (17-CH), 46.3 (13-C), 41.6 (5-CH), 41.5 (14-CH), 39.6 (4-CH<sub>2</sub>), 39.4 (8-CH), 35.4 (1-CH<sub>2</sub>), 35.3 (20-CH), 34.7 (6-CH<sub>2</sub>), 34.6 (10-C), 33.1 (CH<sub>2</sub>), 31.9 (CH<sub>2</sub>), 31.7 (CH<sub>2</sub>), 30.4 (CH<sub>2</sub>), 29.7 (CH<sub>2</sub>), 29.6 (CH<sub>2</sub>), 29.6 (CH<sub>2</sub>), 29.4 (CH<sub>2</sub>),

28.1 (CH<sub>2</sub>), 27.6 (CH<sub>2</sub>), 27.0 (CH<sub>2</sub>), 26.3 (9-CH), 23.3 (CH<sub>2</sub>), 22.7 (CH<sub>2</sub>), 22.4 (19-CH<sub>3</sub>), 17.4 (21-CH<sub>3</sub>), 14.1 (CH<sub>3</sub>), 12.4 (18-CH<sub>3</sub>). - IR (KBr):  $\nu$  = 3324, 2927, 2857, 1646, 1551. - C<sub>36</sub>H<sub>65</sub>NO<sub>4</sub>: calcd. C 75.08, H 11.38, N 2.43; found C 74.90, H 11.71, N 2.25.

**N-Octadecylcholamide (3.1c):** <sup>1</sup>H NMR (CDCl<sub>3</sub>):  $\delta$  = 5.29 (s, 1H, NH), 3.97 (br. s, 1H, 12 $\alpha$ -CH), 3.85 (br. s, 1H, 7 $\alpha$ -CH), 3.45 (m, 1H, 3 $\alpha$ -CH), 3.24 (m, 2H, NCH<sub>2</sub>), 2.40-1.10 (m, 56H, aliphatic H), 0.98 (d, 3H, 21-CH<sub>3</sub>), 0.86 (m, 6H, 2 CH<sub>3</sub>), 0.68 (s, 3H, 18-CH<sub>3</sub>). - <sup>13</sup>C NMR (CDCl<sub>3</sub>):  $\delta$  = 174.0, 73.1, 71.9, 68.5, 46.5, 46.4, 41.6, 41.5, 39.7, 39.6, 39.4, 35.3, 34.7, 33.1, 31.9, 31.7, 29.7, 29.6, 29.6, 29.4, 28.1, 27.6, 27.0, 26.3, 23.3, 22.7, 22.4, 17.4, 14.1, 12.5. - IR (KBr):  $\nu$  = 3314, 2924, 2853, 1648, 1556. - C<sub>42</sub>H<sub>77</sub>NO<sub>4</sub>: calcd. C 76.42, H 11.76, N 2.12; found C 76.41, H 11.82, N 2.00.

**N-(4-Butylphenyl)-cholamide (3.2a):** <sup>1</sup>H NMR (CDCl<sub>3</sub>):  $\delta$  = 8.22 (s, 1H, NH), 7.47 (d, 2H, aromatic H), 7.09 (d, 2H, aromatic H), 3.99 (br. s, 1H, 12 $\alpha$ -CH), 3.85 (br. s, 1H, 7 $\alpha$ -CH), 3.49 (m, 1H, 3 $\alpha$ -CH), 2.54 (t, 2H, Ph-CH<sub>2</sub>), 2.38-1.10 (m, 28H, aliphatic H), 1.00 (d, 3H, 21-CH<sub>3</sub>), 0.89 (m, 6H, 2 CH<sub>3</sub>), 0.67 (s, 3H, 18-CH<sub>3</sub>). - <sup>13</sup>C NMR (CDCl<sub>3</sub>):  $\delta$  = 172.5, 138.5, 136.1, 128.7, 128.1, 120.5, 119.8, 73.2, 71.9, 68.6, 46.3, 41.7, 41.4, 39.4, 35.0, 34.7, 34.0, 33.7, 32.9, 30.9, 30.4, 29.7, 28.1, 26.4, 23.3, 22.4, 22.3, 22.1, 17.5, 14.1, 12.5. - IR (KBr):  $\nu$  = 3404, 2928, 2868, 1666, 1602, 1540. - HRMS calcd for C<sub>34</sub>H<sub>53</sub>NO<sub>4</sub> (M<sup>+</sup>): 539.3975; found 539.3969.

**N-(4-Dodecylphenyl)-cholamide (3.2b):** <sup>1</sup>H NMR (CDCl<sub>3</sub>):  $\delta$  = 8.14 (s, 1H, NH), 7.46 (d, 2H, aromatic H), 7.08 (d, 2H, aromatic H), 3.97 (br. s, 1H, 12 $\alpha$ -CH), 3.83 (br. s, 1H, 7 $\alpha$ -CH), 3.41 (m, 1H, 3 $\alpha$ -CH), 2.53 (t, 2H, Ph-CH<sub>2</sub>), 2.28-1.13 (m, 44H, aliphatic H), 0.99 (d, 3H, 21-CH<sub>3</sub>), 0.85 (m, 6H, 2 CH<sub>3</sub>), 0.66 (s, 3H, 18-CH<sub>3</sub>). - <sup>13</sup>C NMR (CDCl<sub>3</sub>):  $\delta$  = 172.8, 138.2, 136.0, 128.7, 128.4, 120.9, 119.8, 73.2, 72.0, 68.6, 46.3, 45.9, 41.7, 41.4, 39.7, 39.3, 35.4, 34.8, 34.7, 32.9, 31.9, 31.6, 31.2, 30.3, 29.9, 29.7, 29.5, 29.3, 29.3, 28.1, 27.4, 26.4, 23.3, 22.7, 22.4, 17.5, 14.1, 12.5. - IR (KBr):  $\nu$  = 3425, 2923, 2848, 1661, 1601, 1536. - HRMS calcd for C<sub>42</sub>H<sub>69</sub>NO<sub>4</sub> (M<sup>+</sup>): 651.5227; found 651.5222.

**10,12-Henicosadiynylcholamide (3.3):** <sup>1</sup>H NMR (CDCl<sub>3</sub>):  $\delta$  = 5.90 (bs, 1H, NH), 3.95 (br. s, 1H, 12 $\alpha$ -CH), 3.83 (br. s, 1H, 7 $\alpha$ -CH), 3.43 (m, 1H, 3 $\alpha$ -CH), 3.22 (m, 2H, NCH<sub>2</sub>), 2.32-1.08 (m, 54H, aliphatic H), 0.97 (d, 3H, 21-CH<sub>3</sub>), 0.86 (m, 6H, 2 CH<sub>3</sub>), 0.67 (s, 3H, 18-CH<sub>3</sub>). - <sup>13</sup>C NMR (CDCl<sub>3</sub>):  $\delta$  = 174.4, 73.5, 72.3, 68.9, 65.7, 65.6, 46.9, 46.8, 42.1, 41.9, 40.0, 39.9, 39.8, 35.8, 35.7, 35.2, 35.1, 33.5, 32.2, 32.1, 30.8, 30.0, 29.8, 29.7, 29.5, 29.5, 29.5, 29.4, 29.3, 29.3, 29.2, 28.8, 28.5, 28.0, 27.3, 26.7, 23.7, 23.0, 22.8, 19.6, 17.9, 14.5, 12.9. - IR (KBr):  $\nu$  = 3395, 2927, 2855, 1647, 1558. - C<sub>45</sub>H<sub>75</sub>NO<sub>4</sub>: calcd. C 77.87, H 10.89, N 2.02; found C 77.72, H 11.03, N 1.95.

**N-Methyl-N-dodecylcholamide (3.4):** <sup>1</sup>H NMR (CDCl<sub>3</sub>):  $\delta$  = 3.96 (br. s, 1H, 12 $\alpha$ -CH), 3.84 (br. s, 1H, 7 $\alpha$ -CH), 3.44 (m, 1H, 3 $\alpha$ -CH), 3.28 (m, 2H, NCH<sub>2</sub>), 2.93 (d, 3H, N-CH<sub>3</sub>), 2.45-1.06 (m, 44H, aliphatic H), 0.99 (d, 3H, 21-CH<sub>3</sub>), 0.86 (m, 6H, 2 CH<sub>3</sub>), 0.67 (s, 3H, 18-CH<sub>3</sub>). - <sup>13</sup>C NMR

(CDCl<sub>3</sub>):  $\delta$  = 173.5, 73.0, 71.8, 68.4, 50.1, 47.1, 47.0, 46.5, 41.6, 41.5, 39.4, 35.4, 35.3, 34.7, 34.6, 33.4, 31.1, 30.7, 30.5, 29.6, 29.5, 29.4, 29.3, 28.6, 28.1, 27.6, 27.3, 26.9, 26.8, 26.3, 23.3, 22.7, 22.4, 17.5, 14.1, 12.5. - IR (KBr):  $\nu$  = 3421, 2925, 2854, 1635. - C<sub>37</sub>H<sub>67</sub>NO<sub>4</sub>·0.5H<sub>2</sub>O: calcd. C 74.20, H 11.44, N 2.34; found C 74.04, H 11.53, N 2.06.

**N-Dodecyldeoxycholamide (3.5a):** <sup>1</sup>H NMR (CDCl<sub>3</sub>):  $\delta$  = 5.68 (s, 1H, NH), 3.98 (t, 1H, 12 $\alpha$ -CH), 3.62 (m, 1H, 3 $\alpha$ -CH), 3.24 (q, 2H, NCH<sub>2</sub>), 2.26-1.08 (m, 46H, aliphatic H), 0.99 (d, 3H, 21-CH<sub>3</sub>), 0.88 (m, 6H, 2 CH<sub>3</sub>), 0.68 (s, 3H, 18-CH<sub>3</sub>). - <sup>13</sup>C NMR (CDCl<sub>3</sub>):  $\delta$  = 173.5, 73.1, 71.7, 48.2, 47.1, 46.5, 42.1, 39.5, 36.4, 36.0, 35.2, 34.1, 33.6, 33.5, 31.9, 31.7, 30.4, 29.7, 29.6, 29.6, 29.5, 29.3, 29.3, 28.6, 27.5, 27.1, 26.9, 26.1, 23.7, 23.1, 22.7, 17.4, 14.1, 12.7. - IR (KBr):  $\nu$  = 3384, 2926, 2855, 1648, 1558. - C<sub>36</sub>H<sub>65</sub>NO<sub>3</sub>: calcd. C 77.23, H 11.70, N 2.50; found C 77.25, H 12.01, N 2.47.

**N-Dodecylchenodeoxycholamide (3.5b):** <sup>1</sup>H NMR (CDCl<sub>3</sub>):  $\delta$  = 5.73 (s, 1H, NH), 3.84 (br. s, 1H, 7 $\alpha$ -CH), 3.45 (m, 1H, 3 $\alpha$ -CH), 3.21 (q, 2H, NCH<sub>2</sub>), 2.28-1.02 (m, 46H, aliphatic H), 0.91 (d, 3H, 21-CH<sub>3</sub>), 0.85 (m, 6H, 2 CH<sub>3</sub>), 0.63 (s, 3H, 18-CH<sub>3</sub>). - <sup>13</sup>C NMR (CDCl<sub>3</sub>):  $\delta$  = 173.4, 71.9, 68.4, 55.8, 50.4, 42.6, 41.4, 39.8, 39.6, 39.5, 39.4, 35.4, 35.3, 35.0, 34.5, 33.6, 32.8, 31.9, 31.8, 30.6, 29.6, 29.6, 29.5, 29.5, 29.3, 29.3, 28.2, 26.9, 23.7, 22.7, 22.6, 20.5, 18.3, 14.1, 11.7. - IR (KBr):  $\nu$  = 3312, 2926, 2854, 1648, 1558. - C<sub>36</sub>H<sub>65</sub>NO<sub>3</sub>·1.2H<sub>2</sub>O: calcd. C 74.35, H 11.68, N 2.41; found C 74.34, H 11.47, N 2.33.

**N-Cholyldodecanamide (3.6a):** <sup>1</sup>H NMR (CDCl<sub>3</sub>):  $\delta$  = 6.04 (s, 1H, NH), 3.95 (br. s, 1H, 12 $\alpha$ -CH), 3.83 (br. s, 1H, 7 $\alpha$ -CH), 3.44 (m, 1H, 3 $\alpha$ -CH), 3.18 (m, 2H, NCH<sub>2</sub>), 2.35-1.07 (m, 44H, aliphatic H), 0.97 (d, 3H, 21-CH<sub>3</sub>), 0.85 (m, 6H, 2 CH<sub>3</sub>), 0.66 (s, 3H, 18-CH<sub>3</sub>). - <sup>13</sup>C NMR (CDCl<sub>3</sub>):  $\delta$  = 173.3, 73.1, 71.9, 68.5, 46.9, 46.4, 41.6, 41.5, 40.0, 39.5, 39.4, 36.9, 35.4, 34.7, 34.6, 33.0, 31.9, 30.4, 29.6, 29.6, 29.5, 29.4, 29.4, 29.3, 28.1, 27.6, 26.3, 26.1, 25.9, 23.2, 22.7, 22.4, 17.7, 14.1, 12.5. - IR (KBr):  $\nu$  = 3396, 2925, 2854, 1648, 1558. - HRMS calcd for C<sub>36</sub>H<sub>65</sub>NO<sub>4</sub> (M<sup>+</sup>): 575.4914; found 575.4905.

**N-Cholyloctadecanamide (3.6b):** <sup>1</sup>H NMR (CDCl<sub>3</sub>):  $\delta$  = 5.56 (t, 1H, NH), 3.97 (br. s, 1H, 12 $\alpha$ -CH), 3.84 (br. s, 1H, 7 $\alpha$ -CH), 3.45 (m, 1H, 3 $\alpha$ -CH), 3.22 (m, 2H, NCH<sub>2</sub>), 2.31-1.06 (m, 56H, aliphatic H), 0.97 (d, 3H, 21-CH<sub>3</sub>), 0.87 (m, 6H, 2 CH<sub>3</sub>), 0.67 (s, 3H, 18-CH<sub>3</sub>). - <sup>13</sup>C NMR (CDCl<sub>3</sub>):  $\delta$  = 173.3, 73.1, 71.9, 68.5, 46.9, 46.3, 41.6, 41.5, 40.0, 39.5, 39.4, 36.9, 35.4, 34.7, 34.6, 33.0, 31.9, 30.3, 29.7, 29.7, 29.5, 29.4, 29.4, 29.4, 28.1, 27.6, 26.3, 26.1, 25.9, 23.2, 22.7, 22.4, 17.7, 14.1, 12.4. - IR (KBr):  $\nu$  = 3395, 2924, 2853, 1648, 1558. - C<sub>42</sub>H<sub>77</sub>NO<sub>4</sub>: calcd. C 76.42, H 11.76, N 2.12; found C 76.13, H 11.94, N 2.26.

**1,3-Bischolylamidopropane (3.7a):** <sup>1</sup>H NMR (CDCl<sub>3</sub>/CD<sub>3</sub>OD):  $\delta$  = 3.87 (br. s, 2H, 12 $\alpha$ -CH), 3.76 (br. s, 2H, 7 $\alpha$ -CH), 3.35 (m, 2H, 3 $\alpha$ -CH), 3.14 (m, 4H, NCH<sub>2</sub>), 2.30-1.05 (m, 50H, aliphatic H), 0.93 (d, 6H, 21-CH<sub>3</sub>), 0.82 (s, 6H, 19-CH<sub>3</sub>), 0.60 (s, 6H, 18-CH<sub>3</sub>). - <sup>13</sup>C NMR (CDCl<sub>3</sub>/CD<sub>3</sub>OD):  $\delta$  = 175.3, 72.8, 71.4, 68.1, 46.1, 46.1, 41.3, 41.2, 39.1, 39.0, 36.0, 35.3, 35.1,

34.5, 34.3, 32.7, 31.5, 30.8, 29.7, 28.8, 27.7, 27.3, 26.0, 23.0, 22.2, 17.0, 12.1. - IR (KBr):  $\nu$  = 3397, 2934, 2868, 1652, 1542. -  $C_{51}H_{86}N_2O_8 \cdot 1.5H_2O$ : calcd. C 69.43, H 10.17, N 3.18; found C 69.73, H 10.64, N 2.78. - FAB:  $M^+$  = 855, calcd. 855.2.

**1,12-Bischolylamidododecane (3.7b):**  $^1H$  NMR ( $CDCl_3/CD_3OD$ ):  $\delta$  = 3.95 (br. s, 2H, 12 $\alpha$ -CH), 3.82 (br. s, 2H, 7 $\alpha$ -CH), 3.37 (m, 2H, 3 $\alpha$ -CH), 3.19 (t, 4H,  $NCH_2$ ), 2.40-1.13 (m, 68H, aliphatic H), 1.00 (d, 6H, 21- $CH_3$ ), 0.90 (s, 6H, 19- $CH_3$ ), 0.68 (s, 6H, 18- $CH_3$ ). -  $^{13}C$  NMR ( $CDCl_3/CD_3OD$ ):  $\delta$  = 175.1, 72.9, 71.5, 68.2, 46.4, 46.2, 41.4, 41.3, 39.5, 39.3, 39.2, 39.1, 35.3, 35.2, 34.6, 34.4, 33.0, 32.9, 31.8, 29.8, 29.3, 29.3, 29.1, 27.9, 27.4, 26.7, 26.2, 23.1, 22.3, 17.1, 12.3. - IR (KBr):  $\nu$  = 3422, 2926, 2854, 1653, 1558. -  $C_{60}H_{104}N_2O_8$ : calcd. C 73.42, H 10.68, N 2.85; found C 73.44, H 11.09, N 2.83.

**trans-1,2-Bischolylamidocyclohexane (3.7c):**  $^1H$  NMR ( $CDCl_3/CD_3OD$ ):  $\delta$  = 3.92 (br. s, 2H, 12 $\alpha$ -CH), 3.77 (br. s, 2H, 7 $\alpha$ -CH), 3.52 (bm, 2H,  $NCH$ ), 3.34 (m, 2H, 3 $\alpha$ -CH), 2.32-1.10 (m, 56H, aliphatic H), 0.98 (d, 6H, 21- $CH_3$ ), 0.88 (s, 6H, 19- $CH_3$ ), 0.67 (s, 6H, 18- $CH_3$ ). -  $^{13}C$  NMR ( $CDCl_3/CD_3OD$ ):  $\delta$  = 175.6, 175.4, 73.3, 73.2, 72.0, 72.0, 68.7, 53.1, 53.0, 47.7, 47.1, 46.8, 46.7, 41.9, 41.8, 41.8, 41.7, 39.8, 39.7, 39.6, 36.9, 36.1, 35.8, 35.6, 35.1, 35.0, 35.0, 34.8, 32.8, 32.6, 32.5, 30.3, 30.3, 28.3, 28.3, 28.0, 26.7, 26.5, 25.1, 25.0, 23.5, 23.5, 22.7, 22.7, 17.5, 17.5, 12.7. - IR (KBr):  $\nu$  = 3422, 2935, 2865, 1648, 1541. -  $C_{54}H_{90}N_2O_8 \cdot 2H_2O$ : calcd. C 69.64, H 10.17, N 3.01; found C 69.97, H 10.52, N 2.64.

General procedure for the synthesis of alkylcholylurea, based on a literature procedure is as follows:<sup>10</sup> 2 g (4.5 mmol) of 24-aminocholane-3,7,12-triol hydrochloride was neutralized with KOH. The resulting 24-aminocholane-3,7,12-triol was dissolved in 30 ml of dichloromethane. Five millimoles of the appropriate alkyl isocyanate was added dropwise, and the solution was stirred at room temperature for 48 hours. The solvent was evaporated under vacuum and the residue was purified by flash column chromatography on silica using dichloromethane:methanol (95:5) as an eluent. Evaporation of the product-containing fractions under vacuum gave a white solid, generally in about 30% yield.

**N-Hexyl-N'-cholylurea (3.8a):**  $^1H$  NMR ( $CDCl_3/CD_3OD$ ):  $\delta$  = 3.94 (br. s, 1H, 12 $\alpha$ -CH), 3.82 (br. s, 1H, 7 $\alpha$ -CH), 3.41 (m, 1H, 3 $\alpha$ -CH), 3.16 (m, 4H,  $NCH_2$ ), 2.30-1.12 (m, 32H, aliphatic H), 0.96 (d, 3H, 21- $CH_3$ ), 0.85 (m, 6H, 2  $CH_3$ ), 0.65 (s, 3H, 18- $CH_3$ ). -  $^{13}C$  NMR ( $CDCl_3$ ):  $\delta$  = 159.0 (24-C), 73.3 (12-CH), 71.8 (3-CH), 68.5 (7-CH), 46.6 (17-CH), 46.3 (13-C), 41.6 (5-CH), 41.5 (14-CH), 41.0 (4- $CH_2$ ), 40.4 ( $CH_2$ ), 39.5 ( $CH_2$ ), 39.4 (8-CH), 35.5 (20-CH), 35.4 (1- $CH_2$ ), 34.8 (6- $CH_2$ ), 34.2 (10-C), 33.1 ( $CH_2$ ), 31.6 ( $CH_2$ ), 30.4 ( $CH_2$ ), 30.3 ( $CH_2$ ), 29.7 ( $CH_2$ ), 28.0 ( $CH_2$ ), 27.7 ( $CH_2$ ), 26.7 ( $CH_2$ ), 26.3 (9-CH), 23.4 ( $CH_2$ ), 22.6 ( $CH_2$ ), 22.4 (19- $CH_3$ ), 17.7 (21- $CH_3$ ), 14.1 ( $CH_3$ ), 12.4 (18- $CH_3$ ). - IR (KBr):  $\nu$  = 3378, 2931, 2862, 1642, 1569. -  $C_{31}H_{56}N_2O_4 \cdot 1.5H_2O$ : calcd C 67.97, H 10.86, N 5.11; found C 68.12, H 10.65, N 4.77.

**N-Dodecyl-N'-cholylurea (3.8b):**  $^1\text{H}$  NMR ( $\text{CDCl}_3$ ):  $\delta$  = 4.97 (br. t, 1H, NH), 4.90 (br. t, 1H, NH), 3.96 (br. s, 1H,  $12\alpha\text{-CH}$ ), 3.82 (br. s, 1H,  $7\alpha\text{-CH}$ ), 3.42 (m, 1H,  $3\alpha\text{-CH}$ ), 3.10 (m, 4H,  $\text{NCH}_2$ ), 2.40-1.10 (m, 44H, aliphatic H), 0.97 (d, 3H,  $21\text{-CH}_3$ ), 0.87 (m, 6H, 2  $\text{CH}_3$ ), 0.66 (s, 3H,  $18\text{-CH}_3$ ). -  $^{13}\text{C}$  NMR ( $\text{CDCl}_3$ ):  $\delta$  = 158.9, 73.3, 71.9, 68.5, 46.6, 46.3, 41.6, 41.5, 41.0, 40.4, 39.6, 39.4, 35.4, 35.3, 34.8, 33.1, 32.0, 31.9, 30.4, 29.8, 29.8, 29.7, 29.5, 29.4, 29.4, 28.0, 27.7, 27.2, 27.0, 26.3, 26.2, 23.3, 22.7, 22.4, 17.7, 14.1, 12.4. - IR (KBr):  $\nu$  = 3366, 2926, 2854, 1636, 1570. -

$\text{C}_{37}\text{H}_{68}\text{N}_2\text{O}_4 \cdot 0.5\text{H}_2\text{O}$ : calcd C 72.38, H 11.33, N 4.56; found C 72.41, H 11.48, N 4.31.

**N-Octadecyl-N'-cholylurea (3.8c):**  $^1\text{H}$  NMR ( $\text{CDCl}_3$ ):  $\delta$  = 5.03 (br. m, 1H, NH), 4.95 (br. m, 1H, NH), 3.95 (br. s, 1H,  $12\alpha\text{-CH}$ ), 3.82 (br. s, 1H,  $7\alpha\text{-CH}$ ), 3.41 (m, 1H,  $3\alpha\text{-CH}$ ), 3.10 (m, 4H,  $\text{NCH}_2$ ), 2.35-1.12 (m, 56H, aliphatic H), 0.97 (d, 3H,  $21\text{-CH}_3$ ), 0.87 (m, 6H, 2  $\text{CH}_3$ ), 0.66 (s, 3H,  $18\text{-CH}_3$ ). -  $^{13}\text{C}$  NMR ( $\text{CDCl}_3$ ):  $\delta$  = 159.3, 73.7, 72.3, 68.9, 47.1, 46.7, 42.1, 41.9, 41.5, 40.9, 40.0, 39.9, 35.8, 35.8, 35.2, 33.5, 32.3, 31.3, 30.9, 30.8, 30.1, 30.1, 30.1, 29.9, 29.8, 29.6, 28.5, 28.1, 27.4, 26.7, 26.6, 23.7, 23.1, 22.9, 18.2, 14.5, 12.9. - IR (KBr):  $\nu$  = 3364, 2924, 2852, 1632, 1577. -

$\text{C}_{43}\text{H}_{80}\text{N}_2\text{O}_4 \cdot \text{H}_2\text{O}$ : calcd C 73.04, H 11.69, N 3.96; found C 73.23, H 11.71, N 3.62.

General procedure for the synthesis of alkyl cholates is as follows: 2.05 g of cholic acid (5.0 mmol) was dissolved in 10 ml of the appropriate alcohol. A catalytic amount of p-toluenesulfonic acid was added and the mixture was stirred overnight at 80 °C. The excess of alcohol was removed by bulb-to-bulb distillation under vacuum, and the residue was purified by flash column chromatography on silica, using dichloromethane:methanol (96:4) as an eluent. Evaporation of the product-containing fractions in vacuum gave a white solid, generally in about 75% yield.

**Octyl cholate (3.9a):**  $^1\text{H}$  NMR ( $\text{CDCl}_3$ ):  $\delta$  = 4.03 (t, 2H,  $\text{OCH}_2$ ), 3.94 (br. s, 1H,  $12\alpha\text{-CH}$ ), 3.82 (br. s, 1H,  $7\alpha\text{-CH}$ ), 3.42 (m, 1H,  $3\alpha\text{-CH}$ ), 2.40-1.09 (m, 36H, aliphatic H), 0.96 (d, 3H,  $21\text{-CH}_3$ ), 0.86 (m, 6H, 2  $\text{CH}_3$ ), 0.65 (s, 3H,  $18\text{-CH}_3$ ). -  $^{13}\text{C}$  NMR ( $\text{CDCl}_3$ ):  $\delta$  = 174.5 (24-C), 73.1 (12-CH), 71.9 (3-CH), 68.4 (7-CH), 64.5 (O- $\text{CH}_2$ ), 47.0 (17-CH), 46.4 (13-C), 41.6 (5-CH), 41.4 (14-CH), 39.6 (4- $\text{CH}_2$ ), 39.5 (8-CH), 35.3 (1- $\text{CH}_2$ ), 35.2 (20-CH), 34.7 (6- $\text{CH}_2$ ), 34.6 (10-C), 31.8 ( $\text{CH}_2$ ), 31.3 ( $\text{CH}_2$ ), 30.9 ( $\text{CH}_2$ ), 30.3 ( $\text{CH}_2$ ), 29.2 ( $\text{CH}_2$ ), 29.2 ( $\text{CH}_2$ ), 28.6 ( $\text{CH}_2$ ), 28.1 ( $\text{CH}_2$ ), 27.5 ( $\text{CH}_2$ ), 26.3 (9-CH), 25.9 ( $\text{CH}_2$ ), 23.2 ( $\text{CH}_2$ ), 22.6 ( $\text{CH}_2$ ), 22.4 (19- $\text{CH}_3$ ), 17.3 (21- $\text{CH}_3$ ), 14.1 ( $\text{CH}_3$ ), 12.5 (18- $\text{CH}_3$ ). - IR (KBr):  $\nu$  = 3407, 2930, 2859, 1737. -  $\text{C}_{32}\text{H}_{56}\text{O}_5 \cdot 0.5\text{H}_2\text{O}$ : calcd. C 72.54, H 10.84; found C 72.50, H 11.05.

**Decyl cholate (3.9b):**  $^1\text{H}$  NMR ( $\text{CDCl}_3$ ):  $\delta$  = 4.04 (t, 2H,  $\text{OCH}_2$ ), 3.96 (br. s, 1H,  $12\alpha\text{-CH}$ ), 3.83 (br. s, 1H,  $7\alpha\text{-CH}$ ), 3.44 (m, 1H,  $3\alpha\text{-CH}$ ), 2.43-1.02 (m, 40H, aliphatic H), 0.97 (d, 3H,  $21\text{-CH}_3$ ), 0.86 (m, 6H, 2  $\text{CH}_3$ ), 0.67 (s, 3H,  $18\text{-CH}_3$ ). - IR (KBr):  $\nu$  = 3386, 2931, 2858, 1738. -

$\text{C}_{34}\text{H}_{60}\text{O}_5 \cdot 0.5\text{H}_2\text{O}$ : calcd. C 73.20, H 11.02; found C 73.21, H 11.32.

**Dodecyl cholate (3.9c):**  $^1\text{H}$  NMR ( $\text{CDCl}_3$ ):  $\delta$  = 4.03 (t, 2H,  $\text{OCH}_2$ ), 3.95 (br. s, 1H,  $12\alpha\text{-CH}$ ), 3.83 (br. s, 1H,  $7\alpha\text{-CH}$ ), 3.43 (m, 1H,  $3\alpha\text{-CH}$ ), 2.40-1.09 (m, 44H, aliphatic H), 0.97 (d, 3H,  $21\text{-CH}_3$ ), 0.86 (m, 6H, 2  $\text{CH}_3$ ), 0.66 (s, 3H,  $18\text{-CH}_3$ ). -  $^{13}\text{C}$  NMR ( $\text{CDCl}_3$ ):  $\delta$  = 174.5, 73.0, 71.9, 68.4, 64.4, 47.0, 46.4, 41.7, 41.4, 39.6, 39.5, 35.3, 35.2, 34.7, 34.6, 31.9, 31.3, 30.9, 30.4, 29.6, 29.6, 29.6, 29.5, 29.3, 29.3, 28.6, 28.1, 27.5, 26.4, 25.9, 23.2, 22.7, 22.4, 17.3, 14.1, 12.5. - IR (KBr):  $\nu$  = 3396, 2924, 2853, 1738. -  $\text{C}_{36}\text{H}_{64}\text{O}_5\cdot\text{H}_2\text{O}$ : calcd. C 72.68, H 11.18; found C 72.45, H 11.11.

## REFERENCES AND NOTES

- 1 P. Terech, R.G. Weiss, *Chem. Rev.* **1997**, 97, 3133-3159.
- 2 D.J. Abdallah, R.G. Weiss, *Adv. Mater.* **2000**, 12, 1237-1247.
- 3 J.H. van Esch, B.L. Feringa, *Angew. Chem., Int. Ed.* **2000**, 39, 2263-2266.
- 4 D.J. Abdallah, R.G. Weiss, *Langmuir* **2000**, 16, 352-355.
- 5 G. Mieden-Gundert, L. Klein, M. Fischer, F. Vögtle, K. Heuzé, J.L. Pozzo, M. Vallier, F. Fages, *Angew. Chem., Int. Ed.* **2001**, 40, 3164-3166.
- 6 S. Tamaru, M. Nakamura, M. Takeuchi, S. Shinkai, *Org. Lett.* **2001**, 3, 3631-3634.
- 7 K. Hanabusa, H. Nakayama, M. Kimura, H. Shirai, *Chem. Lett.* **2000**, 1070-1071.
- 8 K. Hanabusa, M. Matsumoto, M. Kimura, A. Kakehi, H. Shirai, *J. Coll. Int. Sci.* **2000**, 24, 231-244.
- 9 U. Maitra, V.K. Potluri, N.M. Sangeetha, P. Babu, A.R. Raju, *Tetrahedron: Asymmetry* **2001**, 12, 477-480.
- 10 J. van Esch, S. De Feyter, R.M. Kellogg, F. De Schryver, B.L. Feringa, *Chem. Eur. J.* **1997**, 3, 1238-1243.
- 11 M. de Loos, A.G.J. Ligtenbarg, J. van Esch, H. Kooijman, A.L. Spek, R. Hage, R.M. Kellogg, B.L. Feringa, *Eur. J. Org. Chem.* **2000**, 3675-3678.
- 12 Chapter 2 of this thesis or H.M. Willemen, T. Vermonden, A.T.M. Marcelis, E.J.R. Sudhölter, *Eur. J. Org. Chem.* **2001**, 2329-2335.
- 13 Y. Hishikawa, K. Sada, R. Watanabe, M. Miyata, K. Hanabusa, *Chem. Lett.* **1998**, 795-796.
- 14 U. Maitra, P.V. Kumar, N. Chandra, L.J. D'Souza, M.D. Prasanna, A.R. Raju, *Chem. Commun.* **1999**, 595-596.
- 15 K. Nakano, Y. Hishikawa, K. Sada, M. Miyata, K. Hanabusa, *Chem. Lett.* **2000**, 1170-1171.
- 16 C. Geiger, M. Stanescu, L. Chen, D.G. Whitten, *Langmuir* **1999**, 15, 2241-2245.
- 17 M. Amaike, H. Kobayashi, S. Shinkai, *Bull. Chem. Soc. Jpn.* **2000**, 73, 2553-2558.
- 18 V. Kim, A.V. Bazhenov, K.I. Kienskaya, *Colloid Journal* **1997**, 59, 455-460.
- 19 K. Inoue, Y. Ono, Y. Kanekiyo, T. Ishi-i, K. Yoshihara, S. Shinkai, *J. Org. Chem.* **1999**, 64, 2933-2937.
- 20 K.S. Partridge, D.K. Smith, G.M. Dykes, T.P. McGrail, *Chem. Commun.* **2001**, 319-320.
- 21 K. Hanabusa, A. Kawakami, M. Kimura, H. Shirai, *Chem. Lett.* **1997**, 191-192.
- 22 S. Bhattacharya, S.N. Ghanashyam Acharya, *Chem. Mater.* **1999**, 11, 3121-3132.
- 23 K. Inoue, Y. Ono, Y. Kanekiyo, K. Hanabusa, S. Shinkai, *Chem. Lett.* **1999**, 429-430.
- 24 M. de Loos, J. van Esch, I. Stokroos, R.M. Kellogg, B.L. Feringa, *J. Am. Chem. Soc.* **1997**, 119, 12675-12676.
- 25 G.D. Rees, B.H. Robinson, *Adv. Mater.* **1993**, 5, 608-619.
- 26 A.W. Ralston, R.A. Reck, H.J. Harwood, P.L. Dubrow, *J. Org. Chem.* **1948**, 13, 186-190.
- 27 A.F. Chaplin, D.H. Hey, J. Honeyman, *J. Chem. Soc* **1959**, 3194-3202.
- 28 K.M. Bhattacharai, A.P. Davis, J.J. Perry, C.J. Walter, S. Menzer, D.J. Williams, *J. Org. Chem.* **1997**, 62, 8463-8473.

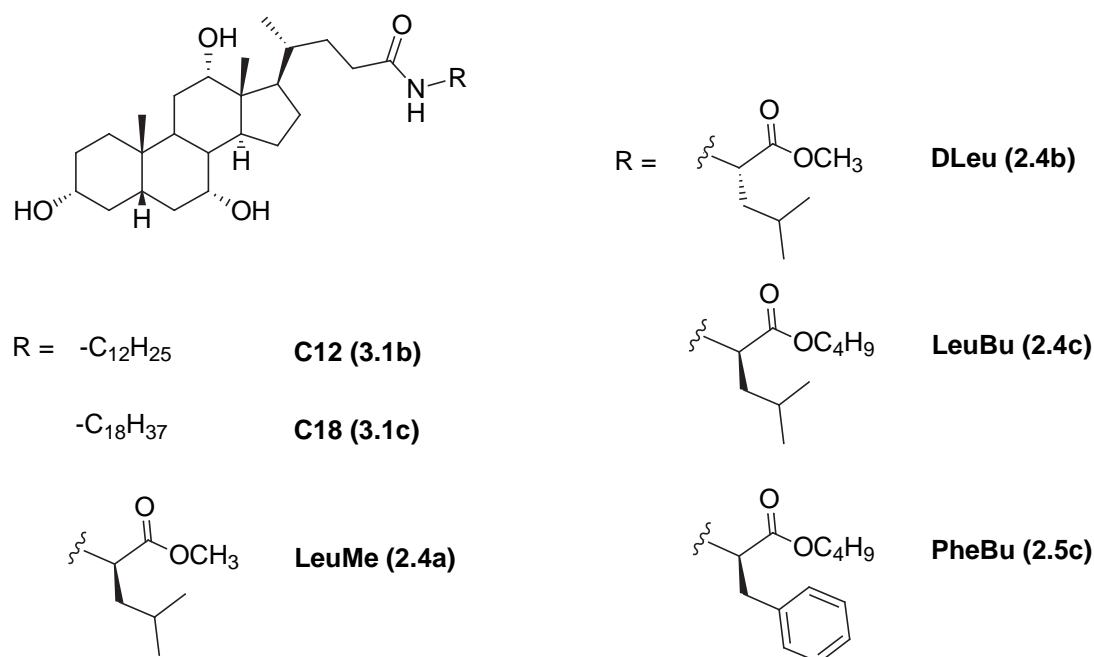
# 4

## **A small angle neutron scattering study on cholic acid based organogel systems**

*Small angle neutron scattering measurements were performed on some of the cholic acid derived gel systems previously described to gain more detailed information about the network structure. The presence of thin fibers with a radius of about 10-20 Å was found for various gelators. Two types of interaction between different sorts of fibers were demonstrated, depending on the gelator's molecular structure. The first type involves the presence of microcrystalline knots with a dimension of about 100-200 Å between the fibers. Upon heating, this network displays a gradual disintegration. The second type involves loose entanglements between flat fibers. The occurrence of these types of interaction is related to the length of the alkyl tail attached to cholic acid. Modeling shows that a major part of the gelator molecules is not taking part in the network, but is in solution.*

## 4.1 INTRODUCTION

In the previous chapters, organogel systems from cholic acid-based gelators in aromatic solvents were described. Although gelators of various molecular structures were used, the hydrogen bonded aggregation mode and corresponding molecular requirements for gelation are similar. Also, macroscopic properties of all gels, such as transparency and rigidity, seem equal. However, detailed information about the network structure and its dimensions is lacking. Electron microscopy (EM) studies revealed some differences between the network of different organogelators. EM-images for N-octadecylcholamide (**C18** in Scheme 4.1) in benzene show thin, almost monomolecular fibers.<sup>1</sup> For another type of gelator, i.e. N-cholyl D-leucine methyl ester (**DLeu** in Scheme 4.1) in benzene, EM images show thicker fibers,<sup>2</sup> but these could also be interpreted as bundles of fibers. Therefore, it would be interesting to obtain information about the structure and dimensions of the single fibers, and about the fiber-fiber interactions in the gel network of the different gelators. In this way, differences on (sub-)microscopic level can be revealed. Furthermore, it is worth investigating possible structural modifications correlated to the thermal behavior of these gels.



Scheme 4.1



A suitable method to obtain this kind of information is small angle neutron scattering (SANS).<sup>3</sup> This is a noninvasive technique, providing data about macromolecular systems on an Angstrom scale, ranging from about 10 to 1000 Å. The principle of SANS measurements is shown in Figure 4.1. Each neutron has a momentum  $k = 2\pi/\lambda$  in which  $\lambda$  is the wavelength of the neutron. A collimated neutron beam is scattered by a sample, and the scattered intensity after collision is measured by an area detector, which can be placed at variable distance. The scattering cross section  $(d\Sigma/d\Omega)(Q)$  is measured as a function of momentum transfer  $Q$ , which describes the relationship between the incident ( $k_i$ ) and scattered ( $k_s$ ) momentum. The following equation applies to  $Q$ :

$$Q = |k_s - k_i| = (4\pi/\lambda) \sin(\theta)$$

in which  $\theta$  is the angle between the  $k_i$  and  $k_s$ . The value  $Q$  quantifies length scales in reciprocal space. By substitution into the Bragg law of diffraction  $\lambda = 2d \sin(\theta)$  one obtains the equation  $d = 2\pi/Q$  in which  $d$  is in 'normal' length scale. This gives direct information about the size of scattering centers from the position of a diffraction peak in  $Q$ -space.

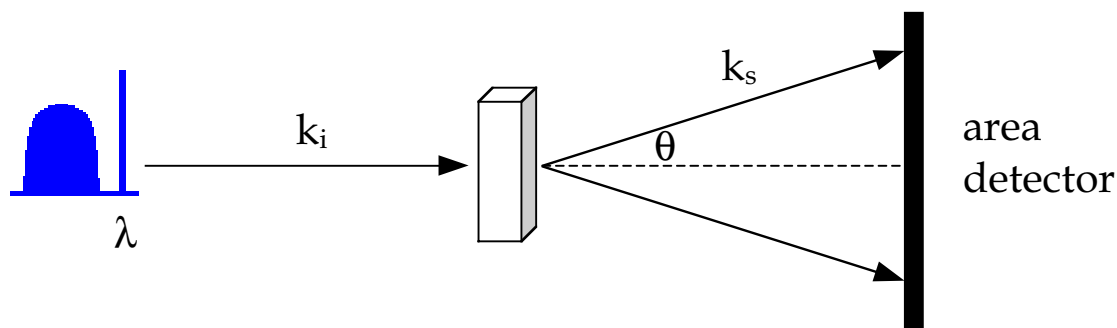


**Figure 4.1** Principle of SANS measurements

The scattered cross section can be related to the structure under study with the following relation for a monodisperse system

$$(d\Sigma/d\Omega)(Q) = \Delta\rho^2 C V^2 F^2(Q) S(Q)$$

in which  $\Delta\rho^2$  is the contrast (see Appendix 4.1),  $C$  is the number concentration of scattering particles,  $V$  is the volume of one particle,  $F(Q)$  is the form factor, and  $S(Q)$  is the structure factor.<sup>4</sup> The form factor describes the shape of the individual particles, such as spheres, rods, or rectangular fibers. The structure factor describes the interaction between the particles. This latter factor becomes more important at

higher concentrations, as for diluted systems  $S(Q)$  approaches 1. Furthermore, the structure factor has the most influence at small values of  $Q$ , where it usually causes a drop in intensity. Both factors will be included in modeling of the scattering curves.

Since the scattered cross section is a Fourier transform of the scattering length density  $\rho$ , and since the  $\rho$  values for hydrogen and deuterium are very different, we can use this to maximize the contrast. In our case, the use of deuterated benzene in combination with normal, hydrogen-containing gelators puts the gelator's structure in large contrast to the surrounding medium. Furthermore, the use of a deuterated solvent decreases the incoherent scattering, which enables measuring at large momentum transfer.

A number of gelators, which were discussed in the previous chapters, were studied with SANS. Scheme 4.1 shows these compounds and the names, which are used in this chapter, together with their original number.

## 4.2 RESULTS AND DISCUSSION

From here on we will only use the abbreviated symbol  $I(Q)$  instead of  $(d\Sigma/d\Omega)(Q)$  for the scattering cross section in the text and figures. Plots of the scattering cross section  $I(Q)$  as a function of momentum transfer  $Q$  were obtained for the various gels. An example for different concentrations of compound **LeuMe** is shown in Figure 4.2 in which the scales are plotted logarithmically.

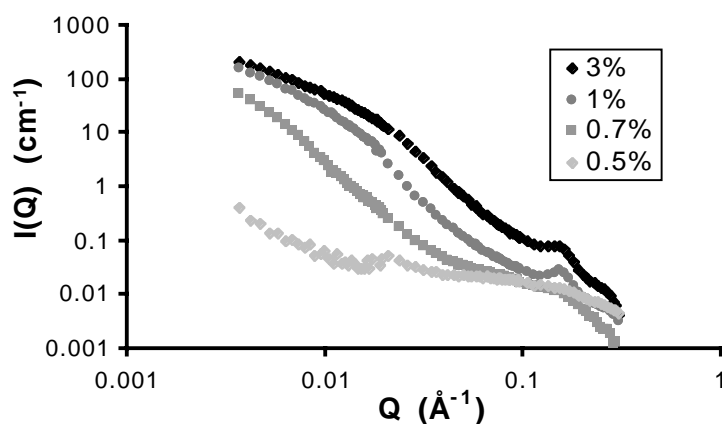


**Figure 4.2** Scattering cross section at various concentrations of **LeuMe**

As we can see, the scattered intensity increases with concentration, because the amount of scattering material increases. A remarkable result of this study is the enormous range in intensity that was obtained. We see that a dynamic range of nearly six orders of magnitude is obtained: from little below  $0.001$  to almost  $500 \text{ cm}^{-1}$ , which is very large for SANS measurements. It is due to the strength of the neutron source, the good quality of the instrument, the low background of the set-up, and the good quality of the samples.

Before looking any further at the results, we have to make some remarks. These gel systems are extremely sensitive to water, because the structure is based on hydrogen bonds. Although we tried to shield the gels from the environment, it is possible that some water diffused into the samples during measurements. Indeed, we noticed a diminishing of the gel's rigidity during the period of a measurement (which is several hours) for some samples, especially the samples with low concentration. So the results from the samples with lower concentrations might be less reliable. This can be seen in Figure 4.2 in which the scattering for a concentration of  $0.5\%$  has decreased considerably in the low  $Q$  range. The discontinuity is caused by the fact that the measurements at small angle (i.e. low  $Q$ ) were obtained last in time in this experiment.

Also, as with all kinds of aggregates, we assume there is a critical aggregation concentration ( $c_{ac}$ ), below which no aggregation takes place. Therefore, we have to keep in mind that part of the material is not contributing to the gel network, but is freely dissolved, and that the actual volume fraction, which causes scattering, is lower than the added volume fraction. This can influence calculations that are performed on basis of these plots. The fraction of gelator that is taking part in the network can also be influenced by the amount of water present. Furthermore, we do not know the exact density  $\delta$  of the materials. For calculations, we assume it equals  $1 \text{ g/ml}$ .

Other usefull ways to plot SANS results are shown in Figure 4.3 and 4.4. The first way is a plot of the product of  $I(Q)$  and  $Q$  vs.  $Q$ , both on a logarithmic scale. In this kind of plot, information can be gained from different  $Q$  ranges. If there is a plateau followed by a decay in the middle  $Q$  range, this usually indicates the

presence of rod-like fibers. For most of our systems we find curves with a plateau and decay, but there are some deviations. Appendix 4.2 shows these plots for all measured compounds, and two typical examples are shown in Figure 4.3. For the plot of **C18** we find a 'bump', instead of a plateau. This was also found for compounds **C12**, **LeuBu** and **PheBu**. In the plot of compound **LeuMe** we see a Bragg peak in the large  $Q$  range. Such a Bragg peak was also found in the plots of **DLeu**, but not in any other plots.

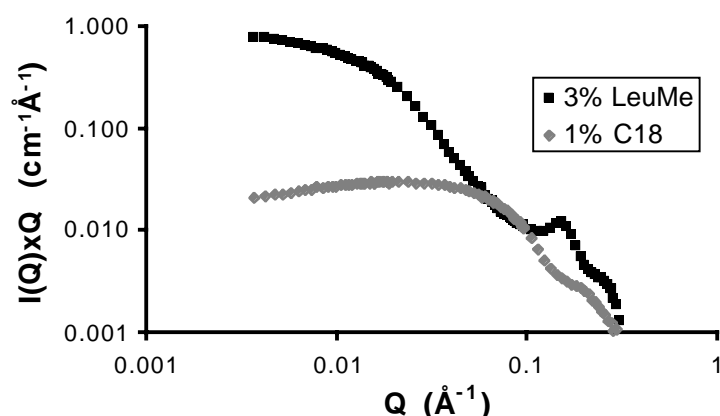


**Figure 4.3** Specially scaled plot of scattering cross section to show the fiber-like structure for compounds **C18** and **LeuMe**

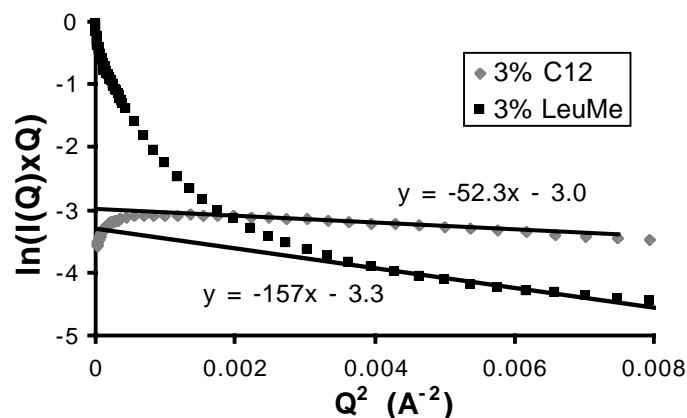


**Figure 4.4** Guinier plots for **C12** and **LeuMe**

The second way is a plot of  $\ln(I(Q) \times Q)$  vs.  $Q^2$ , which is presented in Figure 4.4 for 3% **C12** and 3% **LeuMe** and in Appendix 4.3 for all compounds. For most compounds a straight line with negative slope was found in the low  $Q$  range, a so-called Guinier plot. From these lines the radius of gyration ( $r$ ) can be calculated, assuming rod-like scatterers, using the following equation<sup>5</sup>

$$I(Q) = \{\phi(\pi r \Delta \rho)^2 / Q\} \exp(-Q^2 r^2 / 4)$$

or written as

$$\ln(I(Q) \times Q) = \ln \phi(\pi r \Delta \rho)^2 - Q^2 r^2 / 4$$

in which  $\phi$  is the volume fraction. Now the radius can be determined from the Guinier plot by two methods: from the slope or from the intercept at  $Q = 0$ . As an example, the calculation of the radius for 3% **C12** by both methods is given in Appendix 4.4. The Guinier equation is only valid in the low  $Q$  range, so the calculated values must meet the condition  $rxQ < 1$  in order to be considered reliable. In some cases, a positive slope was found. For **LeuMe** and **DLeu** this is caused by an extra component in the scattering at very low  $Q$ , which will be discussed later. Only negative slopes were used for calculations of the radius. Results are summarized in Table 4.1.

**Table 4.1** Radii calculated from the Guinier plots<sup>[a]</sup>

compound	concentration (wt%)	radius calc. from intercept (Å)	radius calc. from slope (Å)
<b>C12</b>	0.5	10.3	18.2
	1 <sup>[b]</sup>	9.4	15.6
	3	8.0	14.5
<b>C18</b>	0.5 <sup>[b]</sup>	7.8	13.0
	1	11.0	21.7
<b>LeuMe</b>	0.5 <sup>[b]</sup>	ps	ps
	0.7	3.4	9.6
	1	4.9	x
	3	7.3	x
<b>DLeu</b>	0.5 <sup>[b]</sup>	ps	ps
	1	2.8	x
<b>LeuBu</b>	3	7.4	13.8
	10	ps	ps
<b>PheBu</b>	3	5.9	9.8
	10	5.3	2.5

<sup>[a]</sup> ps = positive slope; x = condition  $rxQ < 1$  not met; <sup>[b]</sup> data less reliable because of water

When we compare the radii found with both methods from the Guinier plot, we see that, with an exception for **PheBu** 10%, the value obtained from the intercept is lower than the value obtained from the slope. This is caused by the use of the volume fraction in the first method. As mentioned before, there is an unknown  $\phi$ , which we have to consider. The amount of gelator in the fibers is always lower than the total amount added. So the calculated radius from the intercept is smaller than the actual value. Furthermore, there is quite some variation for the values obtained, as different concentrations of one gelator should give one value. Probably the effect of trace amounts of water on the fraction of dissolved gelator is considerable. This means that the radii obtained from the slope are most reliable.

Generally, the radius of the fibers for all compounds is about 10-20 Å. This means that the fibers are practically monomolecular in thickness. For example, these calculations give a fibrous radius of about 14 Å, and thus a mean diameter of 28 Å for **C12** and **C18**. These molecules in fully stretched conformation have lengths of 30 Å and 38 Å respectively. So the diameter of the fibers corresponds very well with the molecular length. Presumably, the steroid parts of these molecules are stacked in the center of a fiber, and the alkyl tails are located around the center, pointing outwards. One can assume that a larger alkyl tail is somewhat folded. Most fibers in hydrogen bonded gel systems, reported in literature, have diameters of about 100 Å and larger. So compared to other gelators, the fibers from these cholic acid derivatives are very thin. This explains the transparency of these gels. It also means that the obtained values are close to the lower limit of what can be measured using SANS.

From the different plots we can also get information about the way the single fibers interact with each other. When we look in some more detail at the plots for  $I(Q) \times Q$  vs.  $Q$  and  $\ln(I(Q) \times Q)$  vs.  $Q^2$  for all gelators, we see that there are generally two types of interaction in which the fibers are connected to each other, micocrystalline knots or entangled interactions. Both types are common among organogelators.<sup>6,7</sup>

### Microcrystalline knots

This first type of interaction is found for the gelators **LeuMe** and **DLeu**. In the plots of  $I(Q) \times Q$  vs.  $Q$  we find a typical middle  $Q$  range decay, which indicates the presence of rod-like scatterers. This is shown for **LeuMe** in Figure 4.3. However, a remarkable feature in these plots is a clear Bragg peak at  $Q = 0.155 \text{ \AA}^{-1}$ . A Bragg peak indicates the presence of crystalline packing in at least part of the structure. Probably the fibers are occasionally clustered together in micro-crystalline junction zones, or knots. The repeating unit inside the knots has dimension  $d = 2\pi/0.155 \approx 40 \text{ \AA}$ . The average size of the knots can be estimated from the width of the Bragg peak, which is about  $0.06 \text{ \AA}^{-1}$ . This corresponds roughly to an average size of  $2\pi/0.06 \approx 100 \text{ \AA}$ . So each knot contains only about 3 repeating units in length. There is a feature in the Guinier plots, shown in Figure 4.4, which confirms the presence of crystalline knots. At very low  $Q$  values the plot increases drastically, as a result of these crystalline knots. This increase has a considerable influence on the Guinier plot, and it complicates the calculation of the fibrous radius.

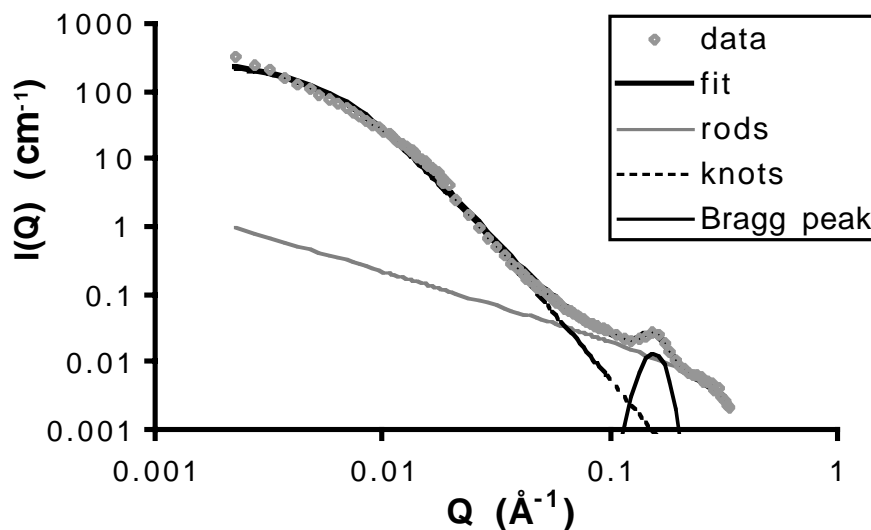


**Figure 4.5** Calculated fit for 1% **LeuMe** with cylindrical fibers

A different approach to gain information from SANS-data is to fit the experimental scattering curves with calculations using geometrical models. The interaction between the fibers may complicate these calculations, but the contribution of the crystalline knots can be calculated separately and taken into account in the

model. We have focused on modeling the scattering curves for **LeuMe**. A model was used, describing the gel's network structure as a mixture of round, rod-like fibers and micro-crystalline knots. In Figure 4.5 a modeled fit for **LeuMe** 1% is displayed, together with the experimental curve. The fit is the sum of three separate contributions: the rod-like fibers, the knots and the Bragg peak, which are also individually shown. Generally, at low Q range the largest contribution comes from the knots, at middle Q range from the rods, and at high Q range from the Bragg peak, which is again caused by the crystalline knots. The knots are described with the Debye-Bueche formula<sup>5</sup>

$$I(Q) = 8 \pi \phi_{\text{knots}} (1 - \phi_{\text{knots}}) (\Delta\rho)^2 d^3 / (1 + d^2 Q^2)^2$$

in which  $\phi_{\text{knots}}$  is the volume fraction of material in the knots and  $d$  is the average size of the knots. The knots do not have one particular shape, but are defined as an exponentially decreasing density. The rod-like fibers are described with equation<sup>8</sup>

$$I(Q) = (\phi_{\text{rods}}/2 Q r^2) [A \Delta\rho (2 J_1(Qr))/Qr]^2$$

in which  $\phi_{\text{rods}}$  is the volume fraction of material in the rods,  $A$  is the cross-sectional area of a rod, and  $J_1$  is the Bessel function of the first kind. The Bragg peak is described with a Gaussian equation with certain position, amplitude, and width.

Parameters describing the dimensions of the network in the model were varied to obtain the best possible fit. In Table 4.2 the resulting data are shown for fits of **LeuMe** at different concentrations. There is variation in obtained values between the different concentrations, but they give a general idea about the order of magnitude for the obtained values. The radius of the rods is about 10 Å and the average size of the knots is about 180 Å. These data are in the same order of magnitude as the results calculated directly from the width of the Bragg peak.

**Table 4.2** Data from modeled fits for **LeuMe**

concentration (wt%)	fiber radius (Å)	knot size (Å)	fraction material in fibers	fraction material in knots
0.7	10.3	300	0.05	0.03
1	6.4	149	0.26	0.14
3	9.5	87	0.16	0.16



Furthermore, we learn that the amount of material that is taken up in the network structure is rather low. For example, for a concentration of 1 wt%, only 40% of the material is taken up in the fibers and knots. This leaves a large amount of added material that is in solution and not taking part in the network structure. Especially for the concentration of 0.7% most material is dissolved; probably this concentration is not far above the cac. We also expected that the fraction of material in the network would increase with the concentration, but this was not found. Again we assume a disturbing effect of water in the samples. Even traces of water are expected to play an important role in the amounts of dissolved material. We do find that for higher concentrations the fraction of material in the knots is relatively larger than the fraction in the fibers, as one could expect. At a concentration of 3% the ratio between the two fractions is equal to one.

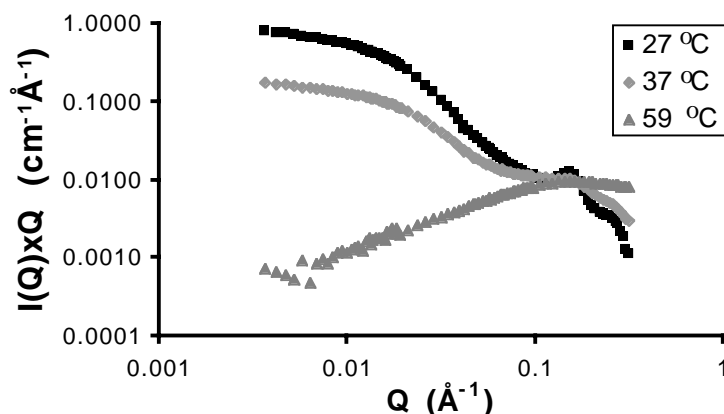


**Figure 4.6** Specially scaled plot of scattering cross section for 3% **LeuMe** at various temperatures

For **LeuMe** temperature-dependent measurements were performed to study the gel structure upon melting. In Figure 4.6 the curves of a 3% gel of **LeuMe** are shown for different temperatures. They show a decrease of scattered intensity at higher temperature. At 37 °C there is mostly a decrease in the scattering intensity at low  $Q$  values. The plot still shows the typical features for rod-like scatterers: a plateau followed by decay in the middle  $Q$  range. Also the radius that can be calculated from the Guinier plot has about the same value as the radius calculated for lower temperature. However, the Bragg peak in the scattering plot is much smaller. This indicates that the crystalline knots disintegrate first, while the fibers are still

intact. At 59 °C there is no scattering left at all, meaning that also the fibers have disintegrated. This gradual breakdown of the gel network corresponds to our earlier suggestion,<sup>1</sup> based on DSC measurements.

### Entangled interactions

This second type of interaction between the fibers is found for the gelators **C12**, **C18**, **LeuBu**, and **PheBu**. In the plots of  $I(Q) \times Q$  vs.  $Q$ , there is not a plateau followed by a decay or only a decay, but in the lower  $Q$  range, there is a "bump". This is shown for **C18** in Figure 4.3 and it indicates a strong interaction between the fibers. However, this interaction does not involve distinct knots, but more loose entanglements. Although SANS gives no information about the dynamics of the system, we assume these are transient entanglements. They can be considered as spaghetti-like interactions. Also the Guinier plots show a remarkable feature. At very small  $Q$  values a decreased intensity is observed, as shown for **C12** in Figure 4.4. This is a typical signature of the structure factor describing correlation between the fibers. This finding supports the idea of entangled interactions between the fibers.

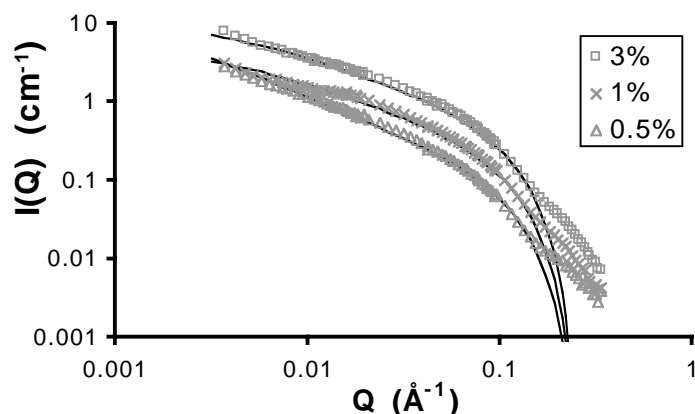


**Figure 4.7** Calculated fits (solid lines) for **C12** with cylindrical fibers

A lot of effort was made to model the experimental scattering curves for a compound with this type of interaction. However, we did not yet succeed in giving a full quantitative description of the measurements. Using the so-called random phase approximation we do effectively describe the low angle part of the scattering, as can be seen in Figure 4.7 for **C12** at various concentrations. The scattering for rod-like

scatterers was expressed in the function  $I(Q)$  in the same way as above. To take the interactions between the fibers into account, the scattering cross-section for correlated rods  $I_{\text{struc}}(Q)$  was expressed using the equation<sup>4</sup>

$$I_{\text{struc}}(Q) \propto I(Q)/[1 + v I(Q)]$$

in which  $v$  is proportional to the concentration of the cylinders. The scattering curve of **C12** with a concentration of 0.5 wt% could be well described with only isolated rods with a radius of 18.2 Å, as determined with the Guinier analysis. Calculations show that a fraction of 0.3 of the material is present in the fibers. The fit is satisfactory up till a momentum transfer of about 0.1 Å<sup>-1</sup>. For the scattering curve with a concentration of 1 wt% it was necessary to take correlation into account, and a good description of the data in the same  $Q$  range was obtained with a value of 0.1 for  $v$ . Again a fraction of 0.3 of the added material was present in the scattering fibers. The curve with a concentration of 3 wt% could be described in the same manner with a value of 0.1 for  $v$ , only with a fraction of 0.2 participating in the fibers. The discrepancies in the fit were again for  $Q$  larger than 0.1 Å<sup>-1</sup>. Thereafter the measured intensity is higher than the calculated intensity. There is a small bump visible at high  $Q$  values that is not described with this model.

The discrepancy between measured and modeled curves for all concentrations of **C12** at high  $Q$  value could indicate that a description with round fibers is not appropriate and that another cross-section for the fibers is more suited. So calculations were performed assuming the presence of rectangular fibers. In Figure 4.8 models are shown for cylindrical fibers and for rectangular fibers with different values for the aspect ratio  $a/b$  in which  $a$  and  $b$  represent half the sides of the rectangular cross-section. These calculations do not fit a particular data set, but are meant to give a general picture. For comparison, experimental data for 3% **C12** are shown. The rectangular model was described using the following equation<sup>9,10</sup>

$$I(Q) = (2C/Q) \Delta b^2 M_L \int_0^{\pi/2} [\{\sin(Qa \sin\phi) \sin(Qb \cos\phi)\} / \{Qa \sin\phi Qb \cos\phi\}]^2 d\phi$$

in which  $\Delta b$  is the specific neutron contrast of the fiber, and  $M_L$  is the mass per unit length of fiber. For these calculations a 10% spread in wavelength was taken into account. In the low  $Q$  range there is little difference between this model and the above described model for round fibers. However, for  $Q$  larger than 0.1 Å<sup>-1</sup> this

rectangular fiber model seems to fit the experimental data better. Especially the curves with aspect ratios of 0.25 and 0.5 seem to give a rather good resemblance to the experimental curve. Further data-analysis is still required and on its way.

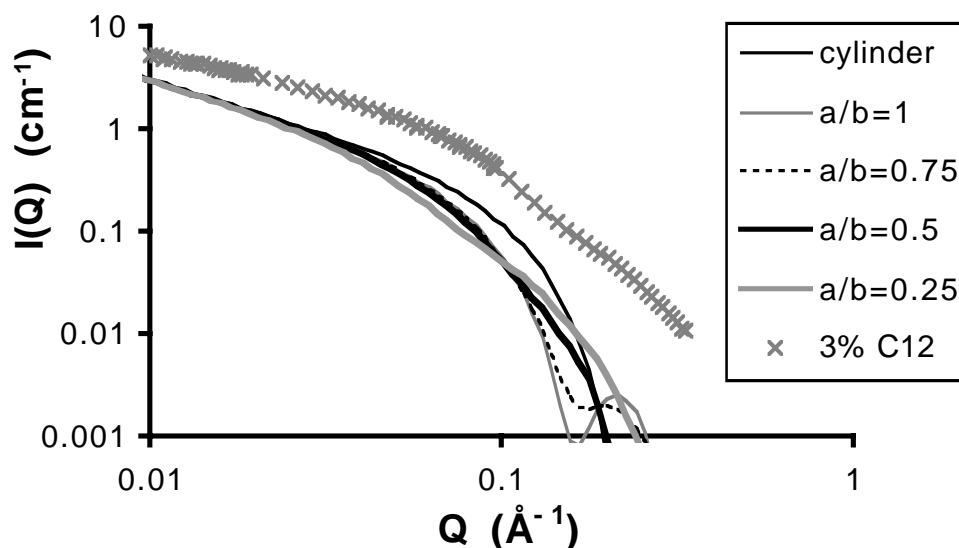


**Figure 4.8** Calculated fits for cylindrical fibers and rectangular fibers with different aspect ratios

This rectangular shape of fiber is formed by compounds **C12**, **C18**, **LeuBu**, and **PheBu**. They all show a similar curve with a characteristic, small bump at high  $Q$  value (above  $0.1 \text{ \AA}^{-1}$ ). Actually, from these calculations we may not conclude that the fibers are rectangular-shaped. They might as well be elliptical-shaped. What we can conclude is that these gelators form flattened fibers, probably with an aspect ratio of about 0.5 or lower. Based on their entangled interactions, we described the interactions in the gel networks from these compounds as spaghetti-like interactions before. Now it seems more correct to describe them as tagliatelle-like interactions.

So we have seen there is not only a difference in the interactions between the fibers of the various cholic acid-based gels. There is also a difference in the shape of the single fibers that are formed. One group of gelators forms a network of round fibers that connect by means of microcrystalline knots. A second group of gelators forms a network of flat fibers with loose entanglements. Comparing the molecular structures from the gelators in these two groups, a possible trend can be seen. In the group with the entangled flat fibers, all compounds contain an alkyl tail of at least 4

carbon atoms, which is attached to cholic acid, whether or not via an amino acid. On the other hand, in the group with the knotted, round fibers the compounds contain only a methyl group at that position. We suggest that the length of the alkyl tail determines the shape of the fiber and also which type of interaction between the single fibers takes place. Generally, a longer alkyl tail hampers a crystalline packing, so it not surprising that the compounds with a longer alkyl tail do not form crystalline knots. A possible explanation for the influence of the molecular structure on the shape of the fibers must lie in the packing inside such a fiber. If the molecules are arranged in an antiparallel fashion the alkyl tails could all lie in one direction, perpendicular to the long axis of the fiber. Increasing the length of the alkyl tail would increase the cross section of the fiber only in this direction, thus going from a round fiber to a flat one. Probably the changeover occurs around an alkyl tail length of 2 or 3 carbon atoms. A remarkable example in this respect is the difference between **LeuMe** and **LeuBu**. The only difference is the presence of a methyl group vs. a butyl group, whereas the rest of the molecule is identical, but both compounds form fibers with different shapes and different interactions.

#### 4.3 CONCLUSIONS

SANS measurements have shown the presence of thin fibers (radius  $\pm 10\text{-}20\text{ \AA}$ ) for all studied cholic acid based organogelators. There are two types of interaction between different, single fibers, depending on the gelator's molecular structure. Compounds with an alkyl tail of at least 4 carbon atoms attached to cholic acid, possibly via an amino acid spacer, have loose entanglements between flat fibers. Compounds with only a methyl group at that position, have crystalline knots with an average size of  $100\text{-}200\text{ \AA}$  between round fibers. This type of network displays a gradual disintegration upon heating. A large part of the gelator is not taking part in the network, but is freely dissolved.

## 4.4 EXPERIMENTAL SECTION

**General Remarks:** Synthesis and characterization of the compounds were previously described.<sup>1,2</sup> Benzene-d<sub>6</sub> (99.6% D) of p.a. quality was purchased from Aldrich. Gels were prepared by heating and subsequently cooling a solution of gelator in deuterated benzene in different concentrations: 0.5, 1, 3, and 10%. A grain of molsieve 4 Å was added to the prepared gels, to ensure they were anhydrous before the measurement.

SANS measurements were performed at the 58 MW reactor at Institut Laue-Langevin (ILL) in Grenoble, France at the D11 facility (Experiment number 9-11-803). The wavelength of the collimated neutron beam was 6 Å. Every sample was measured with a <sup>3</sup>He gas detector (CERCA) of 64x64 cm<sup>2</sup> at three distances: 1.1, 4, and 20m. The investigated Q range was 0.002–0.3 Å<sup>-1</sup>. The wavelength spread was about 10%. Samples in 1 mm pathway quartz cuvettes were placed in a sample holder, kept at constant temperature around 27 °C, unless stated otherwise. Corrections for background and transmission were applied. Background measurements consisted of empty cell and benzene-d<sub>6</sub>. Measurement of H<sub>2</sub>O was used for normalization.

## REFERENCES AND NOTES

- Chapter 2 of this thesis or H.M. Willemsen, T. Vermonden, A.T.M. Marcelis, E.J.R. Sudhölter, *Eur. J. Org. Chem.* **2001**, 2329-2335.
- Chapter 3 of this thesis or H.M. Willemsen, T. Vermonden, A.T.M. Marcelis, E.J.R. Sudhölter, accepted in *Langmuir* **2002**.
- For a more complete introduction to SANS: S.M. King, Chapter 7 of *Modern Techniques for Polymer Characterisation*, Ed R.A. Pethrick, J.V. Dawkins, Wiley, **1999**.
- For a review on analytical models for the interpretation of SANS data: J.S. Pedersen, *Adv. Colloid Interface Sci.* **1997**, 70, 171-210.
- P. Terech, A. Coutin, A.M. Giroud-Godquin, *J. Phys. Chem. B* **1997**, 101, 6810-6818.
- P. Terech, *Progr. Colloid Polym. Sci.* **1996**, 102, 64-70.
- P. Terech, *Ber. Bunsenges. Phys. Chem.* **1998**, 102, 1630-1643.
- Adapted from reference 5.
- P. Mittelbach, G. Porod, *Acta Phys. Austr.* **1961**, 14, 185-211.
- I.M. de Schepper, private communications.

## Appendix 4.1

### Calculation of the scattering length density $\rho$

The contrast  $\Delta\rho^2$  in SANS is the square of the difference in scattering length density  $\rho$  for the solvent and the solute. To calculate  $\rho$ , we use the following equation<sup>1</sup>

$$\rho = (\delta * N_A / M) * \sum_i b_i$$

in which  $\delta$  is the density ( $\delta_{\text{benzene}} = 0.95 \text{ g/cm}^3$ , we assume  $\delta = 1$  for all gelators),  $N_A$  is the Avogadro constant ( $= 6.022 * 10^{23}$ ),  $M$  is the molecular weight, and  $\sum_i b_i$  is the sum of the coherent neutron scattering lengths for all nuclei ( $b_C = 6.646 * 10^{-13} \text{ cm}$ ,  $b_H = -3.741 * 10^{-13} \text{ cm}$ ,  $b_D = 6.671 * 10^{-13} \text{ cm}$ ,  $b_N = 9.362 * 10^{-13} \text{ cm}$ , and  $b_O = 5.803 * 10^{-13} \text{ cm}$ ).  $\Delta\rho$  is the difference in  $\rho$  between benzene and gelator.

benzene-d<sub>6</sub>:  $C_6D_6$ ,  $M = 84.16 \text{ g/mol}$ ,  $\sum_i b_i = 7.9902 * 10^{-12} \text{ cm}$

$$\rho = 5.43 * 10^{10} \text{ cm}^{-2}$$

C12:  $C_{36}H_{65}NO_4$ ,  $M = 575.91 \text{ g/mol}$ ,  $\sum_i b_i = 2.8665 * 10^{-12} \text{ cm}$

$$\rho = 0.30 * 10^{10} \text{ cm}^{-2}$$

$$\Delta\rho = 5.13 * 10^{10} \text{ cm}^{-2}$$

C18:  $C_{42}H_{77}NO_4$ ,  $M = 660.07 \text{ g/mol}$ ,  $\sum_i b_i = 2.3649 * 10^{-12} \text{ cm}$

$$\rho = 0.22 * 10^{10} \text{ cm}^{-2}$$

$$\Delta\rho = 5.21 * 10^{10} \text{ cm}^{-2}$$

LeuMe / D-Leu:  $C_{31}H_{53}NO_6$ ,  $M = 535.76 \text{ g/mol}$ ,  $\sum_i b_i = 5.1933 * 10^{-12} \text{ cm}$

$$\rho = 0.58 * 10^{10} \text{ cm}^{-2}$$

$$\Delta\rho = 4.85 * 10^{10} \text{ cm}^{-2}$$

LeuBu:  $C_{34}H_{59}NO_6$ ,  $M = 577.84 \text{ g/mol}$ ,  $\sum_i b_i = 4.9425 * 10^{-12} \text{ cm}$

$$\rho = 0.52 * 10^{10} \text{ cm}^{-2}$$

$$\Delta\rho = 4.91 * 10^{10} \text{ cm}^{-2}$$

PheBu:  $C_{37}H_{57}NO_6$ ,  $M = 611.86 \text{ g/mol}$ ,  $\sum_i b_i = 7.6845 * 10^{-12} \text{ cm}$

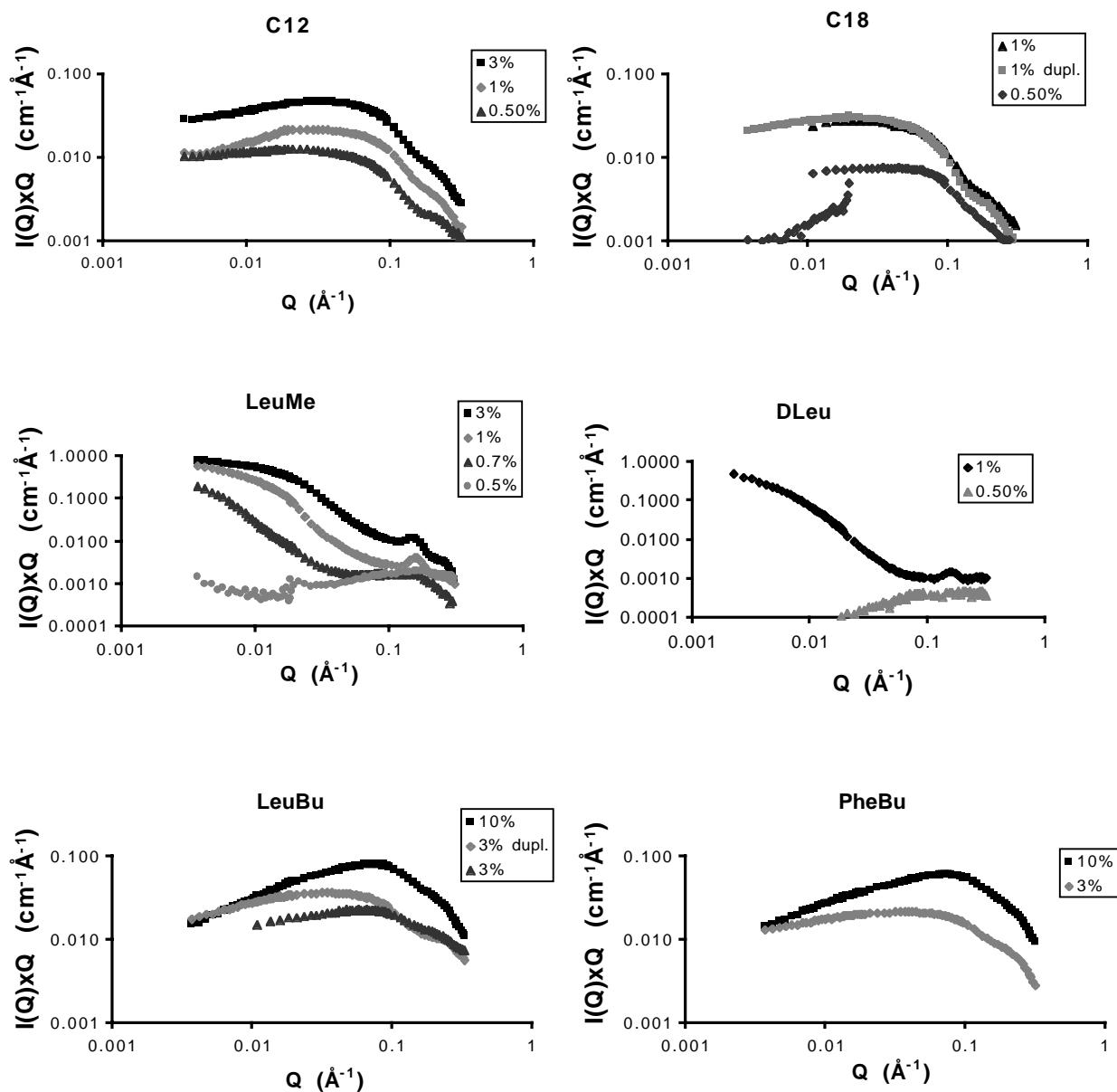
$$\rho = 0.76 * 10^{10} \text{ cm}^{-2}$$

$$\Delta\rho = 4.67 * 10^{10} \text{ cm}^{-2}$$

1 S.M. King, Chapter 7 of *Modern Techniques for Polymer Characterisation*, Ed. R.A. Pethrick, J.V. Dawkins, Wiley, 1999.

## Appendix 4.2

All specially scaled plots of scattering cross section for different compounds at various concentrations

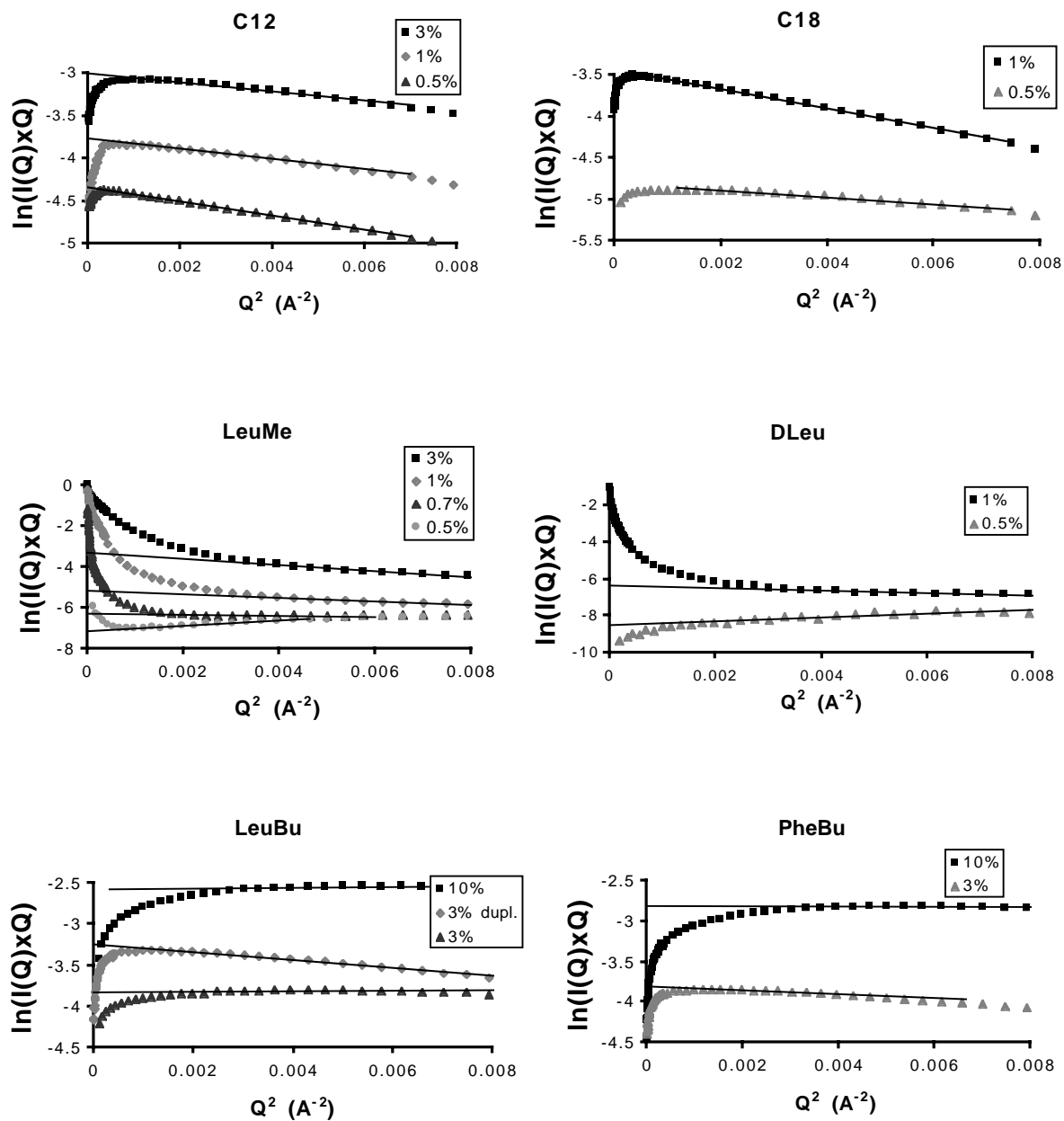


In some plots, the data points decrease drastically at low  $Q$ , caused by deterioration of the sample in time. The measurements at low  $Q$  were done last in time, sometimes a few hours after measuring the middle and high  $Q$  range. In two cases duplicate measurements were done.



## Appendix 4.3

### All Guinier plots for different compounds at various concentrations



## Appendix 4.4

### Calculation of the radius from Guinier-plot

As an example, we look at **C12** in benzene-d<sub>6</sub> in a concentration of 3 wt%, shown in Figure 4.4. In this graph a straight line is observed with the equation  $y = -52.305 x - 2.9979$ .

We calculate the radius of gyration, using the following equation

$$\ln(I(Q) \cdot Q) = \ln \phi(\pi r \Delta \rho)^2 - Q^2 r^2 / 4.$$

In the graph in Figure 4.4 the coordinates from the y-axis and x-axis are  $\ln(I(Q) \cdot Q)$  and  $Q^2$ , respectively. Therefore, the straight line can be described with the general equation

$$\ln(I(Q) \cdot Q) = \text{intercept} + \text{slope } Q^2$$

in which the intercept =  $\ln \phi(\pi r \Delta \rho)^2$  and the slope =  $-r^2/4$ . In the intercept as well as the slope,  $r$  is the only unknown variable, so  $r$  can be calculated from both.

#### Calculation from the intercept

We assume  $\delta = 1 \text{ g/ml}$ ;  $3 \text{ wt\%} = 3 \text{ g/100 ml} \Rightarrow \phi = 3 \text{ ml/100 ml} = 0.03$

$$\Delta \rho_{\text{benzene-C12}} = 5.13 \cdot 10^{10} \text{ cm}^{-2}$$

$$\text{intercept} = \ln \phi(\pi r \Delta \rho)^2 = -2.9979$$

$$\phi(\pi r \Delta \rho)^2 = 0.0499 \text{ \AA}^{-1} \text{ cm}^{-1} = 4.99 \cdot 10^6 \text{ cm}^{-2} = 0.03 (3.14 \cdot r \cdot 5.13 \cdot 10^{10})^2$$

$$\text{gives } r = 8.0 \cdot 10^{-8} \text{ cm} = 8.0 \text{ \AA}$$

#### Calculation from the slope

$$\text{slope} = -r^2/4 = -52.305$$

$$\text{gives } r = 14.5 \text{ \AA}$$

# 5

## **Aggregation of different amino acid conjugates of cholic acid in aqueous solution**

*A series of cholic acid derivatives was synthesized with a variety of  $\alpha$ -amino acids coupled via an amide bond. These conjugates form aggregates in aqueous solutions. Cryo-TEM images show the presence of small micelles with a size of about 5 nm for all compounds. Cmc values vary slightly with the molecular structure. A small decrease in cmc was found upon increasing the hydrophobicity of the amino acid. The cmc of the tyrosine conjugate showed a small pH-effect, increasing at high pH.*

## 5.1 INTRODUCTION

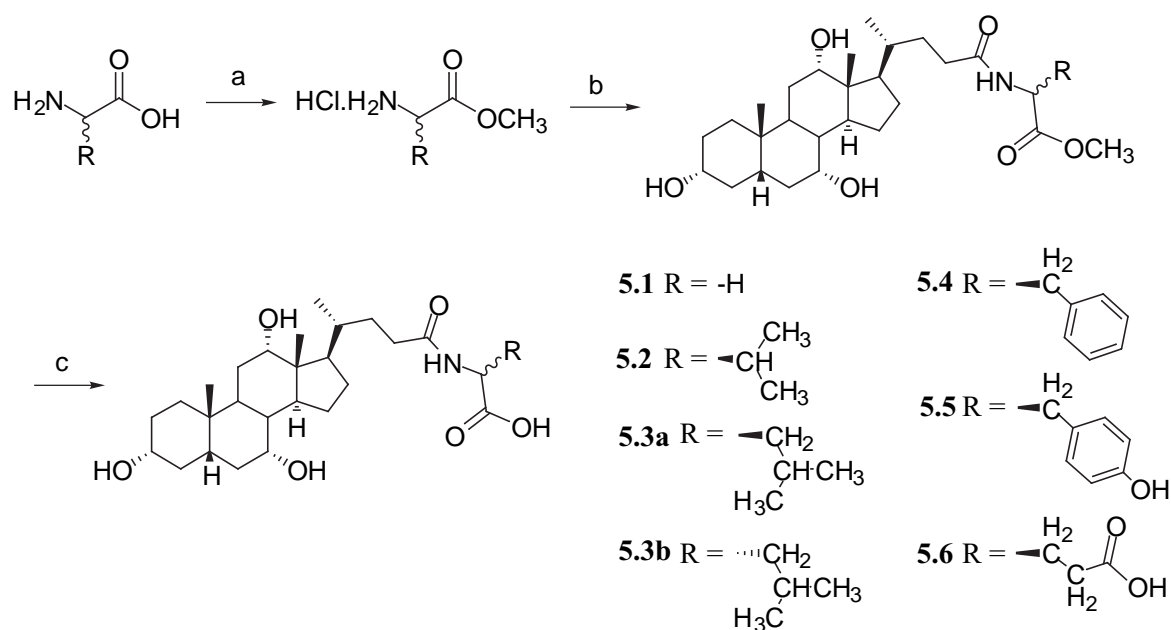
Bile salts are naturally occurring surfactants in mammals with an important function in the digestion of dietary lipids, by solubilizing them in mixed micelles. They are conjugates of bile acids with the sodium salts of the amino acids glycine or taurine. Conjugation lowers the  $pK_a$  value of the bile acids, and therefore increases the water-solubility at low pH.<sup>1</sup> Since cholic acid is the most important bile acid, there has been a lot of research on its conjugates glycocholate and taurocholate. Their synthesis has been reported and improved numerous times.<sup>2-8</sup> Also their aggregation behaviour has been the subject of various studies. The critical micelle concentration (cmc) has been determined for these compounds in many ways, but results are not consistent and were found to depend on the used conditions and techniques.<sup>9,10</sup>

It is interesting to extend this research with other amino acid conjugates besides glycine and taurine. Considering the availability of many naturally occurring amino acids, it is very well possible to couple other amino acids to cholic acid. With the variation in structure it might be possible to extend their applications. The advantage is that these compounds are composed of two natural components, making also medical applications feasible. So far, a number of amino acid conjugates of cholic acid other than with glycine or taurine is reported in literature. Forty years ago, synthesis of a series of amino acid-appended bile acids was reported in two Italian journals.<sup>11</sup> A number of them showed antimicrobial activity.<sup>12</sup> Other amino acid appended cholic acid derivatives with antibiotic activity are reported,<sup>13</sup> but in these compounds the amino acids are coupled to the hydroxyl groups instead of the carboxylate group. The synthesis of an alanine conjugate with a 'reversed' amide bond was described.<sup>14</sup> The metabolism and intestinal absorption of bile salts was studied using cholic acid conjugates with small peptides of 2-6 amino acids.<sup>15</sup> The gastrointestinal absorption of several amino acid conjugates was tested as a model for a possible drug delivery transport system using cholic acid conjugates. In this study, one amino acid analog cholic acid conjugate showed HIV-1 protease inhibitory activity.<sup>16</sup> Further applications for amino acid conjugates of cholic acid could be found as selectors in micellar elektrokinetic chromatography, as chiral stationary phases for HPLC or as chiral receptors in host-guest chemistry.

Although several amino acid derivatives of cholic acid have been prepared, little has been reported on their aggregation behavior in aqueous solution.<sup>17</sup> In this chapter, the synthesis of a series of  $\alpha$ -amino acid derivatives of cholic acid and their aggregation in aqueous solution is described. The aggregation behavior has been studied with UV-spectroscopy using Rhodamine 6G as a polarity sensitive probe. The aggregates were visualized with cryo-Transmission Electron Microscopy.

## 5.2 RESULTS AND DISCUSSION

A series of compounds was synthesized in which different  $\alpha$ -amino acids were attached to cholic acid via an amide bond. Scheme 5.1 shows the synthetic route.



**Scheme 5.1**

a:  $\text{SOCl}_2$ , MeOH, 0 °C, 1h, 95%; b: cholic acid, DEPC, TEA, DMF, 0 °C/rt, 24h, 70%; c:  $\text{K}_2\text{CO}_3$ , EtOH,  $\text{H}_2\text{O}$ , reflux, 24h, 80%

These compounds are well soluble in water at alkaline pH values, in which they spontaneously aggregate. To get an idea of the size of the aggregates, cryo-Transmission Electron Microscopy (TEM) images were made from 1 wt% aqueous solutions of compounds **5.1**, **5.3b** and **5.5**. Some examples are shown in Figure 5.1. It can be seen that the formed aggregates are small micelles. It is difficult to estimate the exact size, but the diameter of the micelles is about 5 nm. In the solution of

compound **5.1** there also are some larger aggregates visible of about 20 nm. These could be secondary aggregates, formed by clustering of the small micelles.

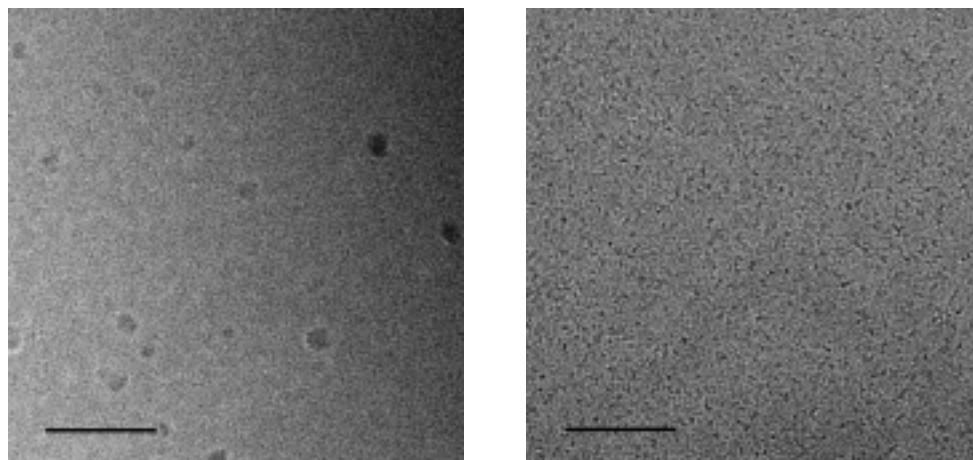
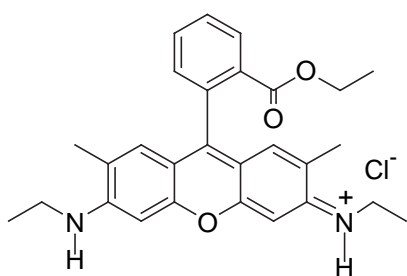


**Figure 5.1** Cryo-TEM images of 1 wt% solutions of compound **5.1** (left) and **5.3a** (right); bar indicates 100 nm

The critical micellar concentration (cmc) for each compound was determined using Rhodamine 6G as a probe.<sup>18</sup> This light-absorbing probe, shown in Scheme 5.2, is sensitive to the polarity of the direct surroundings. When the environment becomes more apolar, there is a shift in wavelength of maximal absorbance ( $\lambda_{\text{max}}$ ) from about 526 nm to about 538 nm.



**Scheme 5.2** Rhodamine 6G

The absorbance was measured for a series of solutions with a constant concentration of Rhodamine 6G, and with increasing concentrations of compounds **5.1-5.6**. An increase in  $\lambda_{\text{max}}$  indicates the formation of aggregates with an apolar interior. The lowest concentration that gives rise to an increase in  $\lambda_{\text{max}}$  is considered the cmc. An example is given in Figure 5.2 for compound **5.4** and results are listed in Table 5.1.

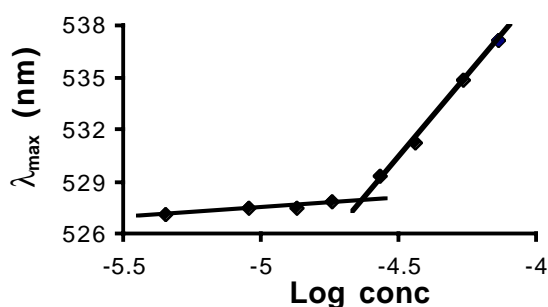


**Figure 5.2** Cmc-determination with Rhodamine 6G for compound 5.4

The cmc for compound 5.1 (glycocholate) was found to be 2.5 mM. Although comparison to literature values is hampered by lack of consistence through variation in circumstances, this value fits nicely in the order of magnitude given by others.<sup>9</sup> The method we use could lead to cmc values that are a bit lower as compared to other methods. Binding of a probe molecule gives a small hazard of inducing micellization, although the concentration Rhodamine 6G is 100-fold lower than the concentration surfactant. Since we use the same method for all compounds within this study, the results for the different conjugates can be compared.

**Table 5.1.** Cmc's of *N*-choly amino acids<sup>[a]</sup>

compound	cmc (mM) <sup>[b]</sup>	
5.1 (gly)	2.5	[±0.2]
5.2 (L-val)	2.1	[±0.3]
5.3a (L-leu)	1.7	[±0.1]
5.3b (D-leu)	2.0	[±0.2]
5.4 (L-phe)	1.4	[±0.1]
5.5 (L-tyr)	1.6	[±0.2]
5.6 (L-glu)	1.9	[±0.1]

<sup>[a]</sup> measured in 0.1M phosphate buffer at pH 8.0; <sup>[b]</sup> deviation in brackets

There is only little variation in cmc. Looking at compounds 5.1-5.4, there is a logical trend of decreasing cmc with increasing hydrophobicity of the amino acid sidegroup. With a larger hydrophobic part in the molecule, the drive to shield this from the polar solvent through aggregation is larger, and the cmc decreases.

A remarkable result is found for compounds **5.3a** and **5.3b**, with different stereochemistry in the leucine side group. The cmc values are 1.7 mM and 2.0 mM for the L and D derivative, respectively. The reason for this difference in physical behavior lies in the difference in diastereomeric interactions.

Compound **5.5** is more polar than compound **5.4**, because of the presence of an extra hydroxyl group, and therefore compound **5.5** has a slightly higher cmc. Compound **5.6** has two carboxylic acid groups, which will both be deprotonated at pH 8. Because of the polarity and high degree of hydration of such a bivalent compound, we expect a higher cmc. The cmc value is indeed higher than for compounds **5.5**, but it is still lower than for compounds **5.1** and **5.2**.

**Table 5.2.** Cmc's of *N*-cholyl amino acids at different pH values<sup>[a]</sup>

compound	pH	cmc (mM) <sup>[b]</sup>	
<b>5.3b</b> (D-leu)	7.0	1.9	[±0.1]
	8.0	2.0	[±0.2]
	9.0	1.9	[±0.2]
<b>5.5</b> (L-tyr)	7.0	1.5	[±0.1]
	8.0	1.6	[±0.2]
	10.5	1.9	[±0.2]
<b>5.6</b> (L-glu)	6.0	1.7	[±0.2]
	8.0	1.9	[±0.1]

<sup>[a]</sup> measured in 0.1M phosphate buffer; <sup>[b]</sup> deviation in brackets

For three compounds the effect of pH on the cmc was investigated. Results for compounds **5.3b**, **5.5** and **5.6** are summarized in Table 5.2. As expected, no effect was found for compound **5.3b** in the pH range 6-8. However, for compound **5.5** a small effect was observable. At pH 10.5 the cmc is higher as compared to pH 7 and 8. The phenolic hydroxyl group in tyrosine has a pK<sub>a</sub> value of 9.11. At higher pH, when the hydroxyl group is deprotonated, compound **5.5** has an extra ionic group. This increases the hydrophilicity and therefore the cmc. Compound **5.6** has two carboxylic acid groups, with pK<sub>a</sub> values of 2.19 and 4.25. Lowering the pH below 4.25 would theoretically decrease the cmc. However, this could not be experimentally



determined, because the solubility of compound **5.6** below pH 6 was too poor. The cmc at pH 6 is only slightly smaller than at pH 8.

### 5.3 CONCLUSIONS

A series of  $\alpha$ -amino acid conjugates of cholic acid was found to form small micelles of about 5 nm in aqueous solution, as was shown with cryo-TEM. Variation of the amino acid side group has a modest influence on the micellization behavior: there is a small decrease in cmc upon increasing the hydrophobicity. The influence of the extra carboxylate group in the bivalent glutamic acid conjugate on the cmc was only small. A small pH-effect was found for the cmc of the tyrosine conjugate, which increased at high pH, due to deprotonation of the phenolic group.

### 5.4 EXPERIMENTAL SECTION

**General remarks:**  $^1\text{H}$ -NMR spectra (200 MHz) were recorded on a Bruker AC200 spectrometer at ambient temperature. FT-IR spectra were recorded on a BIO-RAD FTS-7 spectrophotometer with a resolution of  $4\text{ cm}^{-1}$ . Compounds were measured as a solid in KBr. Elemental analyses were performed with an Elemental Analyzer EMASyst1106. - For cryo-TEM a drop of sample suspension was placed on a glow discharged holey carbon film. Excess liquid was blotted away with filter paper, and the grid was subsequently vitrified in liquid ethane, cooled with liquid nitrogen. The frozen hydrated grid was mounted in a Gatan cryo-stage (Gatan model 626) and observed in a Philips CM120 cryo transmission electron microscope operating at 120 kV. Images were recorded on a slow scan CCD camera under low-dose conditions. - For cmc measurements, a series of solutions was prepared of 0.25-0.5-0.75-1-1.5-2-3-4-5-6-8-10-12 mM of compounds **5.1-5.6** and 5.0  $\mu\text{M}$  of Rhodamine 6G, purchased from Acros, in 0.1 M  $\text{NaH}_2\text{PO}_4/\text{Na}_2\text{HPO}_4$  buffer, set at pH 8.0, unless stated otherwise. The  $\lambda_{\text{max}}$  was determined by measuring the absorbance from 520 to 540 nm, using a Perkin Elmer Lambda 18 UV/VIS spectrometer.

**Synthesis:** Used solvents were of p.a. quality. The purity of the products was verified with NMR, thin layer chromatography, and elemental analysis. Synthesis of these compounds was performed in three steps. The first two steps (preparation of amino acid methyl ester hydrochlorides and N-cholyl amino acids) and spectroscopic data of these compounds were described previously.<sup>19</sup> In the last step the methyl group was removed by base-catalysed

hydrolysis. 7 mmol of the N-cholyl amino acid methyl ester was dissolved in 15 ml of warm ethanol, and 15 ml of a 10 wt% aqueous solution of  $K_2CO_3$  was added. The mixture was refluxed for 24h, and then the ethanol was evaporated under vacuum. Water was added, and the mixture was acidified with HCl to pH 2, causing precipitation of the product. The precipitate was filtered, washed, and dried in a vacuum desiccator, giving a white powder, usually in 80% yield.

**N-Cholyl glycine (5.1):**  $^1H$ -NMR ( $CDCl_3/CD_3OD$ ):  $\delta$  = 3.80 (s, 1H,  $12\alpha$ -CH), 3.78 (s, 2H,  $NCH_2$ ), 3.67 (s, 1H,  $7\alpha$ -CH), 3.22 (m, 1H,  $3\alpha$ -CH), 2.28-0.95 (m, 24H, aliphatic H), 0.84 (d, 3H,  $21-CH_3$ ), 0.73 (s, 3H,  $19-CH_3$ ), 0.52 (s, 3H,  $18-CH_3$ ). - IR (KBr):  $\nu$  = 3375, 2927, 2866, 1736, 1639, 1561. -  $C_{26}H_{43}NO_6 \cdot 1.5H_2O$ : calcd. C 63.39, H 9.41, N 2.84; found C 63.50, H 9.66, N 2.54.

**N-Cholyl L-valine (5.2):**  $^1H$ -NMR ( $CDCl_3/CD_3OD$ ):  $\delta$  = 4.30 (d, 1H,  $C^*H$ ), 3.82 (s, 1H,  $12\alpha$ -CH), 3.68 (s, 1H,  $7\alpha$ -CH), 3.26 (m, 1H,  $3\alpha$ -CH), 2.30-0.98 (m, 25H, aliphatic H), 0.88-0.79 (m, 9H, 3  $CH_3$ ), 0.75 (s, 3H,  $19-CH_3$ ), 0.55 (s, 3H,  $18-CH_3$ ). - IR (KBr):  $\nu$  = 3423, 2935, 2870, 1722, 1656, 1529. -  $C_{29}H_{49}NO_6 \cdot H_2O$ : calcd. C 66.25, H 9.78, N 2.66; found C 66.41, H 9.74, N 2.51.

**N-Cholyl L-leucine (5.3a):**  $^1H$ -NMR ( $CDCl_3/CD_3OD$ ):  $\delta$  = 4.55 (dd, 1H,  $C^*H$ ), 3.84 (s, 1H,  $12\alpha$ -CH), 3.71 (s, 1H,  $7\alpha$ -CH), 3.30 (m, 1H,  $3\alpha$ -CH), 2.24-1.02 (m, 27H, aliphatic H), 0.89 (d, 3H,  $21-CH_3$ ), 0.83 (d, 6H, 2 Leu- $CH_3$ ), 0.78 (s, 3H,  $19-CH_3$ ), 0.57 (s, 3H,  $18-CH_3$ ). - IR: (KBr)  $\nu$  3422, 2937, 2870, 1723, 1656, 1541. -  $C_{30}H_{51}NO_6 \cdot 1.5H_2O$ : calcd. C 65.66, H 9.92, N 2.55; found C 65.75, H 9.69, N 2.45.

**N-Cholyl D-leucine (5.3b):**  $^1H$ -NMR ( $CDCl_3/CD_3OD$ ):  $\delta$  = 4.37 (dd, 1H,  $C^*H$ ), 3.80 (s, 1H,  $12\alpha$ -CH), 3.67 (s, 1H,  $7\alpha$ -CH), 3.21 (m, 1H,  $3\alpha$ -CH), 2.20-0.97 (m, 27H, aliphatic H), 0.86 (d, 3H,  $21-CH_3$ ), 0.80 (d, 6H, 2 Leu- $CH_3$ ), 0.75 (s, 3H,  $19-CH_3$ ), 0.53 (s, 3H,  $18-CH_3$ ). - IR: (KBr)  $\nu$  3422, 2937, 2869, 1722, 1655, 1543. -  $C_{30}H_{51}NO_6 \cdot 1.5H_2O$ : calcd. C 65.66, H 9.92, N 2.55; found C 65.49, H 9.82, N 2.50.

**N-Cholyl L-phenylalanine (5.4):**  $^1H$ -NMR ( $CDCl_3/CD_3OD$ ):  $\delta$  = 7.12 (m, 3H, aromatic H), 7.04 (m, 2H, aromatic H), 4.63 (t, 1H,  $C^*H$ ), 3.81 (s, 1H,  $12\alpha$ -CH), 3.70 (s, 1H,  $7\alpha$ -CH), 3.23 (m, 1H,  $3\alpha$ -CH), 3.00 (m, 2H, Ph- $CH_2$ ), 2.20-0.93 (m, 24H, aliphatic H), 0.83 (d, 3H,  $18-CH_3$ ), 0.76 (s, 3H,  $19-CH_3$ ), 0.53 (s, 3H,  $18-CH_3$ ). - IR (KBr):  $\nu$  = 3422, 2935, 2868, 1726, 1652, 1525. -  $C_{33}H_{49}NO_6 \cdot 2H_2O$ : calcd. C 66.98, H 9.03, N 2.37; found C 67.01, H 8.67, N 2.31.

**N-Cholyl L-tyrosine (5.5):**  $^1H$ -NMR ( $CDCl_3/CD_3OD$ ):  $\delta$  = 6.86 (d, 2H, aromatic H), 6.60 (d, 2H, aromatic H), 4.56 (t, 1H,  $C^*H$ ), 3.80 (s, 1H,  $12\alpha$ -CH), 3.69 (s, 1H,  $7\alpha$ -CH), 3.26 (m, 1H,  $3\alpha$ -CH), 2.90 (m, 2H, Ph- $CH_2$ ), 2.15-0.93 (m, 24H, aliphatic H), 0.81 (d, 3H,  $18-CH_3$ ), 0.76 (s, 3H,  $19-CH_3$ ), 0.53 (s, 3H,  $18-CH_3$ ). - IR (KBr):  $\nu$  = 3421, 2935, 2868, 1725, 1652, 1516. -  $C_{33}H_{49}NO_7 \cdot 1.8H_2O$ : calcd. C 65.60, H 8.78, N 2.32; found C 65.67, H 8.59, N 2.18.

**N-Cholyl L-glutamic acid (5.6):**  $^1\text{H-NMR}$  ( $\text{CDCl}_3/\text{CD}_3\text{OD}$ ):  $\delta$  = 4.41 (m, 1H, C\*H), 3.90 (s, 1H,  $12\alpha\text{-CH}$ ), 3.77 (s, 1H,  $7\alpha\text{-CH}$ ), 3.35 (m, 1H,  $3\alpha\text{-CH}$ ), 2.41-1.05 (m, 28H, aliphatic H), 0.96 (d, 3H,  $21\text{-CH}_3$ ), 0.85 (d, 3H,  $19\text{-CH}_3$ ), 0.64 (s, 3H,  $18\text{-CH}_3$ ). - IR: (KBr)  $\nu$  3405, 2937, 2869, 1724, 1651, 1543. -  $\text{C}_{29}\text{H}_{47}\text{NO}_8 \cdot 3\text{H}_2\text{O}$ : calcd. C 58.86, H 9.03, N 2.37; found C 58.91, H 8.70, N 2.31.

## REFERENCES AND NOTES

- 1 J.B. Carey Jr., in *The Bile Acids, Vol. 2 Physiology and Metabolism*, Eds. P.P. Nair, D. Kritchevsky, Plenum Press - New York, **1973**, pp. 64.
- 2 S. Bondi, E. Müller, *Z. Physiol. Chim.* **1906**, 47, 499-506.
- 3 F. Cortese, L. Bauman, *J. Am. Chem. Soc.* **1935**, 57, 1393-1395.
- 4 F. Cortese, *J. Am. Chem. Soc.* **1937**, 59, 2532-2534.
- 5 E.F. Curragh, D.T. Elmore, *Biochem. J.* **1964**, 93, 163-171.
- 6 L. Lack, F.O. Dorrity Jr., T. Walker, G.D. Singletary, *J. Lipid Res.* **1973**, 14, 367-370.
- 7 K.Y. Tserng, D.L. Hachey, P.D. Klein, *J. Lipid Res.* **1977**, 18, 404-407.
- 8 T. Momose, T. Tsubaki, T. Iida, T. Nambara, *Lipids* **1997**, 32, 775-778.
- 9 D.M. Small, in *The Bile Acids, Vol. 1 Chemistry*, Eds. P.P. Nair, D. Kritchevsky, Plenum Press - New York, **1971**, chapter 8, and references cited herein.
- 10 More recently: E. Bottari, A.A. D'Archivio, M.R. Festa, L. Galantini, E. Giglio, *Langmuir* **1999**, 15, 2996-2998., E. Bottari, M.R. Festa, M. Franco, *Langmuir* **2002**, 18, 2337-2342, and references cited herein.
- 11 G.B. Crippa, A.M. Bellini, A. Crippa, *Ann. Chim. (Rome)* **1963**, 53, 1496-1502 (in Italian).
- 12 A.M. Bellini, G. Vertuani, M.P. Quaglio, *Il Farmaco-Ed. Sc.* **1979**, 34, 967-970 (in Italian with English abstract); A.M. Bellini, M.P. Quaglio, M. Guarneri, G. Cavazinni, *Eur. J. Med. Chem. - Chim. Ther.* **1983**, 185-190.
- 13 Atiq-ur-Rehman, C. Li, L.P. Budge, S.E. Street, P.B. Savage, *Tetrahedron Lett.* **1999**, 1865-1868.
- 14 J.P. Coleman, L.C. Kirby, R.A. Klein, *J. Lipid Res.* **1995**, 36, 901-910.
- 15 P.W. Swaan, K.M. Hillgren, F.C. Szoka Jr., S. Oie, *Bioconjugate Chem.* **1997**, 8, 520-525.
- 16 M. Kagedahl, P.W. Swaan, C.T. Redemann, M. Tang, C.S. Craik, F.C. Szoka Jr., S. Oie, *Pharm. Res.* **1997**, 14, 176-180.
- 17 T. Nakashima, T. Anno, H. Kanda, Y. Sato, T. Kuroi, H. Fujii, S. Nagadome, G. Sugihara, *Colloids Surf., B* **2002**, 24, 103-110.
- 18 M.C. Carey, D.M. Small, *J. Colloid Interface Sci.* **1969**, 31, 382-396.
- 19 Chapter 2 of this thesis or H.M. Willemen, T. Vermonden, A.T.M. Marcelis, E.J.R. Sudhölter, *Eur. J. Org. Chem.* **2001**, 2329-2335.



# 6

## **Micellization, thermodynamics, and antimicrobial activity of cholic acid based facial amphiphiles carrying three permanent ionic head groups**

*The facial amphiphilicity of cholic acid was emphasized by attaching three ionic  $\omega$ -trimethylammoniocarboxylate groups to the hydroxyl groups of the steroid skeleton via a short spacer. Esterification of the carboxylate group with a hydrophobic alkyl tail gave permanently ionic, three-headed surfactants. Electron microscopy of aggregates of these compounds in water showed the formation of spherical micelles, whose size is dependent on the alkyl tail length. The micellization behavior in water was studied as a function of the spacer length and the alkyl tail length: both were found to have a small influence on the cmc. Also ITC was used to gain information on the cmc, but furthermore it provided information on the thermodynamics of micellization. These surfactants show rather normal temperature-dependent behavior: cmc increases and enthalpy of micellization decreases with temperature, Gibbs energy of micellization is almost constant, and micellization is mainly entropy-driven. A possible application of these compounds can be found in their antimicrobial activity: compounds with the shortest alkyl tail inhibit growth of gram-positive as well as gram-negative bacteria.*

## 6.1 INTRODUCTION

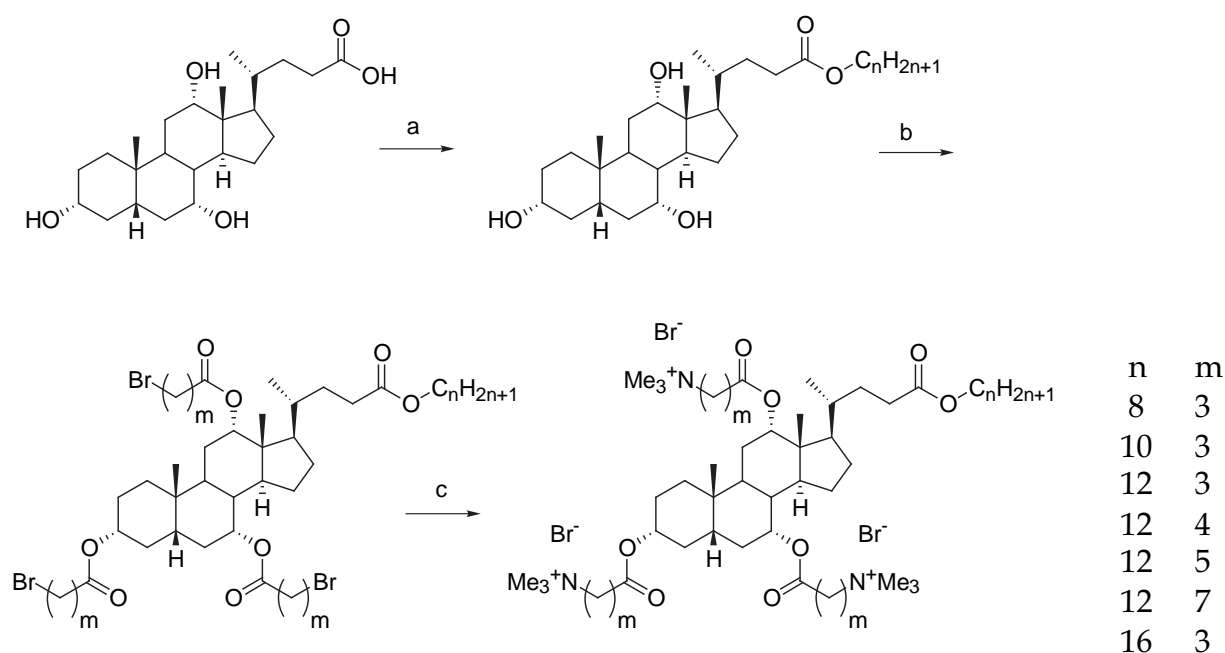
Cholic acid, a main bile acid, is a biosurfactant involved in the digestion of dietary lipids. With the carboxylate group as the ionic head group it resembles a 'classical' surfactant. However, due to the steroid part with three hydroxyl groups on one side, it is often considered a facial amphiphile. These hydroxyl groups can have specific interactions, as found in inclusion compounds,<sup>1,2</sup> organogelators,<sup>3-6</sup> and receptors<sup>7,8</sup> based on cholic acid. Furthermore, the hydroxyl groups, each with a different reactivity,<sup>9</sup> are highly suitable as synthetic handles. Their polarity can be increased to emphasize the facial amphiphilicity of the steroid unit. The resulting facial amphiphiles have excellent applications in ion transport,<sup>10,11</sup> combinatorial chemistry,<sup>12</sup> vesicle fusion,<sup>13</sup> and membrane permeabilization.<sup>14</sup> Even facial amphiphiles with three ionic groups are reported.<sup>15,16</sup> However, the properties of these cationic ( $\text{NH}_3^+$ ) or anionic ( $\text{COO}^-$ ) facial amphiphiles are dependent on the pH of the solution.

In this chapter, a series of new facial amphiphiles with a permanent ionic character is presented. Three cationic trimethylammonium groups were attached to cholic acid, and the carboxylate group was esterified, to yield a new class of three-headed surfactants. A well-known class of surfactants with three head groups is the oligomeric surfactant, but this has also three hydrophobic tails.<sup>17</sup> We know of only one other example of a surfactant with three permanent ionic head groups and one hydrophobic tail.<sup>18</sup> We discuss the aggregation of this new type of surfactant into spherical micelles. Micellization was studied as a function of the alkyl tail length and the spacer length by conductivity measurements and isothermal titration calorimetry (ITC). ITC was also used to obtain information on the thermodynamics of micellization.<sup>19</sup> Furthermore, its antimicrobial activity is discussed.

## 6.2 RESULTS AND DISCUSSION

Synthesis of this new series of ionic facial amphiphiles was completed in 3 steps from cholic acid, as depicted in Scheme 6.1. First, the carboxylate group was esterified with a long alkyl tail. Then, a methylene spacer was attached to all three hydroxyl groups using an  $\omega$ -bromoalkanoic chloride. Finally, the bromine atoms

were substituted by trimethylamine to give trimethylammonium groups. The overall yield of this route is about 45%.



**Scheme 6.1**

a:  $C_nH_{2n+1}OH$ , pTSA, benzene, 90 °C, 24h, 75%; b:  $Br-(CH_2)_m-COCl$ , DMAP, benzene, pyridine, RT, 24h, 65%; c:  $NMe_3$ , EtOH, 100 °C, 24h, 90%

Variation was made in the length of the alkyl tail ( $n = 8, 10, 12, 16$ ) and the length of the spacer ( $m = 3, 4, 5, 7$ ). In addition to NMR and IR, the composition of the compounds was verified by mass spectrometry. For all compounds, a main peak was found at  $m/z [M-Br]^+$ . In Figure 6.1a the mass spectrum of compound **n12m4** is shown. Besides the  $[M-Br]^+$  peak at  $m/z$  1160, also the  $[M-2Br]^{2+}$  peak at  $m/z$  541 stands out. Because of the presence of different isotopes, especially bromine, the spectra show specific peak patterns. Figure 6.1b shows the theoretical peak pattern for a compound with formula  $C_{60}H_{112}N_3O_8Br_2$ , which corresponds to  $[n12m4-Br]^+$ . This peak pattern corresponds very well with the experimental  $[M-Br]^+$  peak pattern from compound **n12m4**, enlarged in Figure 6.1c.

These new compounds are very hygroscopic. Solutions with accurately defined concentration were therefore prepared from lyophilized solutions. Due to the long aliphatic tail, aggregation occurs at rather low concentrations, about 1 mM.

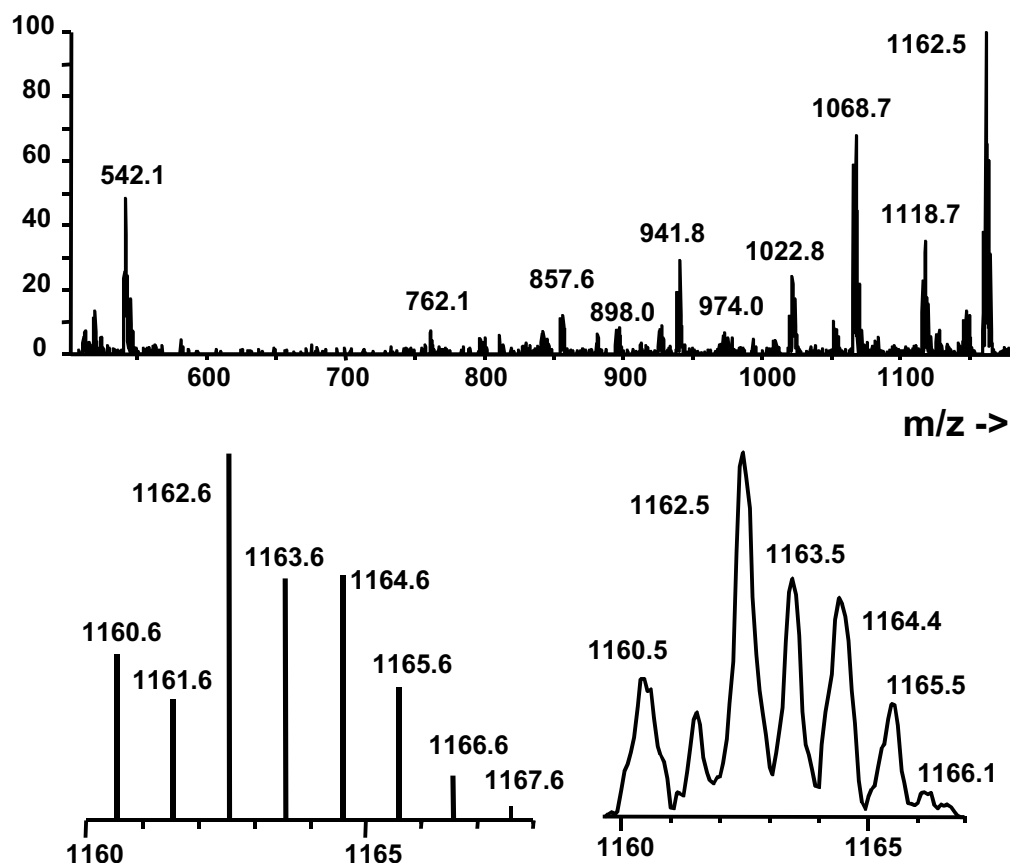


**Figure 6.1** a)(top): Mass spectrum for compound **n12m4**; b)(bottom left): Theoretical isotope peak pattern for  $C_{60}H_{112}N_3O_8Br_2$ , i.e.  $[n12m4-Br]^+$ ; c)(bottom right): Enlarged detail of mass spectrum for compound **n12m4**

Proof for micelle formation was obtained from cryo-Transmission Electron Microscopy (TEM) measurements. For several compounds, cryo-TEM images were made of aqueous solutions of 1 wt% (about 8 mM). Two examples are shown in Figure 6.2. The images show small aggregates with an average diameter of 3-6 nm. The aggregates for **n8m3** are smaller than those for **n16m3** (3-4 nm and 5-6 nm, respectively), displaying the influence of the alkyl tail length on micellar size. No elliptical or bar-shaped aggregates are visible, indicating that the aggregates are spherical micelles. To verify this, a density histogram was created for a single aggregate, showing indeed a Gaussian distribution. Occasionally, larger aggregates with a diameter of 15-50 nm can be seen. These aggregates have the same density variation as the small ones, so they are not vesical structures. We assume the occurrence of secondary micelles, formed by clustering of the small, primary micelles, similar to the two-step aggregation behavior of cholic acid itself.<sup>20</sup> Dynamic



light scattering (DLS) measurements on aqueous solutions of compounds **n10m3** and **n16m3** roughly show the presence of many aggregates with a diameter of about 5 nm and a few larger aggregates with a diameter of several tens of nanometers. These values are calculated, assuming a spherical shape of the aggregates. These values correspond with the ones obtained from cryo-TEM images.

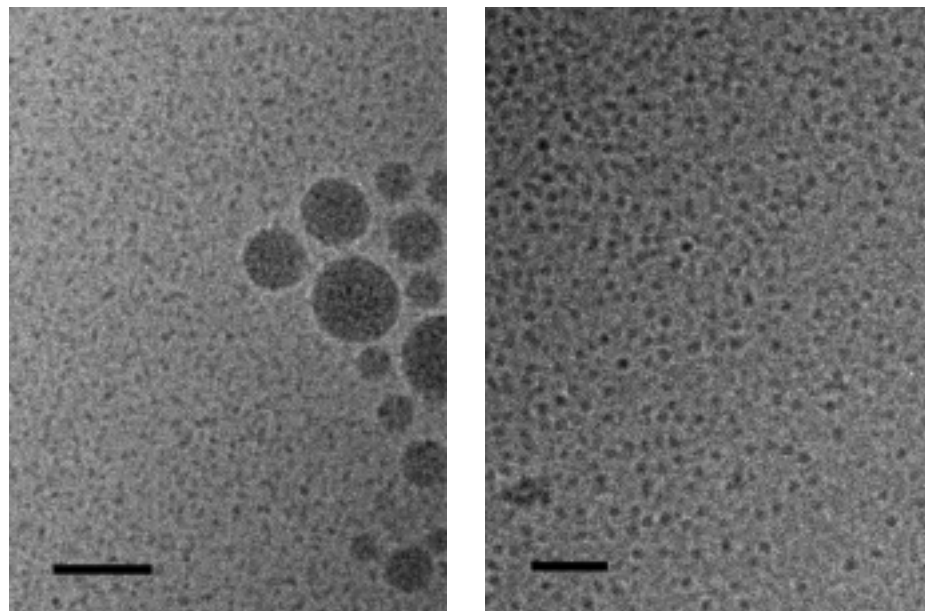


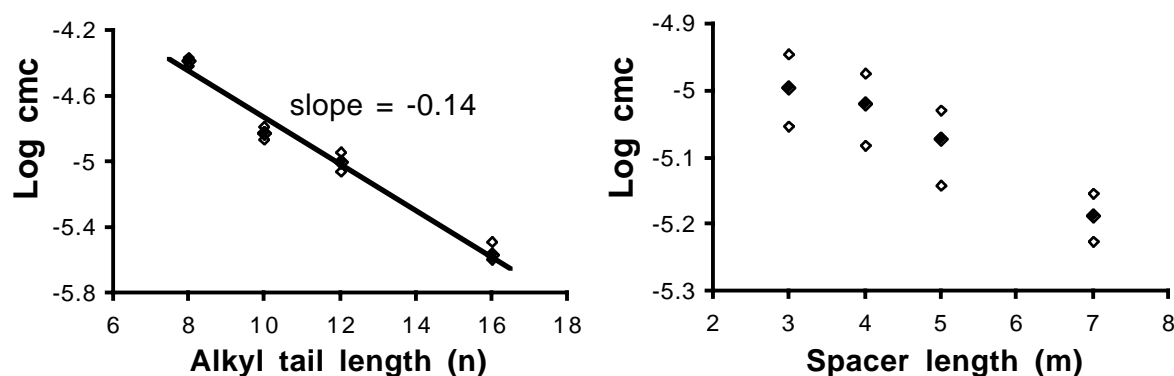
**Figure 6.2** Cryo-TEM images of 1 wt% aqueous solutions of **n12m7**(left) and **n16m3** (right); bar indicates 50 nm

In order to investigate the influence of the alkyl tail length and spacer length on micellization, we determined the critical micellization concentration (cmc) for all compounds using electrical conductivity. Results are given in the second column of Table 6.1. Also counterion binding to the micelles was determined from these measurements and found to be around 60%.

When we compare the compounds with varying alkyl tail length  $n$ , but with a constant spacer length of three methylene units, a normal trend can be seen. A decrease of cmc from 2.3 to 0.15 mM is found with an increase of the alkyl tail length from 8 to 16 carbon atoms. For a more hydrophobic compound, the tendency to aggregate is larger and therefore the cmc smaller. For comparison to other surfactants, a graph was constructed of log cmc (in mole fraction) versus the number of carbon atoms, shown in Figure 6.3a.

**Table 6.1.** Cmc's of three-headed surfactants

compound	cmc from conductivity (mM)	cmc from ITC (mM)
<b>n8m3</b>	2.3	2.5
<b>n10m3</b>	0.84	0.7
<b>n12m3</b>	0.56	0.5
<b>n12m4</b>	0.53	0.5
<b>n12m5</b>	0.47	0.5
<b>n12m7</b>	0.36	0.4
<b>n16m3</b>	0.15	0.1

**Figure 6.3** a)(left): Dependence of cmc on alkyl tail length; b)(right): Dependence of cmc on spacer length; open markers represent spread

A straight line can be drawn through these points with a slope of -0.14. It is known that this value is -0.5 for nonionic surfactants, -0.3 for univalent ionic surfactants, and -0.25 for divalent ionic surfactants. So we see that with an increasing valency of the surfactant, the influence of extra methylene units in the alkyl tail on the cmc decreases. The value for these trivalent ionic surfactants of -0.14 fits nicely in this trend. However, we have to be careful about comparing these compounds to 'classical' head-tail surfactants in which the hydrophobic part consists only of an alkyl tail. In our compounds the hydrophobic part also contains a steroid unit, besides the alkyl tail. Dehydration of the alkyl part may be less important compared to the large contribution of dehydration of the steroid unit to the hydrophobic effect. Furthermore, because of the rigidity of the steroid unit, the flexibility of the hydrophobic part is limited. The packing of the monomers inside the micelle will be

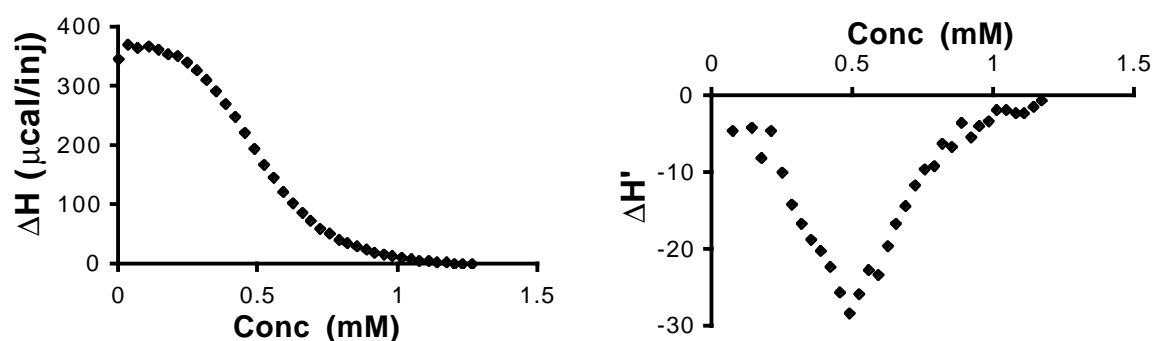
different from that of classical surfactants: due to the space that the steroid unit needs, the monomers are probably less densely packed. So there might be a considerable amount of water still present inside the micelle. A sterical aspect may play a role here too. If the alkyl tails have sufficient freedom to move around between the steroid units in the interior of the micelle, addition of a few more methylene units will make little difference for the micellization process.

Figure 6.3b shows a similar graph of the dependence of log cmc on the number of carbon atoms of the spacer. Apparently, the length of the spacer, within the tested range, has very little influence on cmc. There is a small, nonlinear decrease in cmc from 0.56 mM to 0.36 mM upon increasing the spacer length from 3 to 7 methylene units. It is, however, a well-known feature that the linear relationship falls down at short hydrophobic chain length because the first three methylene groups remain more hydrated under influence of the polar group.<sup>21</sup> In this case the spacer is not only located next to an ionic head group, but also next to a polar ester group and at the exterior of the micelle. Therefore, all methylene groups of the spacer are well hydrated in solution as well as in the micelle. So transfer of a monomer into a micelle, has little effect on hydration of the spacer, and therefore the influence of additional methylene units on the cmc is small. We expect that the linear relationship would be restored if the spacer contains a larger number of methylene units.

There is an extra possible explanation for the small influence that we see. When comparing the signals for the trimethylammonium groups with <sup>1</sup>H-NMR in CDCl<sub>3</sub>, there are three separate signals for compound **n12m3**, whereas for compound **n12m7** there is only one signal for all three groups. So, the longer spacer is flexible enough to move the ammonium groups into the same chemical environment. Similarly, in aqueous solution the longer spacer also has more possibilities to move the charged head groups as far away from each other as possible. When the charges can be distributed better over the micellar surface, the effect of head group repulsion is reduced, micellization is easier, and the cmc decreases.

Isothermal titration calorimetry (ITC) was used to gain information about the thermodynamics of micellization. To the measuring cell, filled with water, a

concentrated solution of surfactant, well above the cmc, was titrated in small steps. In the first number of injections complete demicellization occurs, giving rise to an endothermic heat effect. After a number of additions, the heat effect per injection decreases because the cmc is reached, and finally only dilution of micelles takes place. A typical enthalpogram, obtained with this method, is given in Figure 6.4. It shows a rather gradual decrease instead of a sharp drop, which would occur in the case of most micelles with high aggregation numbers. A curve like this indicates that the aggregation number is rather low. From the enthalpogram the cmc can be determined by looking at the inflection point, i.e. the minimum of its first derivative. Cmc's are comparable to those found with conductivity, as can be seen in Table 6.1.



**Figure 6.4** Enthalpogram (left) and its first derivative (right) for **n12m3**

More information can be obtained from these curves. During the first titration steps complete demicellization occurs, thus the negative equivalent of the initial heat change per injection equals the enthalpy of micellization ( $\Delta H_{\text{mic}}$ ), with a correction for the cmc as the amount of surfactant present in nonmicellar form. The Gibbs energy of micellization ( $\Delta G_{\text{mic}}$ ) can be calculated from the cmc. We look at a salt with general formula  $v_+ Y^{z+} \cdot v_- X^{z-}$  in which  $v_+$  and  $v_-$  are the stoichiometries and  $z^+$  and  $z^-$  the charges for the cation Y and the anion X, respectively. For such a salt  $\Delta G_{\text{mic}}$  can be calculated with the following equation<sup>22</sup>

$$\Delta G_{\text{mic}} = v R T \ln(Q \text{ cmc}')$$

in which  $v$  is the total stoichiometry ( $v = v_+ + v_-$ ),  $Q$  is a stoichiometric parameter ( $Q^v = v_+^{v_+} v_-^{v_-}$ ), and  $\text{cmc}'$  is the cmc in mole fraction. For our compounds with formula  $Y^{3+} \cdot 3X^{1-}$  this results in values of  $v = 4$  and  $Q = 2.28$ . Calculations give values for  $\Delta G_{\text{mic}}$  between -90 and -115 kJ/mol for all compounds.

The obtained values for  $\Delta G_{\text{mic}}$  for these three-headed surfactants are rather high, compared to values for monovalent surfactants calculated using the same equation. For example, hexadecyltrimethylammonium bromide would give a value of  $\Delta G_{\text{mic}} = -55$  kJ/mol. However, we see an increase in the  $\Delta G_{\text{mic}}$  values for surfactants with a stoichiometry other than 1:1, when calculated in the same way. Other surfactants with a 1:3 stoichiometry gave values for  $\Delta G_{\text{mic}}$  of about -100 kJ/mol.<sup>23</sup> Not surprisingly, with this equation the influence of the stoichiometry is considerable.

ITC-measurements for compounds **n12m4** were performed at different temperatures. Upon increasing the temperature from 10 to 40 °C, the cmc increased from 0.45 to 0.7 mM. Figure 6.5 presents all three thermodynamic parameters at different temperatures. There are several observations to be made from this plot. First, the variation in Gibbs energy of micellization with temperature is rather small. Furthermore, both the enthalpy of micellization as the entropy of micellization decrease with temperature. And finally, the entropy of micellization has the largest contribution to the Gibbs energy, so the micellization is mainly entropy-driven. These are three general points, that can also be made for other surfactants, ionic and nonionic.

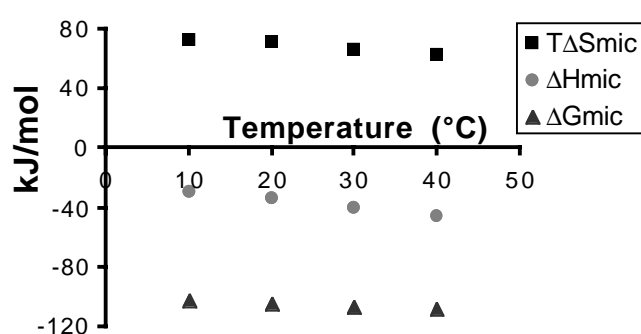


**Figure 6.5** Thermodynamic parameters of micellization for **n12m4** at different temperatures

Several cholic acid derived facial amphiphiles have been reported that permeabilize membranes, like bacterial cell walls.<sup>14</sup> These cholic acid derivatives, which make bacteria vulnerable to other antibiotics, have nitrogen-containing groups, such as amine or guanidine groups, coupled to the hydroxyl groups. The

positive charges associate with the negatively charged membrane. Attaching a hydrophobic chain of about 8 carbon atoms to these molecules facilitates 'self-promoted' transport across the bacterial outer membrane, and therefore results in strong antimicrobial activity.<sup>24,25</sup> Our surfactants contain the same structural elements (three nitrogen-containing, positively charged groups and a hydrophobic alkyl tail), therefore some tests were performed to investigate their antimicrobial activity. The minimum inhibition concentration (MIC) was measured using two bacterial cultures: *Escherichia coli* and *Enterococcus faecalis*. It was found that compounds **n8m3** and **n10m3** inhibited growth of both bacterial cultures. The MIC was established to be 25 and 12.5 µg/ml for **n8m3** and **n10m3**, respectively. This is far below cmc, so the inhibition mechanism does not involve aggregate structures but single molecules. The activity of compound **n10m3** is almost equal to that of the well-known antibiotic chloramphenicol and in the same order of magnitude as other cholic acid-based antibiotics. It is noteworthy that these compounds act as competent bacterial growth inhibitors against both gram-positive and gram-negative bacterial cultures. The compounds with longer alkyl tail (**n12m3** and **n16m3**) showed no inhibitory effect, not even in concentrations up to 200 µg/ml. The hydrophobic tail of 12 or 16 carbon atoms might be too long to facilitate transport through the bacterial membrane due to stronger hydrophobic interaction with the membrane.

### 6.3 CONCLUSIONS

The synthesis of a series of new facial amphiphiles, based on cholic acid, with a permanent ionic character is conducted in three steps. These compounds act as three-headed surfactants, forming mostly small spherical micelles. The micellar size depends on the lengths of the alkyl tail. The cmc depends on the length of the alkyl tail and the spacer, but the dependence is not so strong, compared to monovalent surfactants. Information about the thermodynamics was obtained from ITC. The cmc increases and enthalpy of micellization decreases with temperature, while the Gibbs energy of micellization is rather constant. Micellization is mainly entropy-driven. Two compounds with the shortest alkyl tail display antimicrobial activity against gram-positive as well as gram-negative bacteria.

## 6.4 EXPERIMENTAL SECTION

**General Remarks:**  $^1\text{H}$ -NMR spectra (200 MHz) were recorded on a Bruker AC200 spectrometer at ambient temperature. - FT-IR spectra were recorded on a BIO-RAD FTS-7 spectrophotometer with a resolution of  $4\text{ cm}^{-1}$ . - Mass spectra were obtained by direct injection of aqueous solutions on a Finnigan MAT LCQ mass spectrometer, using ESI, in positive ion scan mode; syringe pump flow  $3\text{ }\mu\text{l/min}$ ; spray voltage 4 kV; capillary temperature  $200\text{ }^\circ\text{C}$ ; capillary voltage 10kV. - For cryo-TEM a drop of sample suspension was placed on a glow discharged holey carbon film. Excess liquid was blotted away with filter paper, and the grid was subsequently vitrified in liquid ethane, cooled with liquid nitrogen. The frozen hydrated grid was mounted in a Gatan cryo-stage (Gatan model 626), and observed in a Philips CM120 cryo transmission electron microscope operating at 120 kV. Images were recorded on a slow scan CCD camera under low-dose conditions. - For DLS measurements 1 wt% aqueous solutions were placed in a Lexel 85 Argon Ion Laser beam with  $\lambda = 514.5\text{ nm}$  and power 100-300 mW; scattering was recorded under an angle of  $90^\circ$ , using an ALV-5000 digital correlator, ALV-125 goniometer, ALV-800 transputerboard from ALV-GmbH (Langen, Germany). 30 measurements of 20s were accumulated and analyzed with Contin-fit. - Conductivity was measured using a Philips PW9527 digital conductivity meter and a PW9550/60 cell at room temperature. - ITC measurements were performed using a MicroCal MCS titration calorimeter. Sample cell ( $V = 1.35\text{ ml}$ ) and reference cell were filled with water. To the sample cell were injected 50 aliquots of  $5\text{ }\mu\text{l}$  of surfactant solution with a concentration of 10-20 times cmc with intervals of 5 min. Temperature was kept constant at 283, 293, 303 or 313 K. - For antimicrobial tests cultures of gram-negative *Escherichia coli* (JM109, Promega) and gram-positive *Enterococcus faecalis* (93103, kind gift from VTT Biotechnology, Finland) were grown in LB broth or M17 broth with 1% of glucose, respectively. A fresh overnight culture of *E. coli* (16 hrs at  $37\text{ }^\circ\text{C}$ ) was inoculated into LB broth containing  $100\text{ }\mu\text{g/ml}$  of a compound and incubated for 24 h at  $37\text{ }^\circ\text{C}$ . On the compounds which showed no turbidity after incubation, a more extensive test was performed.<sup>26</sup> The MIC (defined as the lowest concentration of surfactant that showed no turbidity) was measured using a series of glass test tubes containing the compound in concentrations of 200, 100, 50, 25 and  $12.5\text{ }\mu\text{g/ml}$ . Each tube was inoculated with exponential-growth-phase organisms (*E. coli* or *E. faecalis*) to a concentration of 1% and incubated at  $37\text{ }^\circ\text{C}$  for 20 h. The optical density at 660 nm was measured before and after incubation. Broth containing bacteria alone was used as a positive control, and for comparison bacteria were also tested in broth supplemented with chloramphenicol at  $15\text{ }\mu\text{g/ml}$ . Tests were performed in duplicate.

**Synthesis:** Used solvents were of p.a. quality. The different bile acids were purchased from Acros, as were the  $\omega$ -bromoalkanoic acids, DMAP, and trimethylamine. The purity of the products was verified with NMR, and mass spectroscopy.

**General procedure for the synthesis of 24-(alkyloxy)-24-oxo-3,7,12-tris[[ $\omega$ -(trimethylammonio)alkanoyl]oxy]cholanes:** 3 mmol of alkyl cholate<sup>4</sup> was dissolved in 10 ml of benzene and 2 ml of pyridine. A catalytic amount of DMAP was added and stirred for 45 minutes at room temperature. A solution of 15 mmol of  $\omega$ -bromoalkanoic acid chloride in benzene was added and stirred overnight at room temperature. The reaction mixture was filtered, diluted with  $\text{CH}_2\text{Cl}_2$  and washed with 3 M HCl solution. The organic layer was dried, and the solvent was evaporated under vacuum. The product was purified by column chromatography on silica, using dichloromethane:methanol (99.5:0.5) as eluent, giving a yellow oil. 1 mmol of this 24-(alkyloxy)-24-oxo-3,7,12-tris[[ $\omega$ -bromoalkanoyl]oxy]cholane was dissolved in 15 ml of a 20 wt% solution of trimethylamine in ethanol and stirred for 24 hours in a closed reaction vessel at 100 °C. After cooling and concentrating the mixture, chloroform was added. The precipitate was filtered, and evaporation of the filtrate under vacuum gave a white solid.

**n8m3:**  $^1\text{H-NMR}$  ( $\text{CDCl}_3/\text{CD}_3\text{OD}$ ):  $\delta$  = 5.11 (br. s, 1H, 12 $\alpha$ -CH), 4.92 (br. s, 1H, 7 $\alpha$ -CH), 4.55 (m, 1H, 3 $\alpha$ -CH), 4.01 (t, 2H,  $\text{OCH}_2$ ), 3.58 (m, 6H,  $\text{NCH}_2$ ), 3.24 (s, 9H,  $\text{NCH}_3$ ), 3.21 (s, 9H,  $\text{NCH}_3$ ), 3.16 (s, 9H,  $\text{NCH}_3$ ), 2.60-1.00 (m, 48H, aliphatic H), 0.90 (s, 3H, 19- $\text{CH}_3$ ), 0.84 (t, 3H,  $\text{CH}_3$ ), 0.76 (d, 3H, 21- $\text{CH}_3$ ), 0.70 (s, 3H, 18- $\text{CH}_3$ ). - IR (KBr):  $\nu$  = 3443, 2926, 2857, 1731, 1636. -  $\text{C}_{53}\text{H}_{98}\text{N}_3\text{O}_8\text{Br}_3$ : (M-Br)<sup>+</sup> = 1062.

**n10m3:**  $^1\text{H-NMR}$  ( $\text{CDCl}_3/\text{CD}_3\text{OD}$ ):  $\delta$  = 5.12 (br. s, 1H, 12 $\alpha$ -CH), 4.92 (br. s, 1H, 7 $\alpha$ -CH), 4.56 (m, 1H, 3 $\alpha$ -CH), 3.98 (t, 2H,  $\text{OCH}_2$ ), 3.60 (m, 6H,  $\text{NCH}_2$ ), 3.26 (s, 9H,  $\text{NCH}_3$ ), 3.23 (s, 9H,  $\text{NCH}_3$ ), 3.18 (s, 9H,  $\text{NCH}_3$ ), 2.72-1.05 (m, 52H, aliphatic H), 0.87 (s, 3H, 19- $\text{CH}_3$ ), 0.84 (t, 3H,  $\text{CH}_3$ ), 0.76 (d, 3H, 21- $\text{CH}_3$ ), 0.70 (s, 3H, 18- $\text{CH}_3$ ). - IR (KBr):  $\nu$  = 3442, 2927, 2857, 1730, 1636. -  $\text{C}_{55}\text{H}_{102}\text{N}_3\text{O}_8\text{Br}_3$ : (M-Br)<sup>+</sup> = 1090.

**n12m3:**  $^1\text{H-NMR}$  ( $\text{CDCl}_3/\text{CD}_3\text{OD}$ ):  $\delta$  = 5.15 (br. s, 1H, 12 $\alpha$ -H), 4.96 (br. s, 1H, 7 $\alpha$ -H), 4.60 (m, 1H, 3 $\alpha$ -H), 4.02 (t, 2H,  $\text{OCH}_2$ ), 3.74 (m, 6H,  $\text{NCH}_2$ ), 3.51 (s, 9H,  $\text{NMe}_3$ ), 3.45 (s, 9H,  $\text{NMe}_3$ ), 3.40 (s, 9H,  $\text{NMe}_3$ ), 2.70-1.10 (m, 56H, aliphatic H), 0.94 (s, 3H, 19- $\text{CH}_3$ ), 0.87 (t, 3H,  $\text{CH}_3$ ), 0.81 (d, 3H, 21- $\text{CH}_3$ ), 0.73 (s, 3H, 18- $\text{CH}_3$ ). - IR (KBr):  $\nu$  = 3428, 2927, 2851, 1725, 1634. -  $\text{C}_{57}\text{H}_{106}\text{N}_3\text{O}_8\text{Br}_3$ : (M-Br)<sup>+</sup> = 1118.

**n12m4:**  $^1\text{H-NMR}$  ( $\text{CDCl}_3/\text{CD}_3\text{OD}$ ):  $\delta$  = 5.06 (br. s, 1H, 12 $\alpha$ -H), 4.89 (br. s, 1H, 7 $\alpha$ -H), 4.49 (m, 1H, 3 $\alpha$ -H), 3.99 (t, 2H,  $\text{OCH}_2$ ), 3.46 (m, 6H,  $\text{NCH}_2$ ), 3.22 (s, 9H,  $\text{NMe}_3$ ), 3.20 (s, 9H,  $\text{NMe}_3$ ), 3.18 (s, 9H,  $\text{NMe}_3$ ), 2.54-1.02 (m, 62H, aliphatic H), 0.89 (s, 3H, 19- $\text{CH}_3$ ), 0.82 (t, 3H,  $\text{CH}_3$ ), 0.74



(d, 3H, 21-CH<sub>3</sub>), 0.69 (s, 3H, 18-CH<sub>3</sub>). - IR (KBr):  $\nu$  = 3442, 2926, 2855, 1728, 1636. -

C<sub>60</sub>H<sub>112</sub>N<sub>3</sub>O<sub>8</sub>Br<sub>3</sub>: (M-Br)<sup>+</sup> = 1160.

**n12m5**: <sup>1</sup>H-NMR (CDCl<sub>3</sub>/CD<sub>3</sub>OD):  $\delta$  = 5.07 (br. s, 1H, 12 $\alpha$ -H), 4.87 (br. s, 1H, 7 $\alpha$ -H), 4.49 (m, 1H, 3 $\alpha$ -H), 3.97 (t, 2H, OCH<sub>2</sub>), 3.53 (m, 6H, NCH<sub>2</sub>), 3.24 (s, 9H, NMe<sub>3</sub>), 3.23 (s, 9H, NMe<sub>3</sub>), 3.21 (s, 9H, NMe<sub>3</sub>), 2.45-1.02 (m, 68H, aliphatic H), 0.87 (s, 3H, 19-CH<sub>3</sub>), 0.82 (t, 3H, CH<sub>3</sub>), 0.75 (d, 3H, 21-CH<sub>3</sub>), 0.68 (s, 3H, 18-CH<sub>3</sub>). - IR (KBr):  $\nu$  = 3441, 2926, 2856, 1729, 1636. -

C<sub>63</sub>H<sub>118</sub>N<sub>3</sub>O<sub>8</sub>Br<sub>3</sub>: (M-Br)<sup>+</sup> = 1202.

**n12m7**: <sup>1</sup>H-NMR (CDCl<sub>3</sub>/CD<sub>3</sub>OD):  $\delta$  = 5.04 (br. s, 1H, 12 $\alpha$ -H), 4.86 (br. s, 1H, 7 $\alpha$ -H), 4.51 (m, 1H, 3 $\alpha$ -H), 3.96 (t, 2H, OCH<sub>2</sub>), 3.63 (m, 6H, NCH<sub>2</sub>), 3.38 (s, 9H, NMe<sub>3</sub>), 3.37 (s, 9H, NMe<sub>3</sub>), 3.35 (s, 9H, NMe<sub>3</sub>), 2.38-1.00 (m, 80H, aliphatic H), 0.85 (s, 3H, 19-CH<sub>3</sub>), 0.81 (t, 3H, CH<sub>3</sub>), 0.75 (d, 3H, 21-CH<sub>3</sub>), 0.66 (s, 3H, 18-CH<sub>3</sub>). - IR (KBr):  $\nu$  = 3442, 2927, 2857, 1730, 1636. -

C<sub>69</sub>H<sub>130</sub>N<sub>3</sub>O<sub>8</sub>Br<sub>3</sub>: (M-Br)<sup>+</sup> = 1286.

**n16m3**: <sup>1</sup>H-NMR (CDCl<sub>3</sub>/CD<sub>3</sub>OD):  $\delta$  = 5.07 (br. s, 1H, 12 $\alpha$ -H), 4.88 (br. s, 1H, 7 $\alpha$ -H), 4.51 (m, 1H, 3 $\alpha$ -H), 3.93 (t, 2H, OCH<sub>2</sub>), 3.60 (m, 6H, NCH<sub>2</sub>), 3.24 (s, 9H, NMe<sub>3</sub>), 3.20 (s, 9H, NMe<sub>3</sub>), 3.15 (s, 9H, NMe<sub>3</sub>), 2.71-0.99 (m, 64H, aliphatic H), 0.85 (s, 3H, 19-CH<sub>3</sub>), 0.81 (t, 3H, CH<sub>3</sub>), 0.72 (d, 3H, 21-CH<sub>3</sub>), 0.65 (s, 3H, 18-CH<sub>3</sub>). - IR (KBr):  $\nu$  = 3443, 2924, 2854, 1731, 1635. -

C<sub>61</sub>H<sub>114</sub>N<sub>3</sub>O<sub>8</sub>Br<sub>3</sub>: (M-Br)<sup>+</sup> = 1174.

## REFERENCES AND NOTES

- 1 Y. Hishikawa, R. Watanabe, K. Sada, M. Miyata, *Chirality* **1998**, *10*, 600-618.
- 2 V. Bertolasi, O. Bortolini, M. Fogagnolo, G. Fantin, P. Pedrini, *Tetrahedron: Asymmetry* **2001**, *12*, 1479-1483.
- 3 Chapter 2 of this thesis or H.M. Willemen, T. Vermonden, A.T.M. Marcelis, E.J.R. Sudhölter, *Eur. J. Org. Chem.* **2001**, 2329-2335.
- 4 Chapter 3 of this thesis or H.M. Willemen, T. Vermonden, A.T.M. Marcelis, E.J.R. Sudhölter, accepted in *Langmuir* **2002**.
- 5 K. Nakano, Y. Hiswikawa, K. Sada, M. Miyata, K. Hanabusa, *Chem. Lett.* **2000**, 1170-1171.
- 6 Y. Hishikawa, K. Sada, R. Watanabe, M. Miyata, K. Hanabusa, *Chem. Lett.* **1998**, 795-796.
- 7 J. Tamminen, E. Kolehmainen, *Molecules* **2001**, *6*, 21-46, and references therein.
- 8 L. Vaton-Chanvrier, H. Oulyadi, Y. Combret, G. Coquerel, J.C. Combret, *Chirality* **2001**, *13*, 668-674.
- 9 H. Gao, J.R. Dias, *Org. Prep. Proced. Int.* **1999**, *31*, 145-166.
- 10 Y. Kobuke, T. Nagatani, *Chem. Lett.* **2000**, 298-299.
- 11 P. Bandyopadhyay, V. Janout, L. Zhang, S.L. Regen, *J. Am. Chem. Soc.* **2001**, *123*, 7691-7696.
- 12 J. F. Barry, A.P. Davis, M.N. Pérez-Payan, M.R.J. Elsegood, R.F.W. Jackson, C. Gennari, U. Piarulli, M. Gude, *Tetrahedron Lett.* **1999**, *40*, 2849-2852.
- 13 Y.R. Vandenburg, B.D. Smith, M.N. Pérez-Payán, A.P. Davis, *J. Am. Chem. Soc.* **2000**, *122*, 3252-3253.
- 14 C. Li, A.S. Peters, E.L. Meredith, G.W. Allman, P.B. Savage, *J. Am. Chem. Soc.* **1998**, *120*, 2961-2962.
- 15 S. Broderick, A.P. Davis, R.P. Williams, *Tetrahedron* **1998**, 6083-6086.
- 16 U. Taotafa, D.B. McMullin, S.C. Lee, L.D. Hansen, P.B. Savage, *Org. Lett.* **2000**, *2*, 4117-4120.
- 17 R. Zana, *Adv. Colloid Interface Sci.* **2002**, *97*, 205-253, and references therein.
- 18 J. Haldar, V.K. Aswal, P.S. Goyal, S. Bhattacharya, *Angew. Chem., Int. Ed.* **2001**, *40*, 1228-1232.
- 19 M.J. Blandamer, P.M. Cullis, J.B.F.N. Engberts, *J. Chem. Soc., Faraday Trans.* **1998**, *94*, 2261-2267.
- 20 D.M. Small in *The Bile Acids, Vol. 1 Chemistry*, Eds.: P. P. Nair, D. Kritchevsky, Plenum Press - New York, **1971**, pp. 249-356.

- 21 J.H. Clint, *Surfactant Aggregation*, Blackie - Glasgow, London, **1992**, pp. 107-108.
- 22 M.J. Blandamer, P.M. Cullis, L.G. Soldi, J.B.F.N. Engberts, A. Kacperska, N.M. van Os, M.C.S. Subha, *Adv. Colloid Interface Sci.* **1995**, 58, 171-209.
- 23 Values were calculated using cmc values from reference 18 and from M. Iida, M. Yamamoto, N. Fujita, *Bull. Chem. Soc. Jpn.* **1996**, 69, 3217-3224.
- 24 C. Li, L.P. Budge, C.D. Driscoll, B.M. Willardson, G.W. Allman, P.B. Savage, *J. Am. Chem. Soc.* **1999**, 121, 931-940.
- 25 C. Li, M.R. Lewis, A.B. Gilbert, M.D. Noel, D.H. Scoville, G.W. Allman, P.B. Savage, *Antimicrob. Agents Chemother.* **1999**, 43, 1347-1349.
- 26 W.G. Pitt, M.O. McBride, J.K. Lunceford, R.J. Roper, R.D. Sagers, *Antimicrob. Agents Chemother.* **1994**, 38, 2577-2582.

# 7

## General discussion

*In this chapter some connections are established between the results from the previous chapters. Attempts are made to provide answers, occasionally speculative, for some remaining questions. Also some suggestions are made for experiments to expand this work.*

## 7.1 INTRODUCTION

In this thesis four series of new surfactant compounds have been presented. These series have in common that nearly all of the 51 compounds are based on the main bile acid cholic acid. Only five derivatives of other bile acids can be found (compounds **2.8 - 2.10** and **3.5a-b**). The differences in molecular structure between the members within one series are not so large. Variation can be found, for example, in the length of an appended alkyl tail or in the conjugation of amino acids with different side groups. Nevertheless, we have seen that a small variation in structure can lead to large changes in behavior. Most of the observations and results concerning the aggregation have been discussed in the previous chapters. In this chapter we will focus on some general points.

Furthermore, in this chapter we will try to make some links between the series. The differences in molecular structure between the series of chapter 2 and 5 are relatively small: one methyl group. The differences between the series from the other chapters are more pronounced. Especially, the compounds in chapter 6 in which modifications are made of the hydroxyl groups of cholic acid, differ from the compounds in other chapters in which only the carboxylate group is modified.

Although there is considerable variation in molecular structure, most of the cholic acid derivatives described in this thesis show some form of aggregation in solution, either in water or organic solvent. Apparently the amphiphilic character of cholic acid itself still plays an important role in the behavior of its derivatives. We see that the more apolar derivatives, as described in chapters 2 and 3, are moderately soluble in several organic solvents, and aggregate to form organogels, whereas they are water-insoluble. Following the reversed argumentation, the ionic compounds from chapters 5 and 6 form micelles in water and are insoluble in most organic solvents. So the nature of the added functionalities to cholic acid determines the solubility in certain media, albeit limited, and the facial amphiphilic steroid building block directs the aggregation.

## 7.2 ORGANOGELS

First we will look again at the process of organogel formation. Many compounds in chapters 2 and 3 are potent gelators, affording stable and completely transparent gels. The gels can withstand mechanical shaking without disruption, and they remain intact for months. The gel network is build from thin fibers with diameters of about 30 Å. This fiber thickness was determined with SANS measurements for several gels described in chapters 2 and 3. An estimate of the fiber thickness was also made from EM photographs. For the compounds in chapter 3 the results from the two methods agree rather nicely (about 50 Å from EM). For the compounds in chapter 2, the EM pictures suggest much thicker fibers (about 500 Å) than was found with SANS. It is possible that in this case we did not see the single fibers, but instead bundles of fibers, as a result of the sample preparation. The small diameter of the fibers explains the high transparency of the obtained organogels. The fibers are indeed very thin, as compared to other gel systems: most gel fibers described in literature have diameters higher than 100 Å, although fibers from metal-coordinated gels with stacked molecules have also been found to be this thin.<sup>1</sup> Therefore, the fibers in this thesis are considered to be unimolecular in thickness, with the molecules arranged in some sort of columnar packing. Furthermore, results from chapter 4 show that not all the fibers are cylindrical. Gelators with a longer alkyl tail form flattened fibers.

The logical question that follows from this statement is, how are the gelator molecules inside a fiber organized to obtain such unimolecular columns? We know from structural variations in chapters 2 and 3 that the molecules aggregate though hydrogen bonds in which the amide bond and at least the hydroxyl groups at the 7 and 12-positions are involved. We assume that the hydroxyl group at the 3-position also plays a role in the hydrogen bonded network. We also assume that the apolar parts are located on the outside of the fiber, where they are in contact with the surrounding apolar medium. In the compounds from chapter 3 the alkyl tails are easily recognized as the apolar parts. For the compounds from chapter 2 it is not so clear. Amino acid molecules are not often regarded as apolar groups. In this case, however, both the amine group and the carboxylate group are derivatized. So we can consider the amino acid, especially the side group, as the apolar part of the molecule, although it is very small in some compounds, e.g. compounds **2.1** and **2.2**.

We will assume that the rigid steroid unit is located in the center of the fiber. The simplest idea is to have them stacked on top of each other in a straight line along the long axis of the fiber. This seems, however, not likely because of the facial amphiphilicity of the steroid unit. The preferred way of stacking would be alternately facing up and facing down, with the polar sides facing each other. But this would probably just result in pair formation, instead of fiber formation.

A more feasible model has the steroid units with their polar sides facing the interior of the fiber and the apolar sides facing the outside. Such an organization is schematically drawn in Figure 7.1 for compound **3.1b**. Each amide group can form hydrogen bonds with the 3-hydroxyl group of the opposite molecule. If all molecules are a bit tilted, the molecules form a kind of spiral staircase around the long axis of the fiber. In this arrangement each molecule could also be connected to a neighboring molecule through hydrogen bonds between the 7 and 12-hydroxyl groups.

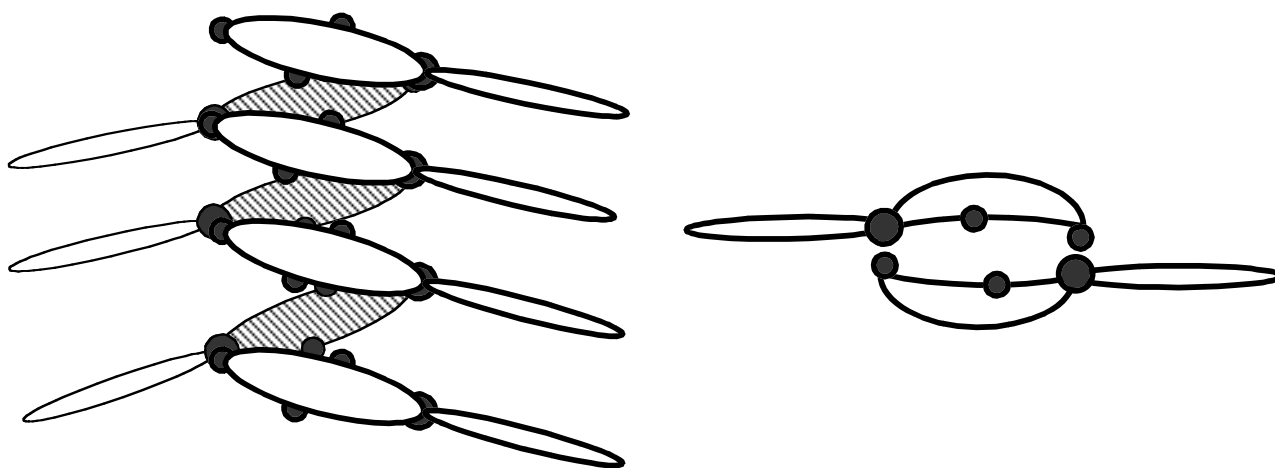


**Figure 7.1** Schematic representation of possible fiber model for compound **3.1b**; side-view (left) and top-view (right); ● = hydroxyl group; ● = amide group

From this model it can also be understood that flattened fibers are found for compounds with a long alkyl group, such as compound **3.1b**. The alkyl tails all lie in one direction, which is elongated, compared to the perpendicular direction. This results in fibers for which the cross section has an aspect ratio of lower than 0.5. One can imagine that for compounds, which lack a long alkyl tail, the aspect ratio increases and the fibers indeed appear cylindrical.

It might be possible that a twisted fiber is formed, as drawn in Figure 7.2. The chirality of the gelators could play a role here, especially in the case of the  $\alpha$ -amino acid derivatives with a chiral center next to the amide bond. Such a helix might be detectable with circular dichroism, but attempts to measure this failed due to lack of a strongly UV-active group, even when a phenyl group containing gelator in cyclooctene was used.

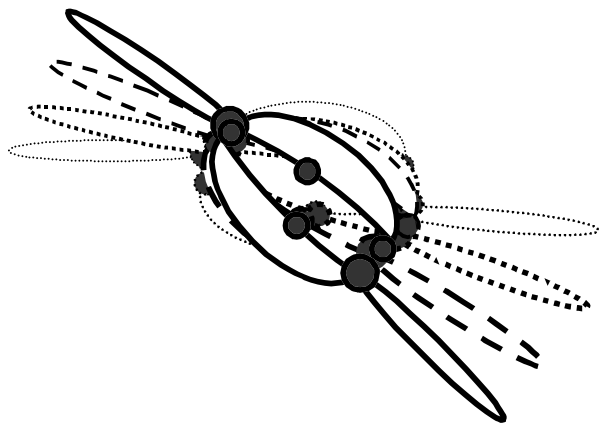


Figure 7.2 Schematic representation of a possible twisted fiber model in top-view; ● = hydroxyl group; ● = amide group

Of course this is not the only design of a fiber from single gelator molecules; there are more possible constructions. A thorough molecular modeling study would be required to determine which organization of molecules is possible and which has the lowest Gibbs energy.

It is possible that the above-described model is also representative for the way the combination gels, reported in chapter 3, are constructed. The alkyl cholates **3.9a-c** could be positioned along the long axis of the fiber with their polar sides facing the center and their apolar sides facing the outside, similar to compound **3.1b** in the model. In the case of the combination gels, the gelators are not always directly linked to each other, but also via water or carbohydrate molecules, which would be located in the center of the fiber. All interactions between the various molecules are via hydrogen bonds.

In chapter 4 two different ways were found in which the fibers were connected to each other: knots and entangled interactions. It is remarkable that two compounds with almost identical molecular structures (**2.4a/LeuMe** and **2.4c/LeuBu**) can show these two different ways of connection. We found that alkyl derivatives and amino acid derivatives with a butyl ester group form gels with entangled interactions, whereas amino acid

derivatives with a methyl ester group form gels with knot-wise interactions. Our suggestion was that the length of the alkyl tail determines the way of interaction, with a border around an alkyl group of 2 or 3 carbon atoms. This also explains why compound **2.5b** is such a poor gelator, as was demonstrated in chapter 2. It seems that compound **2.5b**, which is an amino acid derivative with an ethyl ester group, does not fall in either category, and therefore cannot form a stable gel network, resulting in quick precipitation.

In chapter 2 DSC measurements are reported for several gels, e.g. for compound **2.4a**, which show two endothermic transitions upon heating, as can be seen in Figure 7.3. It was established that the final, sharp transition corresponds to the visual melting of the gel. The first, broad transition was attributed to partial melting of the network, before complete disintegration of the fibers takes place during the last transition. Unfortunately, this was just an assumption, for which no proof was provided. In chapter 4, temperature-dependent SANS measurements for a gel of compound **2.4a (LeuMe)** are reported that provide the information we need. It was found that breakdown of this gel network with knot-like interactions occurs gradually. At a temperature halfway the pre-melting transition, the scattering caused by the knots decreases whereas the typical features for rod-like scatterers are still intact. Also the thickness of the fibers is unaltered. At a temperature above the melting point, the scattering is lost completely. So with the combination of the two techniques, DSC and SANS, we are able to proof the occurrence of step-wise breakdown of the gel structure.

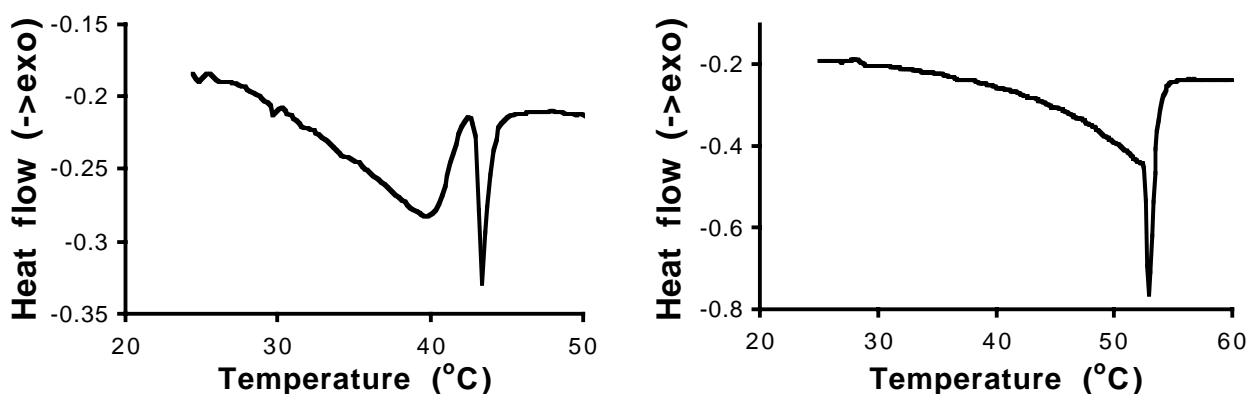


**Figure 7.3** DSC thermograms for 25 mM gels of compounds **2.4a** (left, knots) and **3.1c** (right, entanglements) in benzene; heating rate 0.5 °C/min



This step-wise breakdown was thus shown for a gel system with a knot-like structure. This kind of breakdown seems unlikely for gels with entangled interactions. When we now look again at all DSC thermograms we can indeed see a difference between gels with different interactions. Figure 7.3 also shows the thermogram for a gel of compound **3.1c**, which forms an entangled gel. There is not a clear pre-melting transition, but only a shoulder close to the melting peak. Apparently, this network also disintegrates somewhat before actual melting, but this seems to be a more gradual process. Such melting characteristics were also found for other gels with entangled interactions.

The above explains the presence of one pre-melting transition in the DSC thermograms for knot-like gels. However, in chapter 2 some gels are reported that show two pre-melting transitions instead of just one. These are all gels based on compounds with a phenyl group in the amino acid side group (compounds **2.5a-c** and **2.6b**). A possible explanation for this phenomenon could be found in the steric hindrance of the phenyl group. When the molecules are packed in the gel network, it is imaginable that the phenyl group has little freedom of rotation. If the packing of the molecules becomes looser above a certain temperature, the phenyl group gains extra freedom of rotation, which could be manifested as an extra pre-melting transition.

As was said in the concluding remarks of the second international conference on fibrillar networks SAFIN 2001, it is important to establish some general guidelines by which gels must be characterized to make the comparison between different gelator systems easier. Viscosity should be one of the major keys in achieving this. Although such measurements were not performed on our gels, they would allow a better comparison with other gel systems.

### 7.3 MICELLES

For the last part of this chapter we will focus on the second type of aggregate that was formed with cholic acid derivatives: micelles in aqueous solutions. This was found for two very different series of compounds, although both are ionic in a certain pH range. These molecules do not possess the classical head-tail surfactant shape. The compounds from chapter 5 come closest to this, regarding the steroid unit as more apolar. The

compounds from chapter 6 with three ionic head groups are different from nearly all known surfactants. Other three-headed surfactants are known, but these also possess three tails, the so-called oligomeric surfactants. The difference with the only other known three head groups-one tail surfactant<sup>2</sup> is the presence of a rigid unit in the cholic acid derivatives.

As a consequence, the formed micelles are also different from the classical spherical micelles with high aggregation numbers. The micelles are small, about 5 nm, and because of this it is difficult to see their exact shape with EM, but they seem to be spherical. The micelles described in chapter 6 have rather small aggregation numbers, as can be concluded from the ITC experiments. For the compounds from chapter 5 also larger aggregates can be seen. We assume a two-step aggregation behavior, similar to the aggregation of glycocholate. Considering the fact that these are all  $\alpha$ -amino acid derivatives of cholic acid, this is not surprising.

When we look at the variation within a series of surfactants we see some influence of the molecular structure on micellization behavior. In chapter 6, the distinct influence of the alkyl tail length on cmc fits nicely in the trend of all surfactants. On the other hand, the influence of the spacer length is limited. In chapter 5, increasing the hydrophobicity of the amino acid side group also decreases the cmc only slightly. So we see for both series that variation of molecular structure in the hydrated region near the ionic head group has only little influence on the cmc.

For the compounds in chapter 6 the potential use as antimicrobial compounds was studied. Two compounds (**n8m3** and **n10m3**) inhibit the growth of a gram-positive and a gram-negative bacterial culture. The MIC was determined to be similar to that of chloramphenicol and this is very promising. However, before we could comment on potential use, another value has to be determined in this respect: the MHC. This stands for the minimum hemolytic concentration, i.e. the minimum concentration required to lyse red blood cells. If these compounds display similar MIC and MHC values, they have no membrane selectivity, and are useless as antibiotics. The ideal antibiotic has a low MIC value and a high MHC value, meaning a high selectivity for prokaryotic bacterial membranes over eukaryotic host membranes.<sup>3</sup>

## 7.4 OUTLOOK

Coming to the final section of the last chapter of this thesis, this is the place to look at future work regarding these and other cholic acid derivatives. In general, the possibilities of cholic acid as a building block for new molecules are seemingly endless: the only restrictions lie in the synthetic skills and the imagination of the chemist. We have seen in chapter 1 several examples of functional molecules, derived from cholic acid, with wonderful applications. My impression, however, is that the aggregation behavior of these molecules has been hardly studied. This is a pity because due to the presence of the facial amphiphilic steroid unit, aggregation is to be expected in all kinds of media, as was demonstrated in this thesis. It would be worthwhile to make an effort to investigate the aggregation behavior of more cholic acid derivatives.

On the other hand, the compounds in this thesis were studied with strong emphasis on their aggregation behavior and the properties of their aggregates in various media. But the possible applications of these new compounds were somewhat neglected. Only the use as antibiotics was studied cursorily. It is, however, very well possible that the various classes of compounds in this thesis could be used as receptors, transporters, transmembrane channels or in separation techniques. Also the micelles could be important as mimics for natural bile acid chemistry, and medical applications could be possible.

In order to explore these possible applications, extensive cooperation is needed with research groups with other expertise than our own. For the work described in this thesis we already collaborated with experts in other fields. The SANS measurements in chapter 4 would never have been possible without their much appreciated help. We also value the help from EM-specialists and antimicrobial researchers. To explore the potential applications of these compounds, more of these collaborations are necessary. In this regard I want to stress that the papers with the nicest compounds and applications, referenced in chapter 1, were usually produced by two or more research groups with different expertise, occasionally from different universities. Let us hope that these kinds of collaborations will continue in the future, and that scientists will share their ideas and knowledge. This is the best way to ensure that the most promising molecules will be built from cholic acid, and their possible applications will be examined to the fullest extent so their potential will not be lost.

**REFERENCES AND NOTES**

- 1 P. Terech, R.G. Weiss, *Chem. Rev.* **1997**, 97
- 2 J. Haldar, V.K. Aswal, P.S. Goyal, S. Bhattacharya, *Angew. Chem., Int. Ed.* **2001**, 40, 1228-1232.
- 3 P.B. Savage, *Eur. J. Org. Chem.* **2002**, 759-768.

## Summary

In this thesis various cholic acid derivatives are reported that display aggregation in water or in organic solvents. Spontaneous aggregation of single molecules into larger, ordered structures occurs at the borderline of solubility. Amphiphilic compounds, or surfactants, which possess a hydrophobic as well as a hydrophilic part, have a high tendency to form aggregates to minimize unfavorable polar-apolar interactions with the surrounding solvent. There are different types of aggregates in water as well as in organic solvents. Examples of aggregates in water are micelles and vesicles. The apolar tails of the surfactants are located in the interior of these aggregates, shielded from water, and the polar head groups are located on the surface. The shape of the surfactant determines for a large part the shape of the aggregate. An example of an aggregate in organic solvents is the organogel. Fibers can be formed by means of various interactions between the single organogelator molecules and these fibers then build a network. A small amount of organogelator is sufficient to increase the viscosity of the solvent.

Cholic acid is a main bile acid, a special class of micelle-forming biosurfactants. It has a carboxylate group as an ionic head group attached to a steroid unit via a small spacer. The steroid unit is facial amphiphilic due to the presence of three hydroxyl groups, which are all located on one side. Cholic acid can be easily derivatized via the carboxylate group and hydroxyl groups. In this thesis numerous newly synthesized cholic acid derivatives are reported of which the aggregation behavior in solution has been studied. Special emphasis is on the variation in molecular structure and its influence on aggregation properties.

A large number of cholic acid derivatives with either an amino acid ester group or a long alkyl group attached to the carboxylic acid group via an amide bond display organogel formation in various organic solvents, mostly aromatic solvents. Both types of compounds form thermoreversible gels that are completely transparent and stable for prolonged periods of time. The sensitivity of the gels toward water suggests the construction of a hydrogen bonded gel network. Molecular variation and infrared spectroscopy confirm this and show that both the amide bond and the hydroxyl groups are involved. Electron microscopy shows the presence of thin fibers.

From SANS measurements the diameter of the fibers was established to be around 20 to 40 Å, so the fibers are monomolecular in thickness. Further details about the fibrous shape and network structure were also gained by SANS. Derivatives with an alkyl tail or an amino acid butyl ester form flat fibers that are connected via loose entanglements. Derivatives with an amino acid methyl ester group form round fibers that are connected via crystalline knots of about 100 to 200 Å. This last type of gel network breaks down stepwise upon heating, which could be monitored with DSC.

Small variations in the molecular structure of these organogelators could induce a change in the gelation behavior. Introduction of an aromatic unit in the alkyl tail limits the number of solvents, suited for gelation. Reversing the amide bond increases the melting point of the gels. The stereochemistry of the amino acid unit seems to play a role in some compounds. After substitution of the amide group by a urea group a longer alkyl tail is necessary for gelation, whereas after substitution by an ester group no gelation occurs in aromatic solvents. These alkyl ester derivatives, however, are capable of forming a two-component gel in hexane and octane, in the presence of isomannide or isosorbide. The optimal ratio for the two components is 1:1.

Hydrolysis of the alkyl ester group of several cholyl amino acid ester derivatives creates a series of compounds analogous to the natural bile salt glycocholate. These water-soluble compounds form small micelles of about 5 nm. Only a small variation in the cmc values was found for the various compounds, although the amino acid side groups range from a single hydrogen atom to an aromatic unit or an ionic group. The cmc value of the tyrosine derivative undergoes a small increase at high pH.

Another series of micelle forming cholic acid derivatives was prepared in which the amphiphilicity of cholic acid was completely altered. A long alkyl tail was attached to the carboxylic acid group and ionic groups were attached to the hydroxyl groups via alkyl spacers, resulting in compounds with three ionic head groups. These are the first facial amphiphiles based on cholic acid with three permanent ionic groups. These compounds form micelles in water and the size of the micelles is dependent of the alkyl tail length. Increasing the length of the spacer or of the alkyl tail causes a decrease in cmc, although the decrease is not as large as found for other

surfactants. The thermodynamics of micellization was studied using ITC and the temperature-dependent behavior of these compounds is comparable to other surfactants. Some of these compounds have a strong inhibitory effect on the growth of gram-positive and gram-negative bacteria. In their antimicrobial activity they are comparable to some other facial amphiphiles with nitrogen-containing groups.

## Samenvatting

In dit proefschrift worden verscheidene galzuurderivaten besproken, die aggregatiegedrag vertonen in water of in organische oplosmiddelen. De spontane aggregatie van losse moleculen in oplossing in grotere, geordende structuren vindt plaats op het grensvlak van oplosbaarheid. Amfifiele moleculen, of surfactanten, bezitten zowel een hydrofoob (apolair) gedeelte als een hydrofiel (polair) gedeelte. Daardoor hebben ze een sterke neiging tot de vorming van aggregaten in een poging de ongunstige polair-apolair interacties met het omringende oplosmiddel te minimaliseren. Er zijn verschillende typen aggregaten zowel in water als in organische oplosmiddelen. Voorbeelden van aggregaten in water zijn micellen en vesikels. De apolaire staarten van de surfactanten bevinden zich in het binnenste van zo'n aggregaat, waar ze zijn afgeschermd van het water, terwijl de polaire kopgroepen zich aan de buitenkant bevinden. De vorm van de surfactant bepaalt voor een groot deel de vorm van het aggregaat. Een voorbeeld van een aggregaat in organische oplosmiddelen is de organogel. De vorming van fibers door de losse organogelatoren kan plaatsvinden onder invloed van verschillende soorten interacties en vervolgens vormen deze fibers weer een netwerk. Een kleine hoeveelheid organogelator is voldoende om de viscositeit van het oplosmiddel sterk te verhogen.

Galzuur is een speciaal type micel-vormende biosurfactant. Het heeft een carbonzuurgroep als ionische kopgroep, die vastzit aan een steroïde kern via een klein tussenstukje. Deze steroïde kern is faciaal amfifiel dankzij de aanwezigheid van drie hydroxygroepen, die zich allemaal aan dezelfde zijde bevinden. Het is goed mogelijk om derivaten te maken van galzuur via de carbonzuurgroep en de hydroxygroepen. In dit proefschrift wordt een groot aantal nieuw gesynthetiseerde galzuurderivaten beschreven, waarvan het aggregatiegedrag in oplossing is bestudeerd. De nadruk ligt op de variatie in moleculaire structuur en de invloed hiervan op de aggregatie-eigenschappen.

Een groot aantal galzuurderivaten met een aminozuurester of een lange alkylgroep bevestigd aan de carbonzuurgroep via een amidebinding vertoont de vorming van organogelen in verschillende organische oplosmiddelen, meestal



aromatische oplosmiddelen. Beide type verbindingen vormen thermoreversibele gellen, die volledig doorzichtig zijn en stabiel gedurende langere tijd. De gevoeligheid van de gellen voor water is een aanwijzing dat het netwerk wordt gevormd met waterstofbruggen. Variatie in de moleculaire structuur en infraroodspectroscopie bevestigen dit en laten zien dat zowel de amidebinding als de hydroxygroepen hierbij betrokken zijn. Elektronenmicroscopie toont de aanwezigheid van dunne fibers. Met SANS-metingen is de doorsnede van de fibers vastgesteld op 20 tot 40 Å, dus de fibers zijn monomoleculair in dikte. Ook zijn we meer details te weten gekomen over de vorm van de fibers en de structuur van het netwerk. De derivaten met een alkylstaart of een aminozuurbutylester vormen platte fibers, die losjes met elkaar zijn verweven. De derivaten met een aminozuur methylester vormen ronde fibers, die met elkaar verbonden zijn in kristallijne knooppunten van 100 tot 200 Å. Dit laatste type gel netwerk wordt stapsgewijs afgebroken als het wordt verwarmd. Dit kon worden bekeken met DSC.

Kleine variaties in de moleculaire structuur van deze organogelatoren kan een verandering in het geleergedrag tot gevolg hebben. Introductie van een aromatische groep in de alkylstaart vermindert het aantal geschikte oplosmiddelen voor gelvorming. Omkeren van de amidebinding verhoogt het smeltpunt van de gellen. De stereochemie van de aminozuureenheid lijkt een rol te spelen bij sommige verbindingen. Als de amidebinding wordt vervangen door een ureumbinding is een langere alkylstaart nodig om gelvorming te krijgen. Als zij wordt vervangen door een esterbinding vindt er helemaal geen gelvorming plaats in de aromatische oplosmiddelen. Daarentegen zijn deze alkylesterderivaten in staat om een twee-componenten gel te vormen in hexaan en octaan, in aanwezigheid van isomannide of isosorbide. De optimale ratio voor de twee componenten is 1:1.

Door de alkylestergroep van een aantal van de aminozuuresterderivaten te hydrolyseren is een serie van verbindingen gemaakt die analoog zijn aan het natuurlijke galzure zout glycocholaat. Deze wateroplosbare verbindingen vormen kleine micellen van ongeveer 5 nm. Er werd slechts een kleine variatie in cmc-waardes waargenomen voor de verschillende verbindingen, terwijl de aminozuurrestgroep varieerde van een enkel waterstofatoom tot een aroma-atoom deel of

een geladen groep. De cmc-waarde van het tyrosine derivaat wordt iets groter bij hoge pH.

Een andere serie van micelvormende galzuurderivaten is vervaardigd, waarin de amfifiliciteit van galzuur volledig is veranderd. Een lange alkylstaart werd bevestigd aan de carbonzurgroep en geladen groepen werden bevestigd aan de hydroxygroepen via alkyltussenstukjes. Het resultaat is een serie verbindingen met drie kopgroepen. Dit zijn de eerste faciaal amfifiele verbindingen, gebaseerd op galzuur, met permanent geladen groepen. In water vormen deze verbindingen micellen, waarvan de grootte afhangt van de lengte van de alkylstaart. Door het tussenstukje of de alkylstaart te verlengen daalt de cmc, alhoewel de daling kleiner is dan bij andere surfactanten. De thermodynamica van micellering werd bestudeerd met behulp van ITC en het gedrag van deze verbindingen bij verschillende temperaturen is vergelijkbaar met dat van andere surfactanten. Enkele van deze verbindingen hebben een sterk remmend effect op de groei van gram-positieve en gram-negatieve bacterien. Wat betreft hun antimicrobiele werking zijn ze vergelijkbaar met enkele andere faciaal amfifiele verbindingen met stikstofhoudende groepen.

## Dankwoord

Het dankwoord. Het is dat deel van een proefschrift dat als eerste wordt gelezen maar dat als laatste wordt geschreven. En na de inspanning van lange tijd echte hoofdstukken schrijven mag ik dan nu aan mijn dankwoord beginnen. In de afgelopen jaren heb ik al herhaaldelijk delen ervan bedacht, maar die bleven grotendeels beperkt tot in mijn hoofd. Gelukkig maar, want de inhoud was niet altijd even vriendelijk. Er waren inderdaad de minder leuke tijden. Maar als ik terugkijk, zie ik vooral de positieve dingen: veel leuke momenten met collega's, chemie die lukte, samenwerkingen die mooie metingen hebben opgeleverd. En als ik reeds-gepromoveerden hoor praten, belooft dat nog wat voor deze herinneringen in de toekomst, want ze worden blijkbaar alleen maar beter met de tijd. Een heleboel mensen hebben bijgedragen aan mijn positieve herinneringen en die wil ik hier graag bedanken.

Allereerst Ton Marcelis, mijn dagelijkse begeleider. In een kleine vergelijkende test kom je als een zeer goede begeleider uit de bus. Ik heb het erg gewaardeerd dat ik altijd bij je binnen kon lopen (of dat je toch vanzelf wel langs kwam; nog makkelijker). Ik ken weinig mensen geduldiger dan jij. Dan Ernst Sudhölter, mijn promotor. Ernst, je dacht wel eens dat ik niet zo enthousiast was. Tja, als *jij* "wilde ideeën" gaat spuien, valt eenieder daarbij in het niet. Toch was zo'n brainstormsessie goed voor de motivatie want ik ging daarna altijd weer met frisse moed verder. Ik zou je graag weer nieuwe eerste-geldstroom-aio's wensen voor de toekomst, maar ik vrees dat dat zelfs voor jou niet meer realistisch is.

Op de labzaal kon ik altijd rekenen op Arie Koudijs voor hulp met de synthese of gewoon voor het delen van domme opmerkingen, als de dienst het toeliet. Arie, iedereen zal zich onze trimethylammonium-preparaten herinneren! Ik hoop dat je nog enkele jaren (met je nieuwe *look*) op zaal zult blijven werken. Daarnaast heb ik veel hulp gekregen en ook zelf veel geleerd van mijn studenten. Tina, je hebt zoveel nieuwe verbindingen gemaakt die ook nog leuke dingen deden, dat ze terug zijn te vinden in de hoofdstukken 2, 3 (en dus 4) en 5! Ik vond het erg leuk dat je de laatste jaren mijn collega en kamergenoot bent geweest, tot en met de flams in Lyon toe! Louis, het kostte je veel doorzettingsvermogen, maar dan heb je ook wat: de basis

van hoofdstuk 6 ligt in jouw werk. Leuk dat je inmiddels ook tot de OC-aio's behoort. Werner, jouw werk lag wat verder van het mijne af, waardoor de communicatie wel eens minder goed verliep. Het einddoel is toen niet gehaald, maar ik denk dat je tevreden kunt zijn met de ingeslagen weg van jouw interesse. In hoofdstuk 3 zijn enkele van je 'omgekeerde' verbindingen goed van pas gekomen. Daarnaast zijn ook enkele verbindingen gesynthetiseerd door studenten onderzoeksmethoden: Petra en Patrick, bedankt hiervoor.

Niet alleen met de synthese, maar ook met de verschillende metingen heb ik regelmatig hulp nodig gehad en gekregen. Onder het motto 'beter een goede buur dan een verre vriend' wil ik graag Anton Korteweg en Remko Fokkink van Fysische chemie en kolloïdkunde bedanken voor hun vriendelijke hulp bij de calorimetrie en lichtverstrooiing. Ook iets verderop zijn goede burens in Wageningen: Ineke Heikamp-de Jong van Microbiologie wil ik bedanken voor het uitvoeren van de antimicrobiële test; Elaine Vaughan, thank you for your help with the antimicrobial tests; Adriaan van Aelst van PCB wil ik bedanken voor de verschillende EM-metingen.

Toch is het ook fijn om verre vrienden te hebben. I would like to thank Pierre Terech. Only with your help it was possible for us to come to Grenoble for SANS-measurements. And your experience has been indispensable in gaining all the information we did in 48 hours. I am looking forward to seeing you again at the defense ceremony. Dank is ook verschuldigd aan Marc Stuart en Maaike de Loos, beiden van Rijksuniversiteit Groningen, voor de mooie EM-plaatjes die veel hebben verduidelijkt. Een groot woord van dank gaat uit naar Wim Bouwman van het IRI in Delft. Ik vrees dat zonder jouw kennis de voorbereiding op de trip en de uitwerking van de resultaten behoorlijk desastreus zouden zijn verlopen. Ik heb ook genoten van ons e-mail contact. Ik denk dat ik inmiddels wel donkerblond ben op SANS-gebied.

Ook binnenshuis wil ik een heleboel mensen bedanken. Allereerst Beb voor het snelle meten van de vele NMR's; Rien, Hugo en Elbert voor de elementanalyse (sorry voor de vele hygroscopische glazen); Kees en Maarten voor de massa's. En de dames van het secretariaat en de schoonmaak, heren van het magazijn en gebouwbeheer: zonder jullie is het werken hier onmogelijk of toch op zijn minst zeer onaangenaam.

Eigenlijk zou ik alle (ex-)collega's van OC moeten opnoemen als dank voor allerlei kleine dingetjes: advies over een poster, antwoord op een specifiek synthesevraagje, hulp op computergebied ("Ja, dan moet je onder de instellingen van Windows..." "Laat maar, bedankt"). Speciaal *kudos* voor Han toen iedere aio's nachtmerrie bij mij werkelijkheid werd. Maar vooral voor gezelligheid in de pauzes, fietstochten, labstappen, aio-reizen, borrels, tourtoto's, de persoonlijke bezorging van het lijfblad van deze instelling, enzovoorts, enzovoorts. Een aantal mensen wil ik bij naam noemen: Dorien, Yvonne, Corien, Alex, Tina, Remko, Louis, Cindy, Michael, Patrick, Marjon, Floor, Frédérique, Agnes, Cindy, Helma, René, Dennis, Harald, Peter, Danuta, thank you for a nice time, Theo, Nicole, Matthew, Roel, Tommi, Falko, Harm, Hugo, Maurice, Ton, Arie, Maarten en Gabriëlle: bedankt voor een goede tijd.

Ook buiten het werk waren begrijpende mensen, bij wie ik mijn verhaal kwijt kon, of die juist voor de nodige afleiding zorgden: Marco, Anne, Niels, Angelique, Jules, Karen, Harrold en Bianca, de wereldwinkelmarktkramers, bedankt! Marieke, jij succes in jouw laatste jaar. Voor de meeste van mijn familieleden was het moeilijker te begrijpen wat ik deed, maar jullie zorgden voor des te meer afleiding: Papa, Mama, Doriet, Mark, Anke, Lina, Josien, Sander, Kick, Nina, Pa, Ma, Joost, Conny, Hugo, Stefan, bedankt voor het familie-zijn. En Michiel, bedankt voor de boodschappen, de vele bammetjes, het systeembeheer van Gimo, de buffy-uurtjes, je mailtjes die me regelmatig hebben opgevrolijkt ;-) maar vooral voor je geduld en voor het feit dat in ieder geval één van ons tweeën altijd het vertrouwen in mij behield.

En nu is het af!!!

Hendra

## Curriculum vitae

De schrijfster van dit proefschrift werd geboren op 5 maart 1974 te Roosendaal. Ondanks de originele adviezen van haar oudere zussen en broer kreeg zij de namen Hendrika Maria Willemen, roepnaam Hendra. In haar geboorteplaats behaalde zij het VWO-diploma aan het Gertrudis College. Aansluitend werd in september 1992 begonnen met de studie Moleculaire Wetenschappen aan de toenmalige Landbouwniversiteit Wageningen. Binnen deze studie werden de specialisatierichtingen Chemisch en Chemisch-Biologisch gevolgd met afstudeervakken bij Organische Chemie en Biochemie. In het kader van een Erasmus-project liep zij 5 maanden stage aan de Rijksuniversiteit Gent. Aan het eind van haar studie werkte zij 3 maanden als student-assistent. Twee weken voor het behalen van de doctoraalsbul begon zij op 15 september 1997 aan een promotie onderzoek bij het Laboratorium voor Organische Chemie aan Wageningen Universiteit. Het in dit proefschrift beschreven onderzoek werd begeleid door Prof. dr. Ernst Sudhölter en dr. Ton Marcelis. Sinds september 2002 is zij werkzaam bij het Rijksinstituut voor Volksgezondheid en Milieu in Bilthoven.

## List of publications

Acid- and enzyme-catalysed cyclisation reactions of (Z,E)-1(10),4-cyclodecadiene derivatives as model systems for melampolides. D.P. Piet, H.M. Willemen, T.J.M. de Bruin, M.C.R. Franssen, J.B.P.A. Wijnberg, and Ae. de Groot, *Tetrahedron* **1997**, 53, 11425.

Biotransformation of linalool to furanoid and pyranoid linalool oxides by *Aspergillus niger*. J.C.R. Demyttenaere and H.M. Willemen, *Phytochem.* **1998**, 47, 1029.

Bioreduction of carboxylic acids by *Pyrococcus furiosus* in batch cultures. E.C.D. van den Ban, H.M. Willemen, H. Wassink, C. Laane, and H. Haaker, *Enzyme and Microbial Techn.* **1999**, 25, 251.

N-cholyl amino acid alkyl esters: a novel class of organogelators. H.M. Willemen, T. Vermonden, A.T.M. Marcelis, and E.J.R. Sudhölter, *Eur. J. of Org. Chem.* **2001**, 2329.

Alkyl derivatives of cholic acid as organogelators: one-component and two-component gels. H.M. Willemen, T. Vermonden, A.T.M. Marcelis, and E.J.R. Sudhölter, *Langmuir*, in press.

Micellization and antimicrobial activity of new cholic acid-derivatives with three permanent ionic head groups. H.M. Willemen, L.C.P.M. de Smet, A. Koudijs, M.C.A. Stuart, I.G.A.M. Heikamp-de Jong, A.T.M. Marcelis, and E.J.R. Sudhölter, *Angew. Chem., Int. Ed.*, submitted.

Aggregation of different amino acid-conjugates of cholic acid in aqueous solution. H.M. Willemen, T. Vermonden, A. Koudijs, A.T.M. Marcelis, and E.J.R. Sudhölter, *Colloids and Surfaces A*, submitted.

A small angle neutron scattering study on cholic acid-based organogel systems. H.M. Willemen, W.G. Bouwman, P. Terech, A.T.M. Marcelis, and E.J.R. Sudhölter, manuscript in preparation.

Aggregation and thermodynamics cholic acid-derivatives with three permanent ionic head groups. H.M. Willemen, A.T.M. Marcelis, and E.J.R. Sudhölter, manuscript in preparation.



## Stellingen

1. Gepresenteerde fysische data boeten aan betekenis in, als naam en structuurformule van de betreffende verbindingen niet met elkaar in overeenstemming zijn.  
*T. Nakashima, T. Anno, H. Kanda, Y. Sato, T. Kuroi, H. Fujii, S. Nagadome, G. Sugihara, Coll. Surf., B 2002, 24, 103-110*
2. Publicatie van enkele complete artikelen verdient de voorkeur boven publicatie van vele elkaar overlappende short communications, zoals in sommige onderzoeksgroepen gebruikelijk is.  
*Hanabusa et al., Shinkai et al.*
3. De stap van pyreen naar een pyreenderivaat als fluorescente probe is niet zonder meer een toegestane overgang.  
*F.M. Winnik, M.A. Winnik, H. Ringsdorf, J. Venzmer, J. Phys. Chem. 1991, 95, 2583-2587.*
4. Bij het gebruik van supramoleculaire aggregaten is 'molecular imprinting' een ongelukkige woordkeus.  
*R.J.H. Hafkamp, B.P.A. Kokke, I.M. Danke, H.P.M. Geurts, A.E. Rowan, M.C.A. Feiters, R.J.M. Nolte, Chem. Commun. 1997, 545-546.*
5. Een gel is geen vloeistof.  
*Always commercial 1998*
6. Het vervangen van 25 gedrukte exemplaren van een proefschrift door de elektronische versie is nog minder dan een halfslachtige poging van Wageningen Universiteit om mee te gaan in het elektronische tijdperk.
7. De wijze waarop de Wageningse gemeenteraad de burgemeester heeft behandeld is niet conform de eis die zij zelf aan deze persoon had gesteld.
8. Een gebrek aan systeem in het systeembeheer leidt automatisch tot frustraties.

Stellingen behorende bij het proefschrift

"Aggregation behavior of cholic acid derivatives in organic solvents and in water"

Wageningen, 8 oktober 2002

Hendra Willemsen